Carbon Sharing in a 4-Chlorosalicylate Degrading Bacterial Consortium

Von der Fakultät für Lebenswissenschaften

der Technischen Universität Carolo-Wilhelmina

zu Braunschweig

zur Erlangung des Grades einer

Doktorin der Naturwissenschaften

(Dr. rer. nat.)

genehmigte

D i s s e r t a t i o n

von Sonja Pawelczyk
aus Berlin

1. Referent:	Professor Dr. Kenneth Nigel Timmis
2. Referent:	apl. Professor Dr. Siegmund Lang
eingereicht am:	10.09.2007
mündliche Prüfung (Disputation) am:	16.11.2007
Druckjahr	2007

Vorveröffentlichungen der Dissertation

Teilergebnisse aus dieser Arbeit wurden mit Genehmigung der Fakultät für Lebenswissenschaften, vertreten durch den Mentor der Arbeit, in folgenden Beiträgen vorab veröffentlicht:

Tagungsbeiträge

Pawelczyk, S. and Abraham, W.-R. The incorporation rates of organic carbon in fatty acids of *Pseudomonas putida* are time-dependent. Pseudomonas 2005-10th International Congress on Pseudomonas, Marseille/France. 2005 (Poster)

Pawelczyk, S. and Abraham, W.-R. For some bacteria the incorporation rates of organic carbon in fatty acids are time-dependent. Development and control of functional diversity at micro- and macroscales, Munich/Germany. 2005 (Poster)

Pawelczyk, S. and Abraham, W.-R. Increased fatty acid synthesis rates during stationary in some bacteria species shown by stable isotope labelling. Spring Academy 2006-Systems Biology (German Genetics Society), Magdeburg /Germany. 2006 (Vortrag)

Pawelczyk, S. and Abraham, W.-R. Several bacteria species show increased fatty acid synthesis rates during stationary phase revealed by stable isotope labelling. ISEB 2006 (Poster Presentation)

Pawelczyk S., Müller, S. and Abraham, W.-R. Analysis of carbon sharing in a 4-chlorosalicylate degrading consortium by combining stable isotope labelling and fluorescence activated cell sorting techniques. 16th Annual Meeting of the German Society for Cytometry, Leipzig/Germany. 2006 (Vortrag)

Pawelczyk, S. and Abraham, W.-R. Kinetically analysis of substrate incorporation of bacteria reveals dependencies of growth phase by stable isotope mass spectrometry. Annual Conference of the Association for General and Applied Microbiology, Osnabrück/Germany. 2007 (Poster Presentation)

1. Introduction

2. Material and Methods

3. Results

d	Day
EA	Elemental Analyser
FACS	Fluorescence Activated Cell Sorting
FAMEs	Fatty Acid Methyl Esthers
FISH	Fluorescence *in situ* Hybridization
GC	Gas Chromatography
g	Gravity
Gyr	Gigayear (1 billion years)
h	Hour
HPLC	High Performance Liquid Chromotoghrapy
IgG	Immunoglobulin G
IRMS	Isotopic Ratio Mass Spectrometry
min	Minute
mM	Millimolar
ml	Milliliter
nm	Nanometer
R^2	Proportion of Variability in a Data Set
rpm	Revolution per Minute
rRNA	Ribosomal Ribonucleic Acid
s	Second
STD	Standard Deviation
µ	Growth Rate
µl	Microliter
µM	Micromolar
µm	Micrometer
v / v	Volume per Volume
w / v	Weight per Volume

1. Introduction

Microbes were the first forms of life on earth and have existed twice as long (4 Gyr) as more complex organisms (2 Gyr). They evolved the basic metabolic machinery of all forms of life and evolved a phylogenetic and metabolic diversity that greatly exceeds the collective diversity of all other forms of life. This diversity enables microbes to colonise a vast range of environments too hostile for higher organisms: the range of microbial habitats defines the biosphere. (Schopf 1993). In nature microorganisms tend to live in communities (Caldwell, 1997) in a variety of different habitats (Seckbach, 2000). Within those alliances they are able to cope with a multitude of diverse substrates, for example the pollutants petroleum (Antic, 2006; Nwachukwu, 2001), polychlorinated biphenyls (PCBs) (Pieper, 2005) and chloro-aromatic compounds (König, 2004). The most distinct advantage for bacteria living in a multispecies community is the augmentation of their metabolic potential (Shapiro, 1998). The ability of bacteria to utilize “dead-end” metabolites occurring in the biodegradation of substrates of other species for their own purpose makes such a community the preferred lifestyle (Christensen, 2002; Haug, 1991; Wittich, 1999, Nicodem, 2004).

Much effort was put in the last decades in the analysis of multi-species bacterial communities. The relevance of those studies is obvious if the manifold habitats and duties of microbial consortia are regarded. Those habitats are versatile, they reach from the human body (Falk, 1998; Dethlefsen, 2005; Guarner, 2006) over contaminated sites (Lee, 1998) to the surface of the deep sea (Fuhrmann, 1998).

The diversity of such consortia can only be estimated since the isolation and cultivation of many of its bacterial members is currently not possible. Gans for example revealed that the number of species of a microbial community detected in soil can comprise more than 10,000 (Gans, 2005).

Therefore, culture independent molecular biology techniques for the analysis of such consortia became indispensable tools in microbiology (Amannn,1995). For the analysis of the biodiversity of microbial communities DNA-Finger-Printing techniques like Single Stranded Conformation Polymorphism (SSCP, Orita, 1989), Terminal Restriction Fragment Length Polymorphism (T-RFLP; Liu, 1997) and Denaturing Gradient Gel Electrophoresis (DGGE, Lerman, 1979) were well established in the last decades. Another tool for the dissection of the biodiversity of microbial communities arises from clone libraries (Sakamoto, 2005).

Although those methods delivered an insight in the consistency of a microbial community, they do not allow an assessment about the metabolic activity of its members and their interactions. Therefore, the analysis of metabolomic networks (Hay, 2004; Stolyar, 2007) and the application of isotopic labelled substrates and the analysis of their incorporation in biomolecules of the bacteria developed itself as a useful method in the field of microbial ecology. Biomolecules adopted in those stable isotope probing methods were mostly DNA (Radajewski, 2000; Neufeld, 2007) and RNA (Whiteley, 2007) but also the phospholipid fatty acids of bacteria were proved to be suitable for this method (Lu, 2007). In 1999, Pelz and co-workers (Pelz, 1999) developed a method to unravel the carbon sharing in a pollutant-degrading bacterial consortium by the combination of two techniques: Immunocapture and Isotopic Ratio Mass Spectrometry (IRMS).

For the analysis of the physiological status of individual members of a bacterial consortium flow cytometric approaches (Kell, 1991; Bernender, 1998) turned out as the method of choice in the last years. Müller and co-workers (Müller, 2002) showed that flow cytometric analysis of a binary chemostat culture enabled the monitoring of the proportions and controlling of the population dynamics of the component strains.

In this thesis a further development of the combination of methods Pelz et al. used (Pelz, 1999) was adopted. Here, the techniques of immuno-staining and IRMS were concatenated with Fluorescence Activated Cell Sorting (FACS) to get an insight of the kinetics of carbon sharing in a bacterial consortium. Together with the adaption of DNA patterns revealed by a flow cytometric approach this combination of techniques allowed a deeper insight in bacterial communities.

1.1 Stable Isotope Mass Spectrometry

A chemical element is defined by the number of protons in the nucleus. Isotopes are nuclides of the same element. They possess the same number of protons in the nuclei but differ in its number of neutrons. In contrast to radionuclides, the unstable isotopes of an element, stable isotopes are not radioactive, they do not to decay.

The various isotopes of an element have slightly different chemical and physical properties because of their mass differences. Especially for elements of low atomic numbers, these mass differences are large enough for many physical, chemical, and biological processes or reactions to fractionate or change the relative proportions of various isotopes. Two different types of processes, equilibrium and kinetic isotope effects, cause isotope fractionation. As a consequence of fractionation processes, water and solutes often develop unique isotopic compositions (ratios of heavy to light isotopes) that may be indicative of their source or of the process that formed them.

The isotopic ratio of a solid sample, for example the biomass, can be dissected by employing a combination of an elemental analyser (EA), gas chromatograph (GC) and Isotopic Ratio Mass Spectrometer (IRMS). Therefore, the sample has to be totally combusted in the EA and the emerged gases are introduced to a GC for the separation of CO_2 and N_2. Via the ConFlo II –system the gases are let to the IRMS. At the electron impact ion source of the IRMS the gases are ionised to produce positively charged CO_2 and N_2 which then will be deflected due to their mass differences in a magnetic field and accumulate in collector Faraday cups. Those cups are detecting the masses 44 ($^{12}C\ ^{16}O\ ^{16}O$), 45 ($^{13}C\ ^{16}O\ ^{16}O$) and 46 ($^{13}C\ ^{16}O\ ^{17}O$) for CO_2 and the masses 28 ($^{14}N\ ^{14}N$) and 29 ($^{14}N\ ^{15}N$) for N_2.

For the analysis of the isotopic ratio of volatile compounds in a complex sample by IRMS they have to be separated by an upstream connected GC. The gaseous compounds will than be introduced into IRMS via a Combustion Interface (CI) where they are combusted to CO_2, H_2O and NO_x. In the reduction oven of the CI NO_x will be reduced to N_2 to avoid the false positive detection of NO_2 ($^{14}N\ ^{16}O\ ^{16}O$) as CO_2 ($^{13}C\ ^{16}O\ ^{17}O$) due to their mass of 46. The combustion gas is dried by a water-permeable Nafion membrane to avoid the formation of HCO_2^+-ions which - due to their mass of 45 - could be false positive detected as $^{13}CO_2$. The measurement of the isotopic ratio in the ionised gas delivers the δ-value, the isotopic ratio of the sample. It is calculated

by employing the δ^{13}C-value of Pee Dee Belemnite, a marine calcium carbonate with a relatively high ratio of ^{13}C which serves as an international standard for IRMS.

1.1.1 Stable Isotope Labelling Methods in Microbiology

The technique of stable isotope probing (SIP) is a more and more applied method in the field of environmental microbiology. A labelled substrate (typically 99.95% heavy stable isotope) is added to an environmental sample and biomarkers are purified and analysed to follow the consumption of the substrate (Neufeld, 2006).
The application of this technique reaches from the analysis of interactions between plants and microorganisms in the rhizosphere (Prosser, 2006) to the unravelling of those bacteria from communities, who are involved in the degradation of pollutants. SIP hereby allows following the flow of atoms in isotopically enriched molecules through complex microbial communities into metabolically active microorganisms (Madsen, 2006, Dumont, 2005). The most prominent biomarkers for those studies are DNA and RNA molecules (Neufeld, 2007; Whiteley, 2007) but also phospholipid fatty acids proved to be useful tracer molecules in both identification of metabolic active groups in communities and in substrate flux analysis (Boschker, 1998; Tillmann, 2005; Lu, 2007).

1.1.2 Carbon Isotope Fractionation in Bacteria

Much effort has been spent in research to investigate the isotope fractionation of carbon in bacteria and plants. Due to the fact that lighter isotopes are favored in most biochemical reaction, compounds with heavier isotopes remain in the educt fraction.
Although the chemical and physical properties of stable isotopes are nearly identical, slight differences arise from a quantum mechanical effect depending on different zero-point energies of the heavy and light isotopes. The higher zero-point energy of the lighter isotope means that a chemical bond formed by a lighter isotope is weaker than one by the heavier isotope (Bigeleisen,1959; Meckenstock, 2004). This principle controls the reactivity of the individual stable isotopes in the environment and induces isotope fractionation.
Craig (Craig, 1953) first identified that certain biochemical processes alter the equilibrium between the carbon isotopes. Some processes, such as photosynthesis

for instance, favour one isotope over another, so after photosynthesis, the isotope ^{13}C is depleted by 1.8% in comparison to its natural ratios in the atmosphere.
In general, isotopic fractionation refers to the fluctuation in the carbon isotope ratios as a result of natural biochemical processes as a function of their atomic mass.

1.2 Fatty Acids as Biomarkers

Biomarkers in microbiology are specific molecules which are used to characterise particular organisms. Those can be any kind of molecule indicating the existence of living microbes. In this thesis, bacterial fatty acids are the biomarker of choice.
Bacterial fatty acids are shown in many studies to deliver a useful tool in the phylogenetic and taxonomic analysis of microbial communities (Abraham, 1997; Abraham, 1998; Kohring, 1994; Lechavelier, 1977; Webster, 2006) and represent one of the major modules of cellular components.
In bacterial cells, fatty acids can be found primarily in the cell membranes as phospholipids. Membrane fatty acids can be divided into two major groups regarding to their biosynthetic relationships. The straight-chain fatty acid family counts for the first group, which includes palmitic, stearic, hexadecenoic, octadecenoic, cyclopropanic, 10-methylhexadecanoic, and 2- or 3-hydroxy fatty acids. These fatty acids occur most commonly in bacteria. They are synthesised from acetyl coenzyme A (acetyl-CoA) as the primer and malonyl-CoA as the chain extender, followed, in some cases, by a modification of the fatty acid products. The second family is the branched-chain fatty acid family, which includes iso-, anteiso-, and ω-alicyclic fatty acids with or without a substitution (unsaturation and hydroxylation). The occurrence of these fatty acids in bacteria is not nearly as common as that of the straight-chain fatty acid family, but is still very significant (Kaneda, 1991).
Characteristic fatty acids for bacteria are those with a chain length of C_{12}-C_{19}. Unsaturated fatty acids of this chain length are in general allocated to Gram negative bacteria. Studies of soil samples by Findlay show the potential to assign specific fatty acids to different groups of bacteria (1996). Branched fatty acids with a chain length of C_{14}-C_{16} for example indicate the presence of Gram positive bacteria, while saturated and branched fatty acids with the chain length of C_{16}-C_{19} can be allocated to sulphate-reducing and other anaerobic bacteria (van Elsas, 1997).
In the Eubacteria and Eucaryotes cellular fatty acids have a number of functions.

They are esterified with glycerol which carries a phosphate ester or sugar moieties at its terminal end. To the phosphate a number of different headgroups are attached which form the body of the phospholipids. These phospholipids are organized in a bilayer in the cell membrane protecting the cell against the environment. Some polar lipids carry sugar moieties instead of the phosphate head group, the glycolipids, which are usually found at the outside of the cell mediating e. g. cell contact or cell-cell communication. The functional distinction between phospho- and glycolipids is blurred in *Caulobacteriales* where glycolipids seem to be able to replace many of the phospholipids in the cell wall (Abraham, 1997). Furthermore, fatty acids bound to glycerol alone as triglycerols are storage compounds. Fatty acids can also be found in bacteria as bound lipids, e.g. in lipoproteins and in the lipopolysaccharides.

All fatty acids in the cells in whatever form they occur are called cellular fatty acids. Their composition is often characteristic for a number of taxa and used for their identification (Descheemaker, 1995; Moss, 1974; Miller, 1985).

The formation and metabolism of fatty acids is a critical function of the cell, however, little is know about the kinetics of their formation. It has been reported that phospholipids show high turnover rates and that they are rapidly degraded by phospholipases after the death of the cell (Balkwill, 1988; Fang, 2000; Welch, 1991) qualifying them for valuable markers for living biomass in environmental samples (Zelles, 1992; Vestal, 1989).

1.3 Microbial Consortia

Many studies aim at enriching bacterial communities with distinct metabolic features (Battison, 2007; Cullington, 1999; El-Fantroussi, 2000). A bacterial consortium, which is used as a model consortium in this thesis - initially isolated from the sediment of the creek Spittelwasser - was enriched for its potential to degrade the chloro-aromatic compound 4-chlorosalicylate by Faude (Faude, 1995). The Spittelwasser flows into the river Mulde, a tributary to the river Elbe in a highly polluted site around Bitterfeld in the former German Democratic Republic (GDR). Bitterfeld has been a major industrial site of chemical and metallurgical production in Germany for the last hundred years. Chemical production mainly based on chlorine production by chloralkali electrolysis started in 1894 and included the production of solvents, pesticides, disinfectants, dyes and plastics (Chemie AG Bitterfeld-Wolfen, 1993). High concentrations of numerous organic toxicants as well as heavy metals have been detected in sediments, soils and groundwater of Bitterfeld (Popp, 1994; Kalbitz, 1999; Brack, 1999; Kuballa, 1995; Brack, 2003).

1.3.1 The 4-Chlorosalicylate Degrading Consortium

The bacterial community Faude enriched for its potential to use 4-chlorosalicylate as sole carbon and energy source consists of four strains, MT1, MT2, MT3 and MT4. The sequencing of their 16S rRNA genes revealed a high homology to following strains: *Pseudomonas reinekei* MT1, *Wautersiella falsenii* MT2, *Achromobacter spanius* MT3 and *Pseudomonas veronii* MT4. The cultivation of the community as a chemostat culture revealed strain MT1 with 84 % (± 5%) as the most abundant member of the consortium followed by strain MT3 with 8 % (± 4%), strains MT2 and MT4 are very low abundant with 1 % (Pelz, 1999).

Another remarkable feature of bacterial communities is their potential of carbon sharing during the degradation process. The degradation pathway (Fig. 1.1) of 4-chlorosalicylate (4-CS) is described by Pelz (Pelz, 1999). Strain MT1 is therefore responsible for the initial degradation step, the transformation of 4-CS to 4-chlorocatechol (4-CC). 4-CC can be further degraded by MT1 to 3-chloro-*cis,cis*-muconate or either serve MT3 as a substrate. The further degradation of 3-chloro-

cis,cis-muconate by MT1 can result in the formation of two “dead-end” metabolites, protoanemonin and *cis*-dienlactone, whereby the former can be degraded by strain MT4. *Cis*-dienlactone can be further decomposed by strain MT3. *Wautersiella falsenii* MT2 is not taking part in the degradation of 4-chlorosalicylate, it is assumed to live on cell debris or other metabolites.

Since the isolation and first describtion of the consortium by Faude (Faude, 1995) this community was the inducement of many studies. In addition to the analysis of the above described pathway, Nicodem elucidated a new bacterial pathway of 4- and 5-chlorosalicylate degradation via 4-chlorocatechol and maleylacetate in strain MT1 (Nicoderm, 2004; Pelz, 1999). Camara recently described strain MT1 as *Pseudomonas reinekei* (Camara, 2007). Tillmann dissected the incorporation of ^{13}C-labelled substrate into the rRNA of the individual members of the consortium (Tillmann, 2004) to get further insights in the carbon flux in the community.

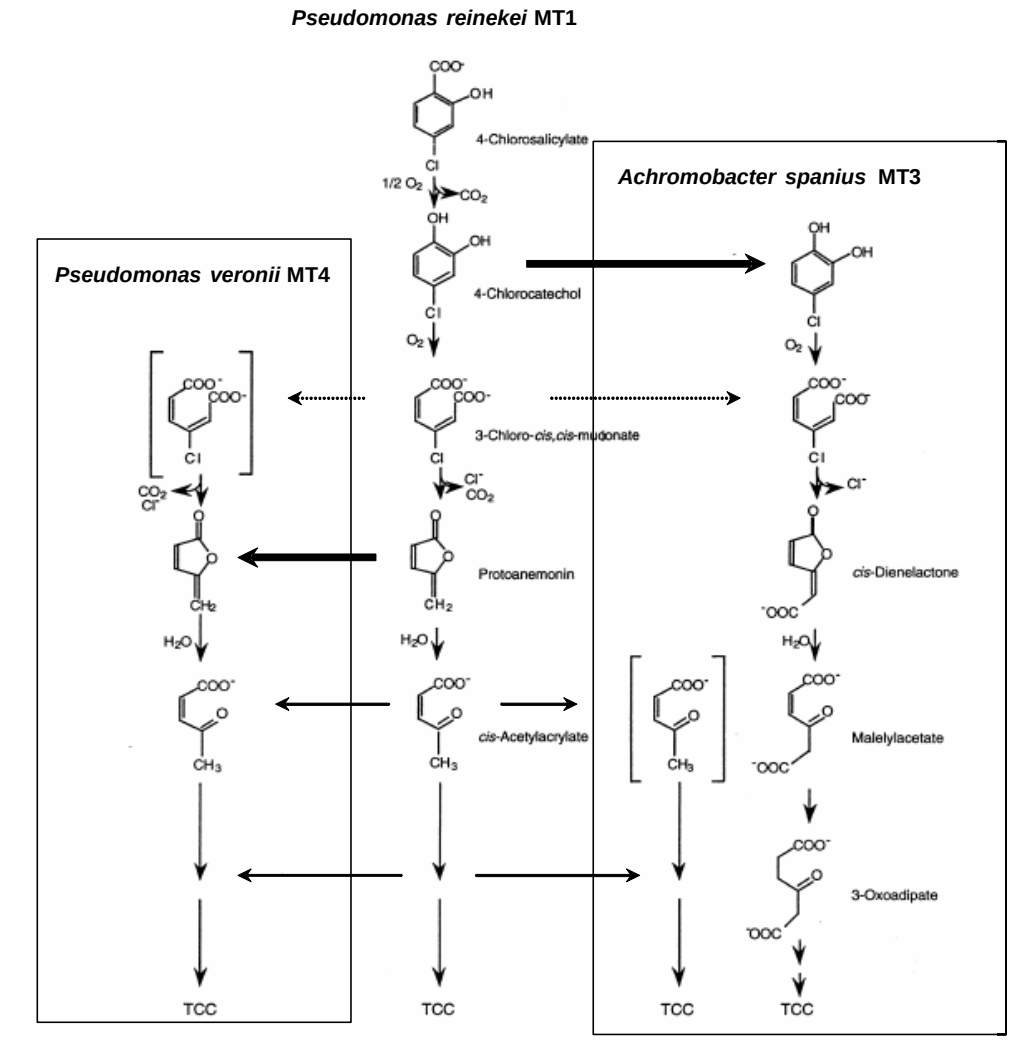

Fig. 1.1: Assignment of metabolic functions and interactions of members of the 4-chlorosalicylate metabolizing consortium. All metabolites shown for MT1 have been identified. The thick solid arrows indicate the experimentally determined release and fate of the corresponding metabolite in the community. The thick outline arrows indicate the experimentally determined release of small amounts of 3-chloromuconate whose fate has not been determined. The thin arrows indicate the possible release of further metabolites. Modified after Pelz (Pelz, 1999).

1.4 Proliferation Assay of a Bacterial Consortium

Flow cytometry is a technology that simultaneously measures and analyzes multiple physical characteristics of single particles, usually cells, as they flow in a fluid stream through a beam of light. The properties measured include relative size, relative granularity or internal complexity and relative fluorescence intensity of a particle. These characteristics are determined by using an optical-to-electronic coupling system that records how the cell or particle scatters incident laser light and emits fluorescence (BD Bioscience, 2000).

A flow cytometer is made up of three main systems: fluidics, optics, and electronics. The fluidics system transports particles by a hydro-dynamically focused stream of fluid to the laser beam for scanning. The optics system consists of lasers to illuminate the particles in the sample stream and optical filters to direct the resulting light signals to the appropriate detectors. The electronics system converts the detected light signals into electronic signals that can be processed by the computer.

An outlier of flow cytometry is the method of Fluorescence Activated Cell Sorting (FACS). Hereby, a vibrating mechanism causes the hydro-dynamically focused stream of cells to break into individual droplets, containing one cell per droplet, after measuring the fluorescence characteristics of the cell by a laser beam. Depending onto those characteristics (sorting criteria) an electrode charges the droplet based on its prior fluorescence intensity. The droplets are deflected due to their charge by positively or negatively charged metal plates and collected in tubes.

Flow cytometric analysis has been shown to be very suitable for probing the dynamics of individual cells within a population and for characterising their physiological status (Allman, 1991; Skarstad, 1986; Kacmar, 2006; Shapiro, 2003; Müller, 2003). Müller and colleagues (Müller, 2002) described a method where they used flow cytometric investigations on pure single cell basis to provide a detailed understanding of the subpopulations' behaviour by following the dynamics and physiological states of their active individuals by analysing the DNA patterns.

The principle that method is based upon is that cells of a bacterial population can differ in their chromosomal content depending on their physiological status (Allman, 1991; Müller, 2003).

Bacteria growing at high rates synthesise more DNA per unit of time than do bacteria that grow slowly. As a result of the delay between times needed for DNA replication

and cell division, fast growing cells can accumulate up to four DNA equivalents per cell. As the growth rate decreases during the deceleration phase, the number of DNA equivalents is readjusted and the number of genomes decreases to one at the early stationary phase (Lebaron, 1994).

To gain information about the physiological status of individual members within the 4-chlorosalicylate degrading consortium (see 1.1.1) the method of Müller is employed in this thesis (Müller, 2002). Hereby, the DNA patterns of the individual members are obtained by analysing samples of pure cultures of the strains on different substrates in proliferation and stationary phase of growth by flow cytometry. The obtained patterns are adapted to samples of the chemostat. Therefore, the individual strains within that sample are immuno-stained with strain-specific antibodies and the DNA-intercalating dye DAPI for the analysis of the DNA content of the subpopulation of the individually stained members of the consortium. Together with conventional analysis of the degradation of the substrate in the consortium, for example by High Performance Liquid Chromatography (HPLC), this method enables an insight in the physiological status of individual members of a pollutant degrading bacterial consortium. Fig. 1.2 precises the analytical procedure of the method.

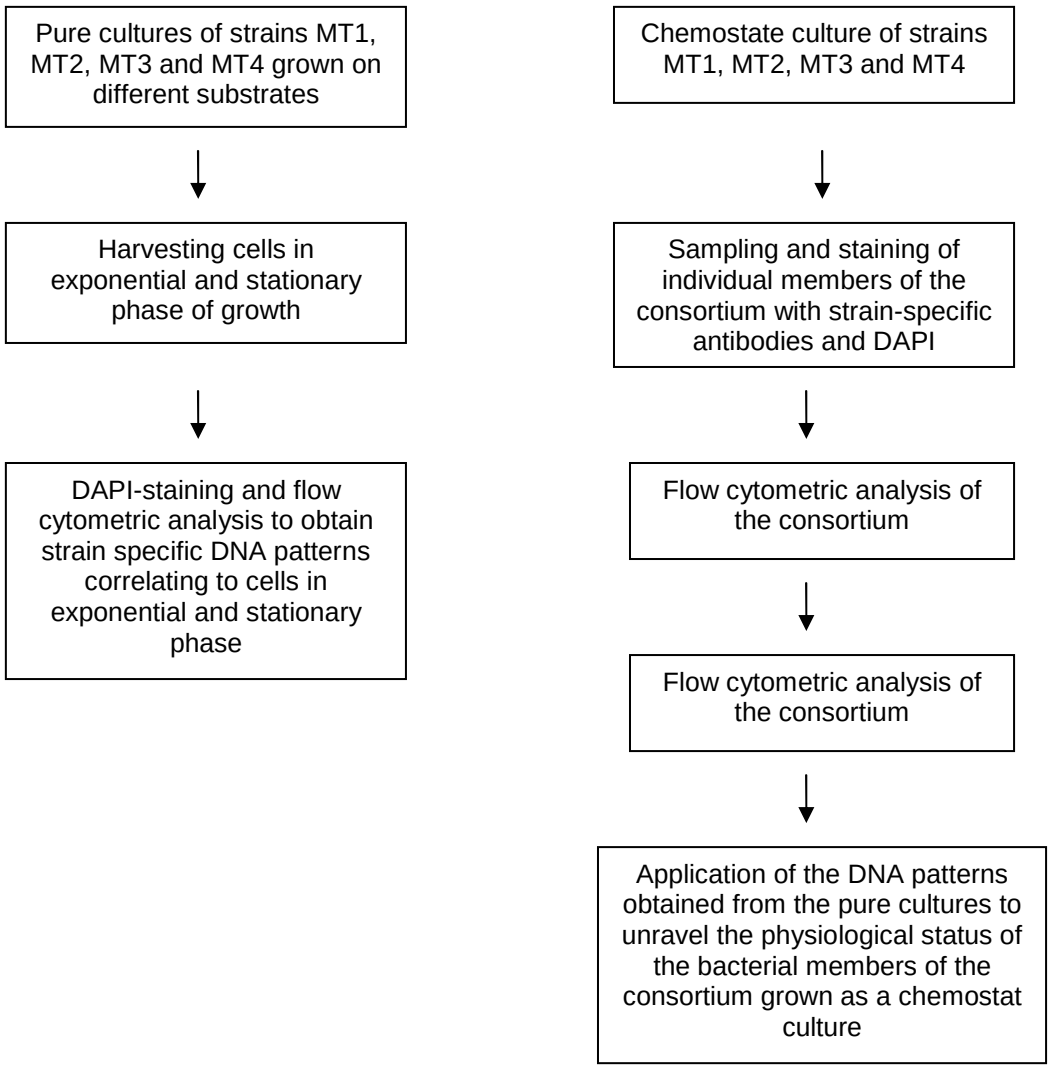

Fig. 1.2: Analysis of the physiological status of Individual members of a bacterial consortium.

1.5 Kinetics of Substrate Uptake in Pure Bacterial Cultures

The analysis of the carbon sharing in a bacterial consortium is difficult because of the often unknown consistency of such a community. The well-caracterised 4-chlorosalicylate degrading microbial consortium delivers therefore a perfect tool since all of its bacterial members could be isolated and identified (Faude, 1995; Pelz, 1999). For three members of this community, *Pseudomonas reinekei* MT1, *Achromobacter spanius* MT3 and *Pseudomonas veronii* MT4, which are actively taking part in the degradation of 4-chlorosalicylate, the kinetics of substrate uptake in pure cultures are analysed. This approach allows a direct comparison of the kinetics of substrate incorporation of the two *Pseudomonas* strains with a strain of a different genus, in that case *Achromobacter spanius* MT3.

The genus *Pseudomonas* is one of the most diverse and ecologically significant taxa of bacteria and its members are found in all of the major natural environments and also in intimate associations with plants and animals (Rainey, 1994). This universal distribution requires a high degree of physiological and genetic adaptability. Evidence of physiological diversity came from early biochemical studies (Stanier, 1966) focusing on the remarkable capacity of *Pseudomonas* strains to degrade a wide range of substrates including aromatic compounds, halogenated derivatives and recalcitrant organic residues (Narbad,1989; Spiers, 2000). Furthermore, the presence of many *Pseudomonas* species in waste water treatment processes confirms the broad metabolic potential of these bacteria. However, to understand and evaluate the physiology of these bacteria, quantitative metabolic studies are required connecting substrate metabolism and biosynthesis of cell components. This study is focused on the metabolism of acetate and fatty acid biosynthesis.

The aim of this study is to elucidate how fast carbon is incorporated into the bacterial fatty acids and whether there are changes in the kinetics of this incorporation along the different stages of growth. This is important because cells which can rapidly incorporate the carbon of the substrates into their fatty acids are also able to switch rapidly from resting cell conditions to exponential growth giving them a temporary advantage against those cells which can do this only at much slower rates.

In this analysis acetate labelled with the stable carbon isotope ^{13}C is used as substrate for the determination of the rates of carbon incorporation into fatty acids in three different bacteria species isolated from a four species consortium degrading 4-

chlorosalicylate (Faude, 1995, Pelz, 1999). Fig. 1.3 demonstrates the analytic procedure of this study. Since strain *Wautersiella* MT2 is not able to live on acetate, this fourth member of the community is not included in this study.

Acetate, activated as acetyl-CoA, can directly be used by acetyl-CoA-carboxylase leading to the fatty acid biosynthesis enzyme complex synthesising long-chain fatty acids (Rock, 1996, Campell, 2000). In parallel experiments [U-^{13}C]-acetate is added at different stages of the growth phase and samples at different time points are taken for analysis of the cellular fatty acids using the isotope IRMS (Goodmann, 1992). This approach allows a direct comparison of the incorporation rates along the growth curve. The incorporation is modelled assuming pseudo-first-order kinetics which is valid because only small amounts of labelled acetate were added in the experiments and the substrate is not the limiting factor for at least 4 of the 6 sampling points. A similar approach has been taken to model the incorporation of substrate carbon along a food chain (Mauclaire, 2003).

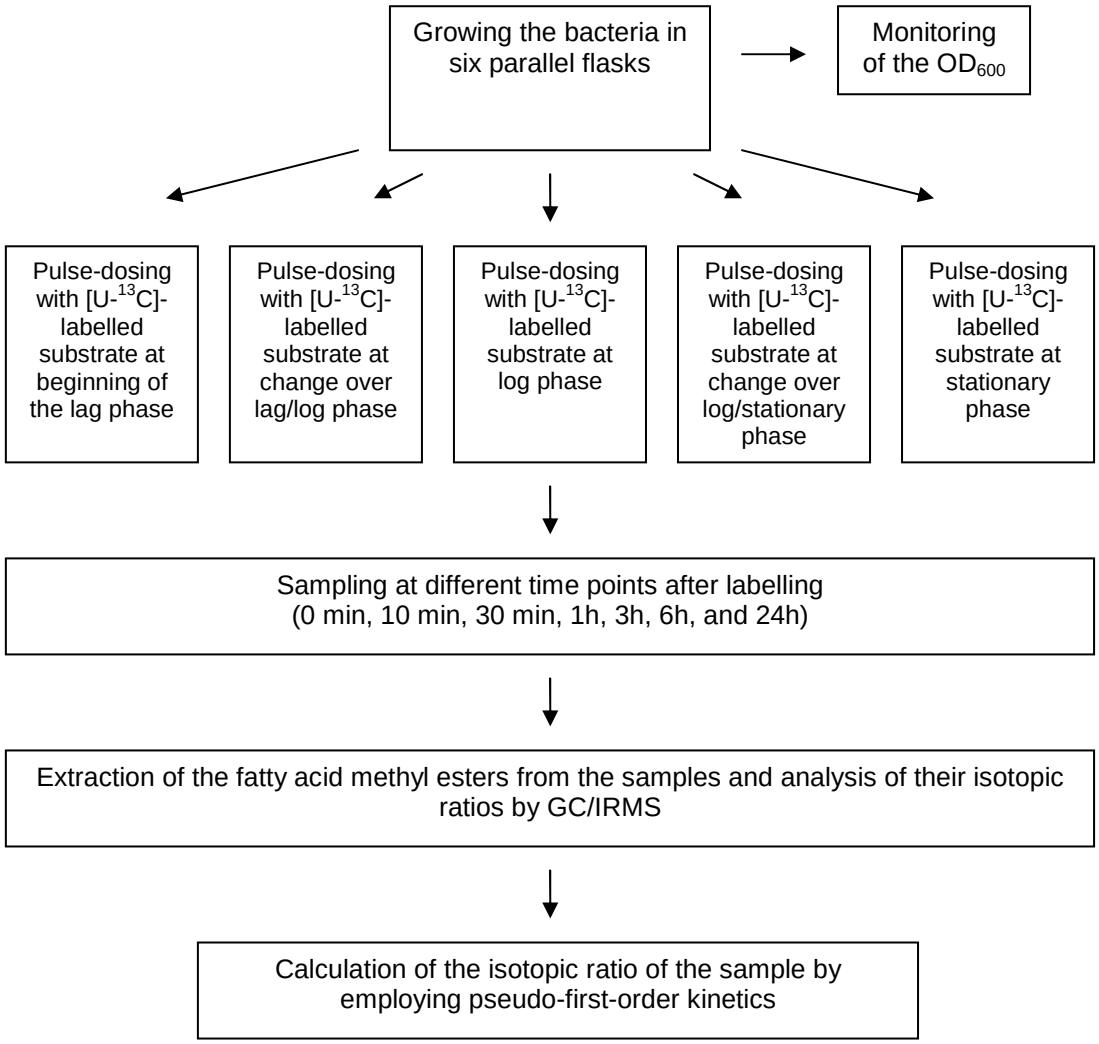

Fig. 1.3: Workflow of the analysis of the kinetics of substrate incorporation in pure bacterial cells.

1.6 Temperature Dependency of Carbon Fractionation in two *Pseudomonas* Strains

Monitoring of isotope fractionation has been developed a powerful tool in elucidating the degradation of hazardous substances in environment (Morasch, 2001; Kaschl, 2005). Until today, little is known about the influence of temperature on the carbon isotope fractionation during bacterial growth. It's ascendancy on the carbon fractionation is mostly analysed in plants. The effect of the growth temperature on carbon isotopic ratios in plants was deconstructed by Smith and colleagues. They found more ^{13}C incorporation during growth at low temperatures than at higher, but the change in isotopic ratio was not linear over the temperature range employed (Smith, 1973). Studies of the isotopic ratio of marine plankton collected from diverse locations differing in temperature showed also a dependency on this parameter (Sackett, 1965). Leclerc and colleagues showed a clear dependence by plotting the temperature of diatome growth as a function of the isotopic enrichment between biogenic silica and water (Leclerc, 1987).

In this study the temperature dependency of the carbon isotopic fractionation during bacterial growth is tested in two *Pseudomonas* strains, *Pseudomonas reinekei* MT1 and *Pseudomonas veronii* MT4. Therefore, biomass, extracted fatty acids and amino acid derivatives from exponential-phase-harvested cells are dissected for carbon isotope fractionation when grown at different temperatures. Additionally, the influence of the growth temperature on the composition of the extracted amino acids and fatty acids is analysed (Fig. 1.4).

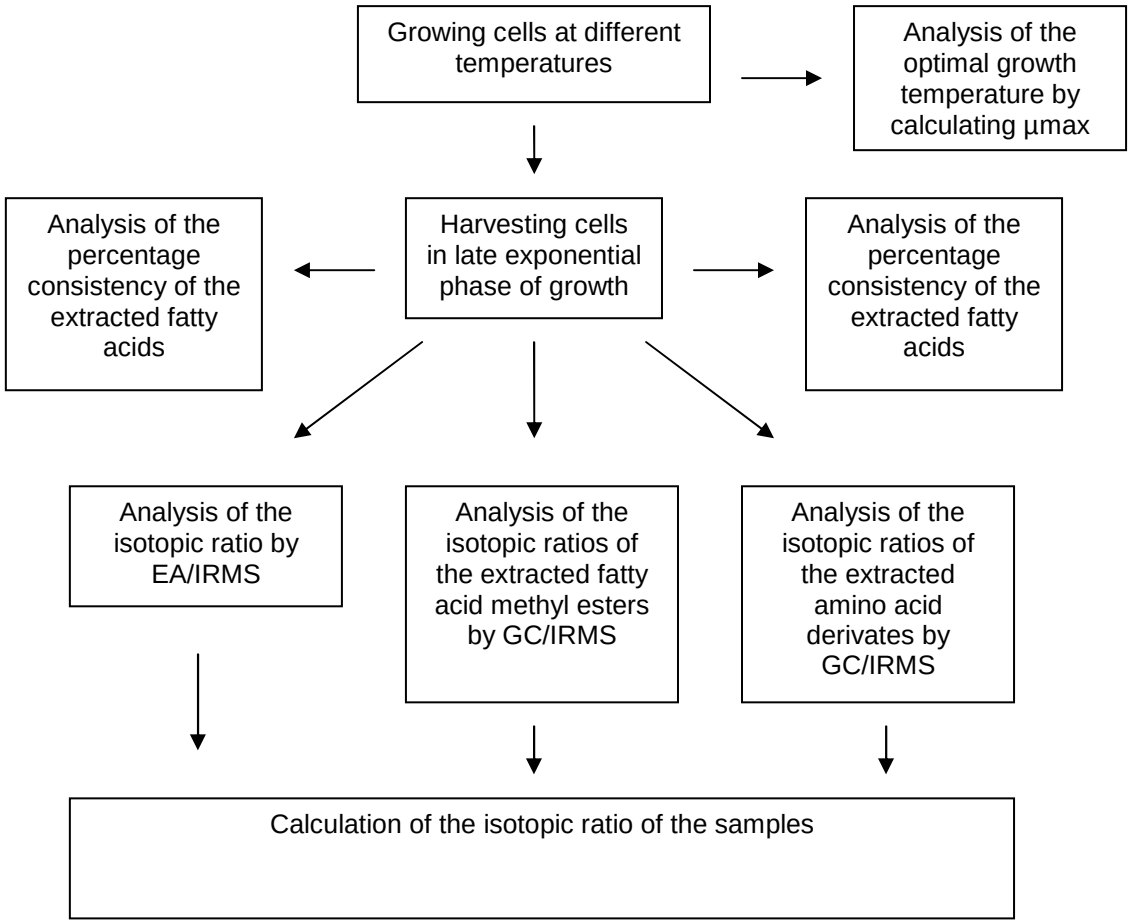

Fig. 1.4: Analysis of the temperature dependency of carbon fractionation in two *Pseudomonas* strains.

1.7 Kinetics of Carbon Sharing in a Bacterial Consortium

Until today little is known about carbon fluxes in bacterial communities. Two approaches were performed to meet the challenge of unravelling the trophic networks within microbial or benthic communities.

Pelz and colleagues developed an approach to dissect the metabolic pathways of the bacterial consortium (Pelz, 1999). This employed immunocapture of the individual members after pulse-dosing the chemostat culture with ^{13}C-labelled substrates. In this study fatty acids were used as biomarkers. The incorporation of the isotopic labelled substrate into the fatty acids of the separated strains revealed first insights into the trophic network of the consortium. For unravelling the carbon sharing within bacterial or benthic consortia the separation of the individual members is essential since the similarity of their fatty acid profiles does not always allow the differentiation of the incorporation of the ^{13}C-labelled substrate. Pel and colleagues (Pel, 2004) introduced a new approach where they employed FACS for the separation of zooplankton after pulse-dosing with $^{13}CO_2$ –spiked unfiltered lake water. Therefore, they took the advantage of the different pigmentation and cell-light-scatter properties to separate four different cell fractions by flow cytometry.

In this thesis a combination of both techniques is applied to get further insights in the kinetics of carbon sharing in a pollutant-degrading bacterial community (1.3.1). This new approach affiliates the well established techniques of immuno-staining of bacteria with strain specific antibodies, their separation by FACS and the analysis of the ^{13}C-labelled substrate incorporation into bacterial fatty acids by IRMS. The incorporation is modelled assuming pseudo-first-order kinetics which is valid because only small amounts of [U-^{13}C]-4-chlorocatechol are added in the experiments and the substrate was not the limiting factor for at least 4 of the 6 sampling points. This approach aims at dissecting the kinetics of the carbon flux in a well-studied bacterial model consortium. A scheme of the analytical workflow can be found in Fig. 1.5. This method enables not only insights in the carbon flux of this particular well-studied community, it also allows the analysis of substrate fluxes in unknown consortia, since the fluorochromising of the bacteria is also possible by employing Fluorescence In Situ Hybridizing (FISH) probes (DeLong, 1989). Therefore, this combination of bacterial staining methods with FACS and IRMS enables the understanding of carbon sharing in complex systems as bacterial consortia.

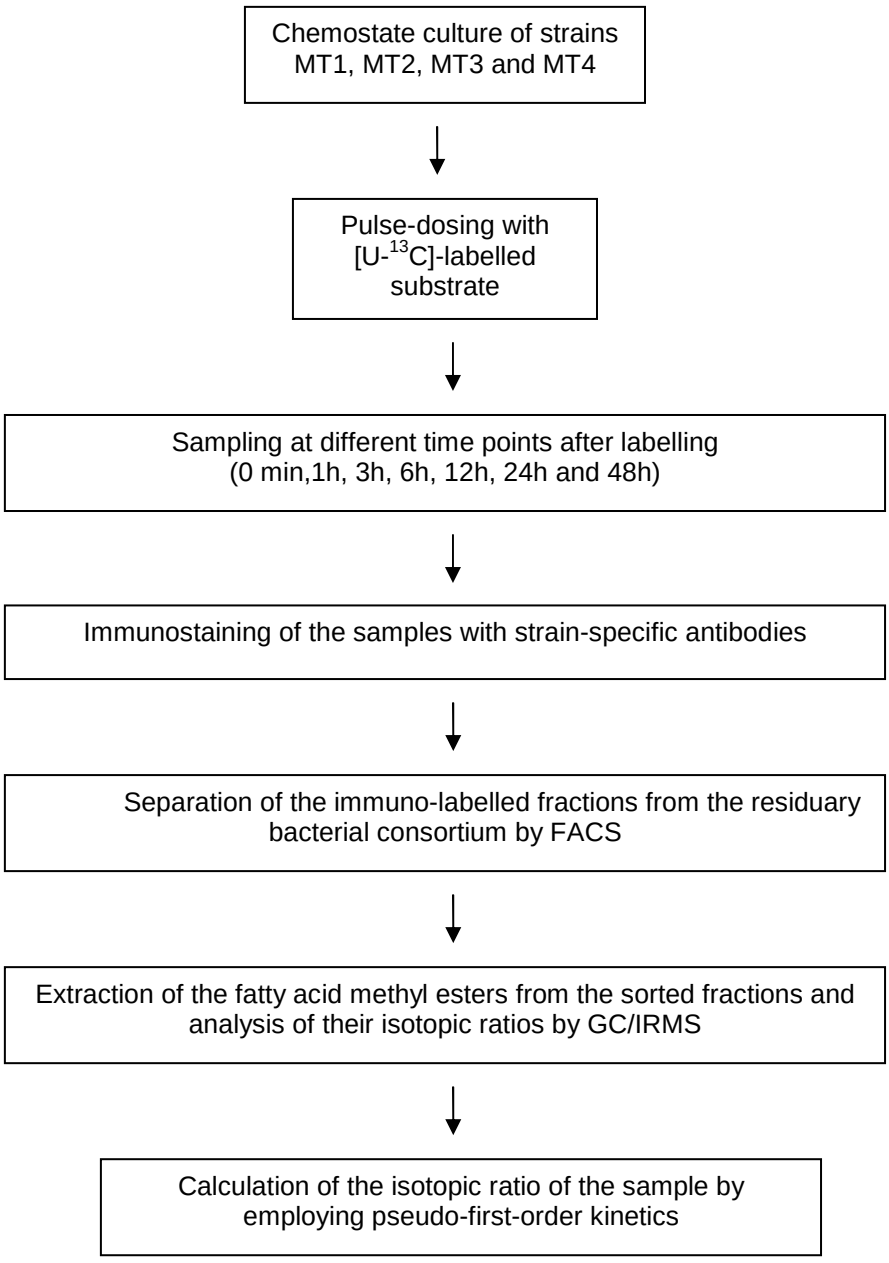

Fig. 1.5: Analysis of the kinetics of carbon sharing in a bacterial consortium.

2. Material and Methods

2.1 Equipment

Autoclave	Tecnoclav 50, Tecnomara AG, Zürich, Schweiz
Centrifuges	Multifuge 1 S-R, Heraeus; RC3C, Sorvall
Evaporator	TR-L 288, Liebisch
Magnetic stirrer	M20/1, Framo-Gerätetechnik
Peristaltic pump	202 U 1, Watson Marlow, England
Rotary shaker (flasks)	Pilot-shake RC-6-U, System Kühner
Thermo block	5018 6101, Liebisch
Vortex Mixer	Velp Scientifica

2.2 Chemicals

All solvents used in this thesis were purchased from Baker (Deventer, Netherlands) and Merck (Darmstadt, Germany) in p.a. quality.

Other chemicals were supplied from Sigma-Aldrich (Steinheim, Germany), Merck (Darmstadt, Germany), Fluka (Buchs, Switzerland), Roth (Karlsruhe, Germany) and Riedel de Haën (Seelze, Germany).

The isotopic labelled compounds [U-^{13}C]-sodium acetate and [U-^{13}C]-4-chlorocatechol were purchased from Sigma-Aldrich (Steinheim, Germany) and Promochem (Wesel, Germany).

Bacterial media supplements were purchased from Difco (Le Pont de Claix, France).

2.3 Media, Buffer and Staining Solutions

Minimal Growth Medium M9

100 ml	Mineral-Buffer Solution
0.67 ml	Magnesium Solution
4 ml	Iron-EDTA Solution
1.33 ml	Trace Elements Solution

ad 1000 ml distilled water

(sterile filtered, pH 7.0)

Mineral-Buffer Solution

87.78 g $Na_2HPO_4 * 2\ H_2O$

30 g KH_2PO_4

12.37 g $(NH_4)_2SO_4$

ad 1000ml distilled water

(autoclaved)

Magnesium Solution

246.48 g $MgSO_4 * 7\ H_2O$

ad 1000ml distilled water

(autoclaved)

Iron-EDTA Solution

3.20 g $FeSO_4 * 7\ H_2O$

12.37 g EDTA

ad 1000ml distilled water

(autoclaved)

Trace Elements Solution

10.75 g MgO

4.5 g $FeSO_4 * 7\ H_2O$

2.0 g $CaCO_3$

1.44 g $ZnSO_4 * 7\ H_2O$

0.87 g $MnSO_4 * 2\ H_2O$

0.28 g $CoSO_4 * 7\ H_2O$

0.25 g $CuSO_4 * 5\ H_2O$

0.06 g $H_3BO_3 * 7\ H_2O$

51.3 ml conc. HCl

ad 1000ml distilled water

(sterile filtered)

EM Medium

20 g	tryptone
5 g	yeast Extract
5 g	NaCl
5 g	glucose
15 g	agar (for solid medium)

ad 1000ml distilled water
(autoclaved, pH 7.0)

PMS Minimal Medium

7,8 g	$Na_2HPO_4 \times 2H_2O$
6,8 g	KH_2PO_4
0,41 g	$MgSO_4 \times 7H_2O$
1 mg	NH_4-Fe-citrat
50 mg	$Ca(NO_3)_2 \times H_2O$
85 mg	$NaNO_3$
0.7 mg	$ZnCl_2$
1 mg	$MnCl_2 \times 4H_2O$
0.62 mg	H_3BO_3
1.9 mg	$CoCl_2 \times 6H_2O$
0.17 mg	$CuCl_2 \times 2H_2O$
0.24 mg	$NiCl_2 \times 6H_2O$
0.36 mg	$NaMoO_4 \times 2H_2O$
13µl	conc. HCl
ad 1000ml	distilled water

(sterile filtered, pH 7.0)

Peptone Medium

5 g	peptone from meat (pancreatic)
3 g	NaCl
2 g	K_2HPO_4
10 g	meat extract
10 g	yeast extract
5 g	glucose

ad 1000ml distilled water
(autoclaved, pH 7.5)

Phosphate Buffered Saline (PBS)

0.54 g	NaH_2PO_4
2.85 g	Na_2HPO_4
8.77 g	NaCl

ad 1000ml distilled water
(autoclaved, pH 7.0)

TE Buffer

5 ml	Tris-HCL (2-amino-2-(hydroxymethyl)-1,3-propanediol HCl, 1M, pH 8.0)
1 ml	EDTA (ethylenedinitrilotetraacetic acid, 0.5M, pH 8.0)

ad 100 ml distilled water
(autoclaved)

Modified DAPI Staining Solutions

Solution A

2.1 g citric acid

0.5 g Tween 20 in

ad 100 ml distilled water

(sterile filtered, pH 7.0)

Solution B

1.5 µM DAPI 4 (‘,6-diamidino-2‘-phenylindole)

400 mM Na_2HPO_4

ad 100 ml distilled water

(sterile filtered, pH 7.0)

Solutions for the Preparation of Fatty Acid Methyl Esters (FAMES)

Solution 1

100 ml Methanol

100 ml 15% NaOH (w/v)

Solution 2

100 ml Methanol

20 ml 37% HCl

Solution 3

100 ml Hexane

100 ml tert-Butyl ethyl ether

Solution 4

0,5 M NaOH

2.4 Bacterial Strains

The bacterial community consisting of four strains was initially isolated from the sediment of the river Spittelwasser, a tributary of the river Elbe in Bitterfeld, Germany (Faude, 1995) highly polluted with chloro-organic substances. Due to their origin from this contaminated region, the chloro-aromatic compound 4-chlorosalicylate served as carbon source in the chemostat culture.
The isolated strains of the consortium were identified by sequencing their 16S ribosomal RNA genes.

2.4.1 Sequencing of bacterial 16S rRNA Genes

2.4.1.1 Extraction of DNA

A bacterial colony of strains was picked and resuspended in 100µl TE-buffer and boiled for 15 min at 96°C in a heating block. The suspension was centrifuged for 1 min at 15700 x g to pellet the cell remains. The DNA-containing supernatant was utilised for the following PCR. Alternatively, the bacterial DNA was extracted by employing the FastDNA® Spin Kit for Soil (Q-Biogene (MP Biomedicals), Heidelberg) by following the supplier's manual.

2.4.1.2 Amplification of the DNA by Polymerase Chain Reaction (PCR)

The extracted DNA was amplified by PCR (Mullis, 1990), a method that enabled the exponential augment of particular sequences of the DNA by enzymatic replication. Those were appointed by using specific sets of primer pairs which enabled the amplification of a special region of the DNA template. The primers, short oligonucleotides, bind at specific regions coding for the 16S ribosomal RNA gene (16S rRNA) of the denaturised bacterial DNA template. The polymerase enables the synthesis of the new complementary DNA strand by the accumulation of free desoxynucleosidtriphosphates (dNTP's) to the primers. The PCR reaction (Table 2.1) was performed in a thermocycler at a total volume of 50 µl by using the temperature program described in Table 2.2.

Table 2.1: Composition of the PCR

1µl	Forward Primer 16F27 (1 pmol end conc.)
1µl	Reverse Primer 16R1492 (1 pmol end conc.)
2µl	dNTP's (25µM each)
5µl	10 x Taq-Buffer
39.5µl	ddH2O
1µl	Template
0.5µl	Taq-Polymerase
50µl	PCR Reaction

Table 2.2: Temperature program of the PCR

Temperature		Time	
94℃	Initial Detnaturation	1 min	
94℃	Denaturation	10 sec	30 cycles
60℃	Annealing	20 sec	
72℃	Elongation	1 min	
72℃	Final Elongation	3 min	

2.4.1.3 Sequencing Reaction

The 16S rRNA gene was sequenced to enable a phylogenetic analysis of the bacterial strains. This was performed by employing the classical chain-termination or Sanger method which requires a single-stranded DNA template, a DNA primer, a DNA polymerase, fluorescence labelled nucleotides and modified nucleotides that terminate DNA strand elongation.

The DNA sample is divided into four separate sequencing reactions, containing the four standard deoxynucleosidtriphosphates (dATP, dGTP, dCTP and dTTP) and the DNA polymerase. To each reaction one of the four fluorescence labeled dideoxynucleosidtriphosphates (ddATP, ddGTP, ddCTP, or ddTTP) is added. These ddNTP’s are the chain-terminating nucleotides, lacking a 3'-OH group required for the formation of a phosphodiester bond between two nucleotides during DNA strand elongation. Incorporation of a ddNTP into the elongating DNA strand therefore terminates DNA strand extension, resulting in various DNA fragments of varying length. The dideoxynucleotides are added at lower concentration than the standard deoxynucleotides to allow strand elongation sufficient for sequence analysis.

For the sequencing reaction the PCR product (2.4.1.2) was purified by employing the QIAquick- PCR Purification Kit (Qiagen, Hilden) by following the supplier's manual.
The sequencing reaction (Table 2.3) was performed in a thermocycler at a total volume of 10 µl by using the temperature program described in Table 2.4.

Table 2.3: Composition of the sequencing reaction

2µl	BigDye RR Mix (Applied Biosystems, Darmstadt)
1µl	BigDye Buffer (Applied Biosystems, Darmstadt)
3µl	purified PCR Product
1µl	Primer
3µl	ddH2O
10µl	PCR Reaction

Table 2.4: Temperature program of the sequencing reaction

Temperature		Time	
96℃	Initial Detnaturation	1 min	
96℃	Denaturation	15 sec	25 cycles
60℃	Annealing	15 sec	
60℃	Elongation	4 min	

The sequencing reaction products were purified by employing the DyeEx 2.0 Spin Kit (Qiagen, Hilden) by following the supplier's manual. The purified sequencing reaction products were dried in vacuum centrifuge and sequenced by employing a 3130xl Genetic Analyzer (Applied Biosystems, Darmstadt).
The gene sequences were annotated by using the computer program Sequencher™ 4.0.5 (Gene Codes Corporation, Ann Arbor, USA). Phylogenetic and molecular evolutionary analyses were conducted using the computer programs ClustalW (EMBL, Hinxton, UK) and MEGA version 3.1 (Kumar, Tamura, Nei 2004).

2.5 Cultivation Conditions

2.5.1 Stock Cultures

An inoculating loop of a pure bacterial culture was added to 750 µl sterile EM-medium in a 2 ml cryo-vial and incubated over night at 30℃ on a continuous shaker (110 rpm). After adding of 500 µl sterile glycerine and vigorous vortexing the vial was frozen at -20℃.

2.5.2 Liquid Cultures

Bacterial strains from frozen stock cultures were streaked on solid EM medium agar plates and incubated at 30℃ until colony formation was visible. Single colonies served as inoculum for liquid cultures.

2.5.3 Chemostat Culture

For the chemostat culture strains *Pseudomonas reinekei* MT1, *Achromobacter spanius* MT3 and *Pseudomonas veronii* MT4 were grown as pure pre-cultures on 30 ml M9-medium with 5 mM sodium acetate as sole carbon source. Strain *Wautersiella falsenii* MT2 was grown as a pure pre-culture on 30 ml M9-medium supplied with 1 g/L yeast extract. Pre-cultures were incubated over night at 30℃ with continuous shaking at 110 rpm. After incubation, the pure culture cells were washed with PBS and resuspended in M9-medium with 5 mM 4-chlorosalicylate (M9-4CS) as sole carbon source to an optical density of 1 measured at 600 nm (OD_{600}) and equal volumes of 7,5 ml of each culture were combined for a 30 ml inoculum consisting of all four strains. This was added to 470 ml of M9-4CS into a 1000 ml glass vessel of the bioreactor (Fig. 2.1). The continuous flow of the medium was controlled by a peristaltic pump. To guaranty a sufficient oxygen supply to the culture the reactor was provided with a magnetic stirrer. The parameters for the continuous culture were shown in Table 2.5.

Table 2.5: Bioreactor parameters

Parameter	Settings
Temperature	20°C
Revolution speed of the magnetic stirrer	300rpm
Flow rate	0,1/d

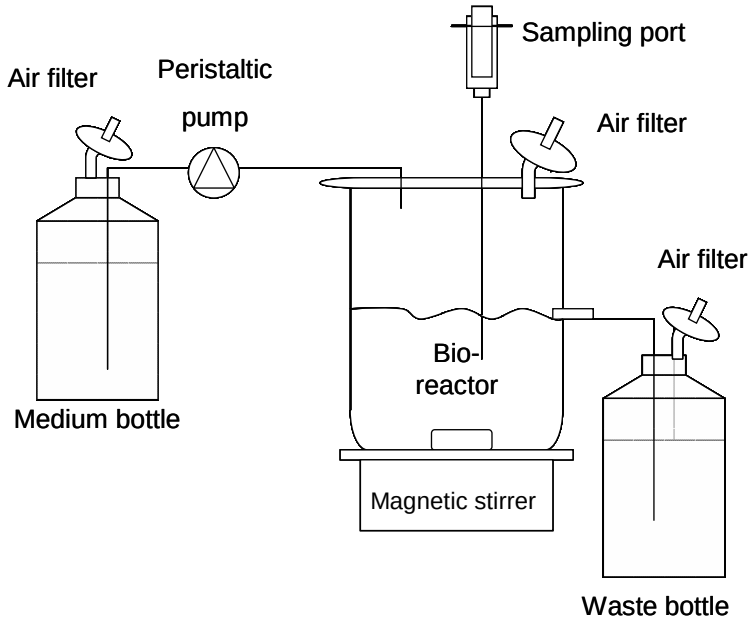

Fig. 2.1: Scheme of the bioreactor

10 ml samples of the chemostat culture were taken via the sampling port. The OD_{600} was measured by using a biophotometer. The samples were centrifuged at 4700 rpm for 10 min. 1 ml of the supernatant was stored at -20℃ for metabolic analysis.
The remaining supernatant was decanted and the cell pellet was resuspended in 2 ml 10% Sodium azide (w/v) and stored at 4℃ for fur ther dissection.

2.5.4 Analysis Dependent Cultivation Conditions

2.5.4.1 Temperature Dependency of Carbon Fractionation in *Pseudomonas sp.*

Pure cultures of strains MT1 and MT4 grown on EM-agar plates (2.5.2) were used to inoculate 30 ml of M9 medium with 10 mM sodium acetate as sole carbon source (M9-NaAc). The inoculating cultures were incubated at 30℃ over night shaking at 110 rpm. The cultures were then diluted with fresh medium to an OD_{600} of 0.1 and incubated at different temperatures (15℃, 20℃, 25 ℃, 30℃ and 37℃) shaking at 110 rpm. OD_{600} was monitored during growth. Cells were harvested in exponential growth phase by centrifugation at 6400 x g for 20 min. The resulting bacteria pellets were stored at -20℃ until further analysis of the isotopic ratio of their fatty acids (2.6.1), their amino acids (2.6.2) and their biomass (2.6.4). These experiments were performed in triplicates.

2.5.4.2 Kinetics of Substrate Incorporation in Pure Bacterial Cultures

Pure cultures of strains MT1, MT3 and MT4 grown on EM-agar plates (2.5.2) were used to inoculate 100 ml of M9 medium with 10 mM sodium acetate as sole carbon source (M9-NaAc). The inoculating cultures were incubated at 30℃ over night shaking at 110 rpm. The cultures were then distributed into six 100 ml flasks and diluted with fresh medium to an OD_{600} of 0.1. OD_{600} was monitored during growth. Five of these flasks were pulse-labelled with 100 µl 1 mM [U-^{13}C]-sodium acetate at several time points of their growth curve. These time points were 15 min (lag phase), 1 h (transition lag to logarithmic phase), 2.5 h (logarithmic phase), 4.75 h (transition logarithmic to stationary phase) and 6.5 h (stationary phase) for strain MT1 and 15 min, 1 h, 3 h, 7 h and 9 h for strains MT3 and MT4 to adopt for different growth rates of the strains. 5 ml samples were taken at time points 0 min, 10 min, 30 min, 1h, 3h, 6h and 24h after labelling. After centrifuging the samples at 4600 x g the cell pellets were employed for the fatty acid methyl ester preparation (2.6.1) prior to the IRMS analysis (2.6.5). These experiments were performed twice.

2.5.4.3 Kinetics of Carbon Sharing in a Bacterial Consortium Revealed by Combining Immuno-Staining, FACS and IRMS Techniques

The bacterial consortium consisting of strains MT1, MT2, MT3 and MT4 was grown as a chemostat culture (2.5.3). After adding 500 µl of [U-^{13}C]-4-chlorocatechol (1 mg/ml) via the sampling port 60 ml samples were taken after different time points (0 h, 1 h, 3 h, 6 h, 12 h, 24 h and 48 h). Samples were centrifuged at 6400 x g for 20 min. The pellets were washed with 30 ml PBS and centrifuged again at 6400 x g for 20 min. The supernatants were decanted and the pellets were resuspended in 8 ml 10% sodium azide (w / v) and stored at 4°C for further immuno-staining (2.7.2.1) prior to the cell sorting (2.8.1) and the IRMS analysis (2.6.5) of the prepared fatty acid methyl esters from the separated fractions (2.6.1). These experiments were performed twice.

2.5.4.4 Analysis of the Physiological Status of Individual Members of a Bacterial Consortium

For the analysis of the physiological status of pure cultures of strains MT1, MT2, MT3 and MT4 they were grown at 30°C on 300 ml peptone media or on the minimal medium PMS with 0.2 % sodium acetate (w / v) or 4-chlorosalicylate (0.8 mM) as sole carbon source shaking at 110 rpm. The optical density was monitored during incubation time. Cells were harvested in exponential and stationary phase of growth by centrifuging at 3200 x g for 5 min. The pellets were fixed in 10 ml 10% sodium azide (w / v) and stored at 4°C for further analysis.

For the analysis of the physiological status of the individual members of the bacterial consortium strains MT1, MT2, MT3 and MT4 were grown as a chemostat culture (2.5.3). Due to stability reasons the community was build up strain by strain. After running a continuous culture of strain MT1 the other strains were added one by the other. Samples of 10 ml were taken on a daily base. The OD_{600} was monitored spectrometrically during cultivation. The samples were centrifuged at 4600 x g for 10 min. 1 ml of the decanted supernatant was stored at -20°C for further HPLC analysis (2.6.6). The bacterial pellet was resuspended in 10% sodium azide (w / v) and stored at 4°C for further immuno-staining (2.7.2.2) and flow cytometry analysis (2.8.2).

2.6 Analytical Methods

2.6.1 Preparation of Fatty Acid Methyl Esters (FAMES)

For the saponification of the bacterial fatty acids 40 mg wet cells or bacteria concentrated onto a Durapore membrane filter (2.8.1) were resuspended in 1 ml of solution 1 in a 4 ml glass vial and securely sealed with a teflon lined cap. The suspension was boiled for 1h at 100°C in a heating block.
To methylize the saponificated fatty acids 2 ml of solution 2 was added followed by another heating step at 80°C for 10 min. The reaction was then stored on ice until cooled. For the extraction of the fatty acid methyl esthers (FAMEs) from the aqueous phase 1.5 ml of solution 3 was added. After vigorous vortexing for 30 s the upper organic phase was transferred to a new 4 ml vial. This extraction step was performed twice. To prevent any contamination from the organic phase during gas chromatography analysis 3 ml basic solution 4 was added. After vortexing again for 30 s the organic phase was transferred to a 2 ml crimp top vial. The solvent was evaporated by a gentle stream of N_2. For the gas chromatographic analysis FAMEs were resuspended in octane containing an internal standard of alkanes $C_{24}H_{50}$ and $C_{16}H_{34}$.

2.6.2 Analysis of Amino Acids

For the hydrolyzation of the bacterial proteins to amino acids ca. 100 mg of wet cells were suspended in 2 ml of 6M HCl in a 4 ml glass vial. The sample was hydrolysed for 24h at 100°C in a thermo block. To remove solid particles from the cooled hydrolysate the sample was filtered. The hydrochloric acid was removed by an evaporation step at 80°C with N_2. Remainders were resuspended in 1 ml 60% methanol (v / v) and stored at -20°C until further analysis. 0.5 ml of the sample was transferred to a new 4 ml glass vial and evaporated by a gentle stream of N_2. To the dried remainders 0.4 ml dichloromethan (DCM) were added and evaporated again to remove H_2O from the sample. For the derivatization the amino acids in the sample were esterified with 0.8 ml isopropanol / acetylchloride 5:1(v / v) for 45 min at 100°C.
For the removal of the remaining derivatisation solution the sample was evaporated. Remainders were resuspended in 0.4 ml DCM and again evaporated.

After adding 0.4 ml trifluoroacetic acid / DCM 1:1 (v/v) the sample was heated at 100℃ for 15 min. The mixture of trifluoroacetic acid/DCM was evaporated on ice by a gentle stream of N_2. For the gas chromatographic analysis the remainders were resuspended in 0.2 ml ethylacetate.

2.6.3 Gas Chromatography (GC)

The extracted fatty acid methyl esters and amino acid derivates were analysed by employing the Hewlett Packard 6890 gas chromatograph equipped with an Optima 5 capillary column (50 m by 0.32 mm; film thickness 0.35 µm) and a Flame Ionization Detector (FID). Hydrogen served as the carrier gas. For FAMEs and amino acid derivatives analysis the injector temperature was set to 250 ℃ and detector temperature was 300 ℃. The oven program for the FAMEs analysis was 100 ℃ for 2 min, subsequently increasing the temperature to 290 ℃ at 4℃/ min. An isothermal period of 14 min followed the heating steps.
The oven program for the amino acid derivatives was 60 ℃ for 2 min, subsequently increasing the temperature to 170 ℃ at 3℃/ min. The temperature was then increased up to 288℃ with heating steps of 10℃/ min. An isothermal period of 6 min followed the heating steps. The temperature was then lowered to 100℃ for an isothermal period of 30 min.

2.6.4 Elemental Analysis-Isotope Ratio Mass Spectrometry (EA/IRMS)

20-100 µl of bacterial suspensions were applied to tin cups and dried at 80℃ until samples were anhydrous. In the elemental analyser the samples were burned at a temperature of 1020℃. The thereby emerging gases were led by a stream of helium to the oxidation column filled with chromium oxide and silver plated cobalt oxide of the elemental analyser. Here, the gases were oxidised to CO_2 and NO_x. In the reduction column packed with copper oxide and copper the NO_x was reduced to N_2. H_2O was then removed by a water trap. The gases were led to a gas chromatograph coupled to the elemental analyser to separate CO_2 and N_2. After entering the Isotope Ratio Mass Spectrometer (IRMS) via a ConFlo II System the gases were ionised and

deflected in the magnetic field of the IRMS due to their masses resulting from different isotope content. Deflected ions were detected in Faraday cups.
NBS 22 with a $\delta^{13}C$ value of 29.74 ± 0.12‰ (International Atomic Energy Agency, Vienna/Austria) served as a standard in this study. Data were analysed by using the Isodat software (Finnigan MAT, Bremen).

2.6.5 Gas Chromatography-Isotope Ratio Mass Spectrometry (GC-IRMS)

The IRMS analysis of the FAMEs and the amino acid derivatives was performed by a Hewlett Packard 5890 Series II gas chromatograph using the conditions described before (see 2.6.3) for those substances but here helium served as the carrier gas. The gas chromatograph was coupled via a combustion interface to a MAT 252 isotope ratio mass spectrometer. In the oxidation oven of the combustion interface the gas chromatographically separated FAMEs respectively amino acid derivatives were combusted at 980℃ to CO_2, H_2O and NO_x. The gases were led to the reduction oven were NO_x was reduced to N_2 followed by ionisation of the gases by an electron impact source. The helium carrier stream led the ionised compounds to the IRMS. In the electric field of the magnet of the spectrometer the CO_2 was deflected due to its different masses resulting from different isotope contents of the gas and separately detected in Faraday cups. Data were analysed by using the Isodat software (Finnigan MAT, Bremen). The calucalation of the $\delta^{13}C$ values of the samples was carries out by applying equation 1:

Equation 1:

$$\delta^{13}C(‰) = \left(\frac{R_{Sample}}{R_{Standard}} - 1 \right) \times 1000$$

R_{Sample}: Isotopic ratio of the sample

$R_{Standard}$: Isotopic ratio of the standard (Pee Dee Belemnite)

The incorporation is modelled assuming pseudo-first-order kinetics which is valid because only small amounts of labelled acetate were added in the experiments and therefore, the substrate is not the limiting factor.

Due to the methylation of the fatty acids as additional carbon atom is introduced to the resulting FAME which could be detected by mass spectrometry ($\delta^{13}C_{FAME}$). For the calculation of the $\delta^{13}C$ value of the original fatty acid a mass balance was employed (Goodman, 1992):

$$\delta^{13}C_{FA} = \frac{(C_{FAME} \times \delta^{13}C_{FAME}) - (C_{ME} \times \delta^{13}C_{ME})}{C_{FA}}$$

$\delta^{13}C_{FA}$:	$\delta^{13}C$ value of the fatty acid
$\delta^{13}C_{FAME}$:	$\delta^{13}C$ value of the FAME
$\delta^{13}C_{ME}$:	$\delta^{13}C$ value of the methyl group
C_{FA}:	Numbers of carbon atoms of the fatty acid
C_{FAME}:	Numbers of carbon atoms of the FAME
C_{ME}:	Numbers of carbon atoms of the methyl group

2.6.5.1 Calculation of the Fitting Curves

The obtained $\delta^{13}C$ values of the samples were plotted versus time. The kinetics of the substrate incorporations were calculated with the program Sigmaplot 7.1(SPSS, Inc., USA) using the law of first order kinetics based on the isotope ratios of the unlabelled fatty acids:

Equation 2:

$$\delta^{13}C = \delta^{13}C_{t=0} + \mathbf{a}\,(1 - e^{-\mathbf{b}t})$$

$\Delta\,\delta^{13}C$:	$\delta^{13}C - \delta^{13}C_{t=0} = \mathbf{a}\,(1 - e^{-\mathbf{b}t})$
$\delta^{13}C$:	measured $\delta^{13}C$ at time t
$\delta^{13}C_{t=0}$:	measured $\delta^{13}C$ at time t=0
a:	asymptote (maximal incorporation)
b:	rate constant of substrate incorporation
t:	time [h]

The constants **a** and **b** were calculated by minimising the square sum of the difference between measurements and calculations. The constants were independently determined for each experiment and their means were calculated for each time point.

2.6.5.2 Calculation of the $\delta^{13}C$ Values of the Amino Acid Derivatives

For the calculation of the $\delta^{13}C$ values of amino acid derivatives a correction of the $\delta^{13}C$ values is required due to their trifuoroacetate and isopropyl moieties (equation 3 and 4; Abraham, 2003).

Equation 3:

$$\delta^{13}C_{AA} = (\delta^{13}C_{DAA}\,(n_{AA}+x n_{iso}+y n_{TFA}) - \delta^{13}C_{korr}\,(x n_{iso}+y n_{TFA})) / n_{AA}$$

Equation 4:

$$\delta^{13}C_{korr} = (\delta^{13}C_{DAA}\,(n_{AA}+x n_{iso}+ y n_{TFA}) - \delta^{13}C_{AA} n_{AA}) / (x n_{iso}+y n_{TFA})$$

$\delta^{13}C_{AA}$: $\delta^{13}C$ of amino acid
n_{AA} : number of carbons in the amino acid
n_{iso} : number of carbons in isopropyl = 3
n_{TFA} : number of carbons in trifluoroacetic acid = 2
x : number of isopropyls in amino acid derivative
y : number of trifluoroacetates in amino acid derivative
$\delta^{13}C_{DAA}$: $\delta^{13}C$ of amino acid derivative

2.6.6 Reversed Phase-High Performance Liquid Chromatography (RP-HPLC)

The analysis of the metabolites resulting from the degradation of the 4-chlorosalicylate by the bacterial consortium was carried out by Reversed Phase-High Performance Liquid Chromatography (RP-HPLC).

This technique operated on the principle of hydrophobic interactions resulting from repulsive forces between a relatively polar solvent methanol, the relatively non-polar metabolites and the non-polar stationary phase - a silica which has been covered with a straight chain alkyl group. A UV/VIS Photodiode-Array-Detector recorded the chromatogram as a function of retention time, wave length and absorption.

Therefore, 50 µl of the supernatant of the chemostat culture were injected to a Waters Alliance 2695 Separation Module. The system was equipped with a Nucleosil 100-3 C18 reversed phase column (Macherey-Nagel, Düren/Germany). Methanol-H_2O containing 0.1% (v/v) H_3PO_4 was used as eluent at a flow rate of 0.25 ml/ min. The concentration of methanol increased from initially 20% up to 80%. The column effluent was monitored at 260 nm by a Waters 996 UV/VIS Photodiode-Array-Detector (Eschborn/Germany). Data were analysed by using the Empower 2 software (Waters, Eschborn/Germany)

2.7 Immuno-Staining Techniques

2.7.1 Antibodies

For the immunodetection of individual members of the bacterial community consisting of strains MT1, MT2, MT3 and MT4 indirect immunofluorescence was employed. Therefore, the individual strain within the community was labelled with a strain specific primary antibody reacting against the surface of the bacteria. The immunodetection resulted from the binding of the fluorescence-conjugated secondary antibody which binds to its IgG heavy chains and all classes of immunoglobulin light chains. For the immunochemical labelling of the individual members of the bacterial consortium primary poly-and monoclonal antibodies shown in Table 2.6 and 2.7 were employed.

Table 2.6: Polyclonal antibodies used for indirect immunostaining

Polyclonal Antibodies		
Strain	**Taxonomy**	**Antibody**
MT1	Pseudomonas reinekei	#200
MT2	Wautersiella falsenii	#201
MT3	Achromobacter xylosoxidans	#202
MT4	Pseudomonas veronii	#170

Table 2.7: Monoclonal antibodies used for indirect immunostaining

Monoclonal Antibodies		
Strain	**Taxonomy**	**Antibody**
MT1	Pseudomonas reinekei	3G8
MT3	Achromobacter xylosoxidans	1A3

The polyclonal sera against the individual members of the community were produced by Tesar and colleagues (Faude, 1996; Frech, 1996; Tesar et al., 1996). The monoclonal antibodies reacting against outer membrane proteins of the individual members were assembled by Faude and Tesar et al. (Faude, 1996; Tesar et al., 1996). The immunodetection of the primary antibody labeled bacteria was carried out with the secondary antibodies shown in Table 2.8.

Table 2.8: Secondary antibodies used for indirect immunostaining

	Secondary Antibodies	
Antibody	**Fluorescence Dye**	**Host**
anti-mouse IgG+IgM DTAF	Dichlorotriazinylamino-Fluorescein	Goat
anti-rabbit IgG alexa635	Alexa Fluor 635	Goat

2.7.2 Analysis Dependent Immunostaining of Bacteria

2.7.2.1 Analysis of the Physiological Status of Individual Members of a Bacterial Consortium

To obtain DNA patterns corresponding to the physiological status of the bacteria FACS analysis were performed with fixed cells harvested in exponential and stationary phase of growth (2.5.4.4). Cells were centrifuged at 5900 rpm for 5 min and washed with PBS. After resuspending the cells in PBS up to a concentration of 3 x 10^8 cells/ ml the suspension was DAPI –stained according to the modified protocol. Therefore, 2 ml of the diluted cell suspension were incubated with 1 ml solution A for 10 min, washed and resuspended in 2 ml solution B. After incubating for at least 20 min in the dark at room temperature the suspension was analysed by flow cytometry. For the analysis of the DNA patterns of the bacterial community consisting of strains MT1, MT2, MT3 and MT4 the DAPI-stained solution was counterstained with 2.5 µl of the polyclonal strain-specific antibodies (Table 2.6) for 1 h. The solution was then incubated with 1.5 µl of the alexa635-conjugated secondary antibody (Table 2.8) for 1 h in the dark and analysed by flow cytometry.

2.7.2.2 Kinetics of Carbon Sharing in a Bacterial Consortium Revealed by Combining Immunochemical, FACS and IRMS Techniques

For the Fluorescence Activated Cell Sorting (FACS) of the [U-^{13}C]-labelled bacterial consortium (2.5.4.3) 2 ml of the 10% sodium azide fixed cell suspension was incubated for 1 h with 340 µl of the primary mouse antibody 3G8 reacting against strain MT1 or 340 µl 1A3 reacting against strain MT3. For the immunodetection of the antibody–bound cells 10 µl of the DTAF-conjugated secondary antibody reacting against the IgG heavy chains and all classes of immunoglobulin light chains from mouse were added to the suspension and incubated for 1 h in the dark. For the FACS analysis the cell suspension was diluted with 4 ml sterile filtered PBS and incubated with 100 µl DAPI (4',6-diamidino-2-phenylindole, dilactate, 1 µg/ ml), a DNA-intercalating fluorescence dye, for 5 min. This staining allowed the detection of all cells by the cytometer.

2.8 Analysis Dependent Flow Cytometry

2.8.1 Analysis of the Physiological Status of Individual Members of a Bacterial Consortium

Flow cytometric measurements were carried out by using a MoFlo cell sorter (DakoCytomation, Fort Collins, USA) equipped with two water-cooled argon-ion lasers (Innova 90C and Innova 70C from Coherent, Santa Clara, USA). Excitation of 580 mW at 488 nm was used to analyse the forward scatter (FSC) and side scatter (SSC) as a trigger signal at the first observation point. DAPI was excited by 180 mW of ML-UV (333-365 nm) at the second observation point.

The orthogonal signal was first reflected by a beam-splitter and then recorded after reflection by a 555 nm long-pass dichroic mirror, passage by a 505 nm short-pass dichroic mirror and a bandpass filter at 488 nm with a bandwidth of 10 (BP-488/10). DAPI fluorescence was passed through a 450/65 band pass filter, green fluorescence through BP- 520/15 and, red fluorescence through BP-620/45.

Photomultiplier tubes were obtained from Hamamatsu Photonics (models R 928 and R 3896; Hamamatsu City). Amplification was carried out at linear or logarithmic

scales, depending on the application. Fluorescent beads (Polybead Microspheres: diameter, 0.483 µm; flow check BB/Green compensation Kit, Polyscience, USA) were used to align the MoFlo. Also, an internal DAPI-stained bacterial cell standard was introduced for tuning the device up to a CV value not higher than 6%.

2.8.2 Kinetics of Carbon Sharing in a Bacterial Consortium Revealed by Combining Immunochemical, FACS and IRMS Techniques

For the separation of the immuno-stained cells from the residuary bacterial community (2.7.2.2) Fluorescence Activated Cell Sorting (FACS) was employed. The analysis was performed by using the FACSAria^{TM} Cell-Sorting System, data analysis was performed by the FACSDiva^{TM} software (BD Bioscience, Heidelberg, Germany). Appropriate gates were set to distinguish the immuno-stained cells from the residuary bacterial community.

The separated bacterial fractions were concentrated by filtration onto hydrophilic Durapore membrane filters (pore size 0.22µm, Millipore,Schwalbach, Germany). The filters were then used for the direct preparation of the fatty acid methyl esters.

3. Results

3.1 Phylogenetic Analysis of the 4-Chlorosalicylate Degrading Community

The consortium, consisting of four bacterial strains, was initially isolated (Faude, 1996) from the sediment of the creek Spittelwasser in Bitterfeld, Germany. By sequencing the 16S ribosomal RNA genes of the four isolated strains it revealed that the community was composed of bacterial strains of the genera Pseudomonas, Achromobacter and Wautersiella. Former studies of the bacterial consortium (Pelz, 1999; Tillmann, 2004) identified its members by sequencing their 16S rRNA genes. Those sequences were compared to the database of the National Centre for Biotechnology Information. The four community members showed the highest homology towards following bacterial strains: *Pseudomonas putida* MT1, *Empedobacter brevis* MT2, *Achromobacter spanius* MT3 and *Pseudomonas veronii* MT4. Due to the continuous expansion of the sequence database of the National Center of Biotechnology Information the sequences of the four bacterial members of the 4-chlorasalicylate degrading consortium were recently compared within this thesis to those stored in the database. This analysis revealed changes towards the highest homology of strains MT1, MT2 and MT3 to the database reference strains. Strain MT1 showed the highest homology towards strain *Pseudomonas reinekei* (Camara, 2007), strain MT2 towards *Wautersiella falsenii* (Kämpfer, 2006) and strain MT3 showed the highest homology towards the 16S rRNA gene of strain *Achromobacter spanius* (Coenye, 2003). The sequence analysis of strain MT4 still revealed the highest homology towards *Pseudomonas veronii* (Table 3.1).

Table 3.1: Analysis of the 16S rRNA gene sequence homology of the consortium members

Base Pairs	Homology (%)	Greatest Homology (Type strain)
1495	99	*Pseudomonas reinekei* (AM293565)
1441	98	*Wautersiella falsenii* (AM084341)
1454	99	*Achromobacter spanius* (AY170848)
1449	99	*Pseudomonas veronii* (AF064460)

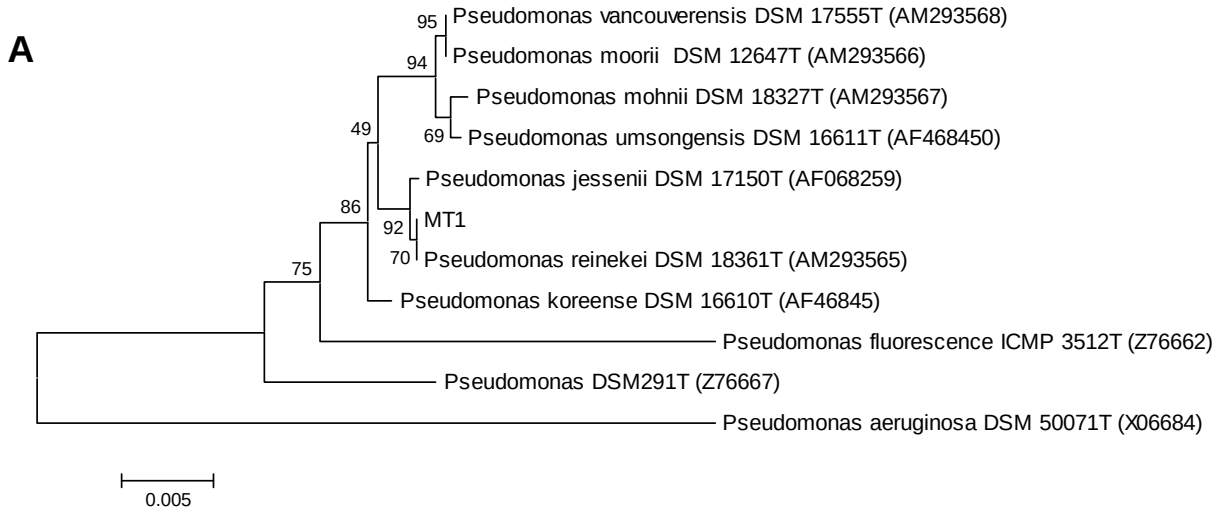
A
95
Pseudomonas vancouverensis DSM 17555T (AM293568)
94
Pseudomonas moorii DSM 12647T (AM293566)
Pseudomonas mohnii DSM 18327T (AM293567)
49
69
Pseudomonas umsongensis DSM 16611T (AF468450)
Pseudomonas jessenii DSM 17150T (AF068259)
86
92
MT1
70
Pseudomonas reinekei DSM 18361T (AM293565)
75
Pseudomonas koreense DSM 16610T (AF46845)
Pseudomonas fluorescence ICMP 3512T (Z76662)
Pseudomonas DSM291T (Z76667)
Pseudomonas aeruginosa DSM 50071T (X06684)
0.005

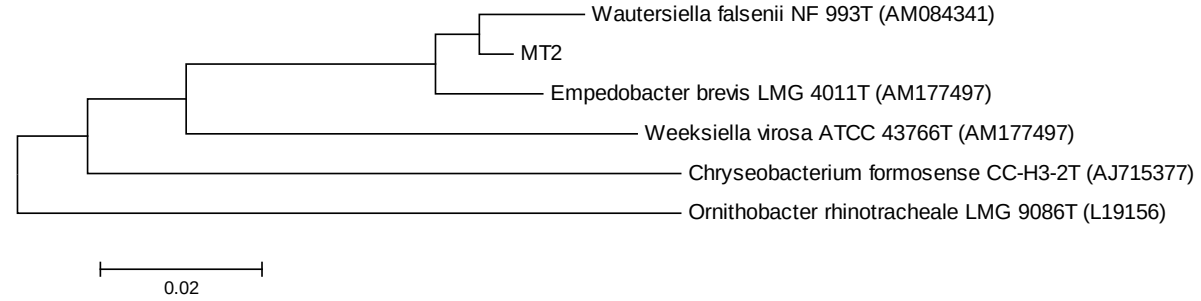
B
Wautersiella falsenii NF 993T (AM084341)
MT2
Empedobacter brevis LMG 4011T (AM177497)
Weeksiella virosa ATCC 43766T (AM177497)
Chryseobacterium formosense CC-H3-2T (AJ715377)
Ornithobacter rhinotracheale LMG 9086T (L19156)
0.02

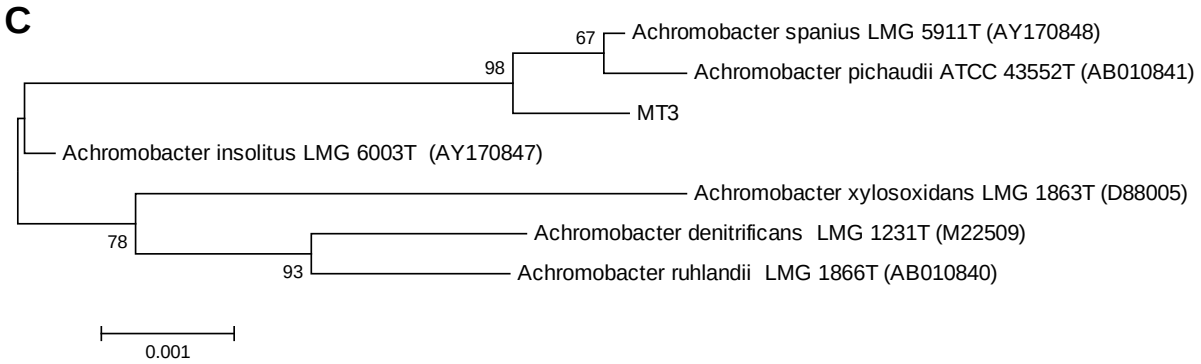
C
67
Achromobacter spanius LMG 5911T (AY170848)
98
Achromobacter pichaudii ATCC 43552T (AB010841)
MT3
Achromobacter insolitus LMG 6003T (AY170847)
Achromobacter xylosoxidans LMG 1863T (D88005)
78
Achromobacter denitrificans LMG 1231T (M22509)
93
Achromobacter ruhlandii LMG 1866T (AB010840)
0.001

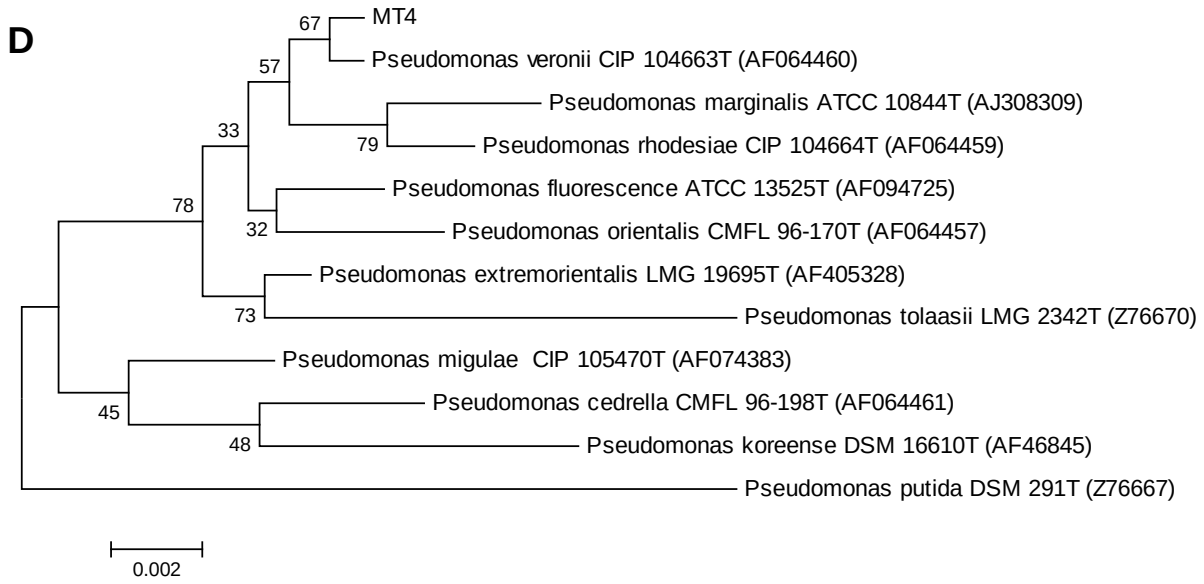

Fig. 3.1: Phylogenetic classification of the isolated members of the 4-chlorosalicylate degrading consortium. **A** Phylogenetic classification of strain MT1. Bar, 0,5% sequence dissimilarity. **B** Phylogenetic classification of strain MT2. Bar, 1% sequence dissimilarity. **C** Phylogenetic classification of strain MT3. Bar, 0,1% sequence dissimilarity. **D** Phylogenetic classification of strain MT4. Bar, 0.2% sequence dissimilarity.

3.2 Temperature Dependency of Carbon and Nitrogen Fractionation in *Pseudomonas*

The dependency of the carbon and nitrogen fractionation towards the growth temperature was tested in two *Pseudomonas* strains, *P. reinekei* MT1 and *P. veronii* MT4. Therefore, cells were harvested in exponential phase of growth at different temperatures on minimal medium supplemented with 5 mM sodium acetate as sole carbon source. For the analysis of the growth temperature influence towards bacteria, cells of both strains were deployed for the analysis of the isotopic ratio of whole cells, the isotopic ratio of extracted amino and fatty acids and the dependency of the growth temperature on the percentage distribution of the bacterial amino and fatty acids.

3.2.1 µ Values of Strains MT1 and MT4

The comparison of the growth rates µ calculated from the optical density values at 600 nm in exponential phase of growth revealed the optimal growth temperature between 30℃ and 37℃ for strain *Pseudomonas reinekei* MT1 and a temperature ranging between 25° and 30℃ for *Pseudomonas veronii* MT4 (Fig 3.2).

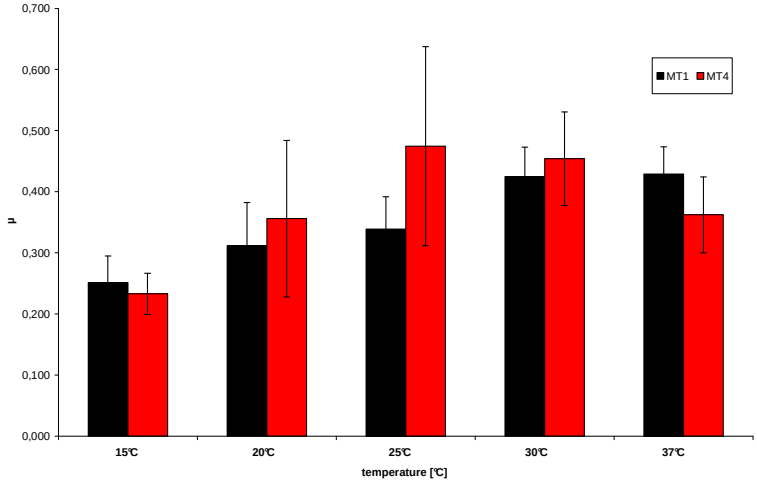

Fig. 3.2: Analysis of the optimal growth temperature. µ values from strains MT1 (black bars) and MT4 (red bars) were obtained from cells of both strains grown at different temperature.

3.2.3 Analysis of the Carbon and Nitrogen Fractionation by EA/C/IRMS

The analysis of the carbon and nitrogen fractionation by EA/C/IRMS of bacterial biomass harvested in exponential phase of growth of strains *Pseudomonas reinekei* MT1 and *Pseudomonas veronii* MT4 revealed no dependency on the optimal growth temperature for strain MT1 (Fig. 3.3). The measurements showed no clear tendency for dependence on the growth temperature. The $\delta^{15}N$ values of MT1 cells grown at 30℃ showed a slight depletion of the heavier isotope. When grown at 15℃ or 25℃ cells of this strain revealed a slight enrichment of the heavier isotope ^{15}N. The $\delta^{13}C$ values of strain MT1 showed no dependency on the growth temperature. The obtained $\delta^{13}C$ values from MT1 cells grown at 25℃ revealed an enrichment of the heavier isotope. A slight enrichment in ^{12}C could be seen in the $\delta^{13}C$ values of cells grown at 15℃.

The $\delta^{15}N$ and $\delta^{13}C$ values of MT4 cells revealed an enrichment of the heavier isotopes when grown at 25℃, the optimal growth tem perature of this strain. A slight depletion of ^{12}C and respectively ^{14}N could be found in MT4 cells grown at 20° and 30℃ and even higher in cells grown at 15° and 37℃ .

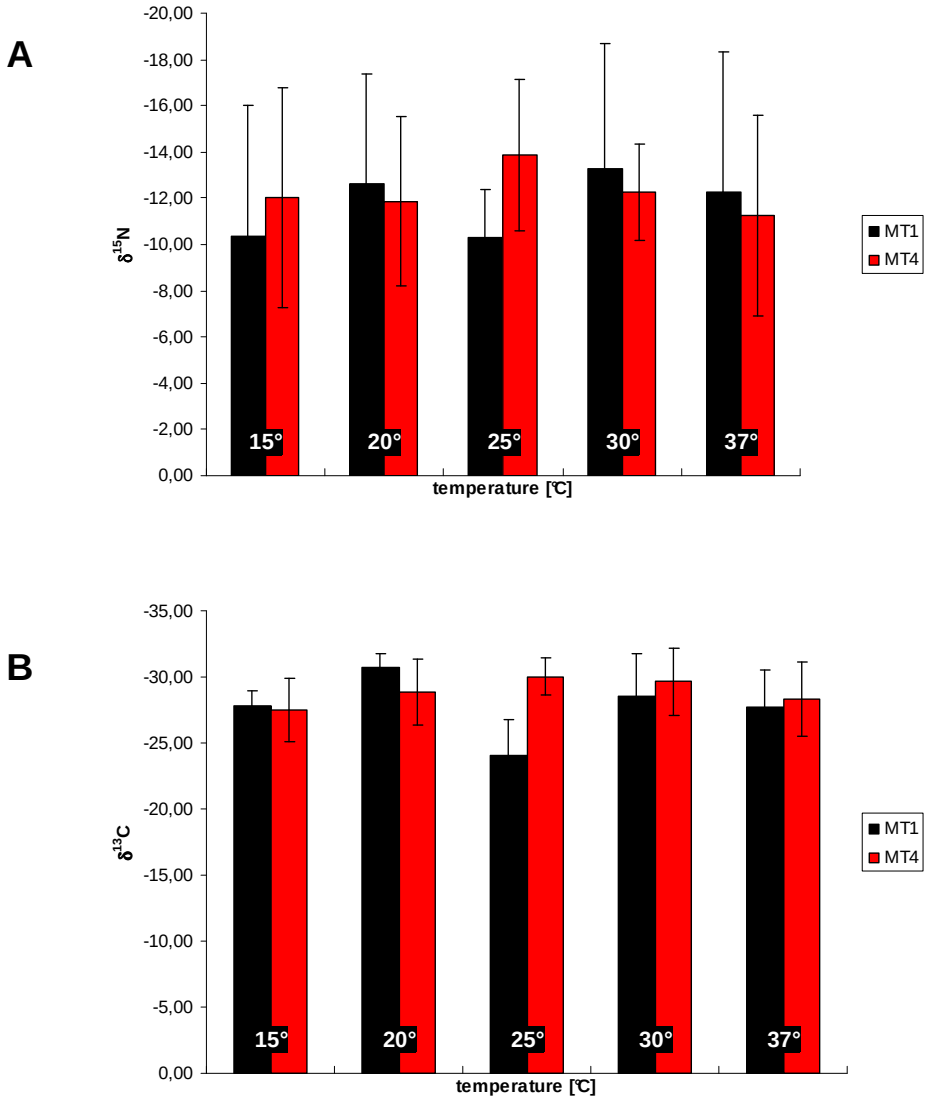

Fig. 3.3: Analysis of the carbon fractionation by EA/C/IRMS. **A** Cells in exponential phase of growth at different temperatures of strains MT1 (black bars) and MT4 (red bars) were analysed for their $\delta^{15}N$ value **B** Cells in exponential phase of growth at different temperatures of strains MT1 (black bars) and MT4 (red bars) were analysed for their $\delta^{13}C$ values

3.2.4 Carbon Fractionation of the Bacterial Amino Acids

The carbon fractionation in the amino acids extracted from strains *Pseudomonas reinekei* MT1 and *Pseudomonas veronii* MT4 in exponential phase of growth revealed significant differences depending on the strain and the growth temperature. The most obvious difference in the measured isotopic ratios can be found in the amino acids alanine, serine and glycine in both strains (Fig. 3.4).

The $\delta^{13}C$ value of the amino acid alanine of strain MT4 showed an increasing enrichment of the lighter isotope towards rising growth temperature, while the $\delta^{13}C$ value of this amino acid in strain MT1 remained on a constant level up to a growth temperature of 30°C, a significant enrichment of ^{13}C could only be found in cells growing at 37°C.

A clear dependency on the growth temperature in the carbon fractionation in the amino acids could be found for serine in both strains. The MT1 $\delta^{13}C$ values showed a tremendous enrichment in the heavier isotope when grown at temperatures between 15° and 25°C and at 37°C. At a growth temperature of 30°C the MT1 $\delta^{13}C$ value revealed a high depletion in the heavier isotope, it descended from -8.1 ‰ at 25°C to -28.3 ‰ at 30°C. A similar development of the $\delta^{13}C$ values of serine could be shown in strain MT4. The amount of ^{13}C depleted rapidly, reflected by decreasing $\delta^{13}C$ value in the growth temperature range of 15°-25°C. The rising $\delta^{13}C$ values of the amino acid serine in strain MT1 grown at 30° and 37°C indicated an enrichment of the lighter isotope at those temperatures.

In comparison to the $\delta^{13}C$ values of the residual amino acids, glycine showed significantly higher $\delta^{13}C$ values in both strains, MT1 and MT4. Those values ranged between -6.6 ‰ and -14.8 ‰ for strain MT1 and -10.5 ‰ and -16.1 ‰ for MT4. The $\delta^{13}C$ value of glycine from MT1 showed enrichment in ^{13}C when grown at 15°C. Grown at temperatures of 20° and 37°C a depletion of the heavier isotope could be revealed in strain MT1. When grown at temperatures of 25° and 30°C a clear enrichment of ^{13}C in the stable isotope ratios of glycine could be seen.

In general the analysis of the carbon fractionation in amino acids extracted from two bacterial strains grown at different temperatures showed a dependency on this parameter, although this study revealed no dependency on the optimal growth temperature in those strains. The $\delta^{13}C$ values of all extracted amino acid derivatives from strains MT1 and MT4 can be found in Table 3.2.

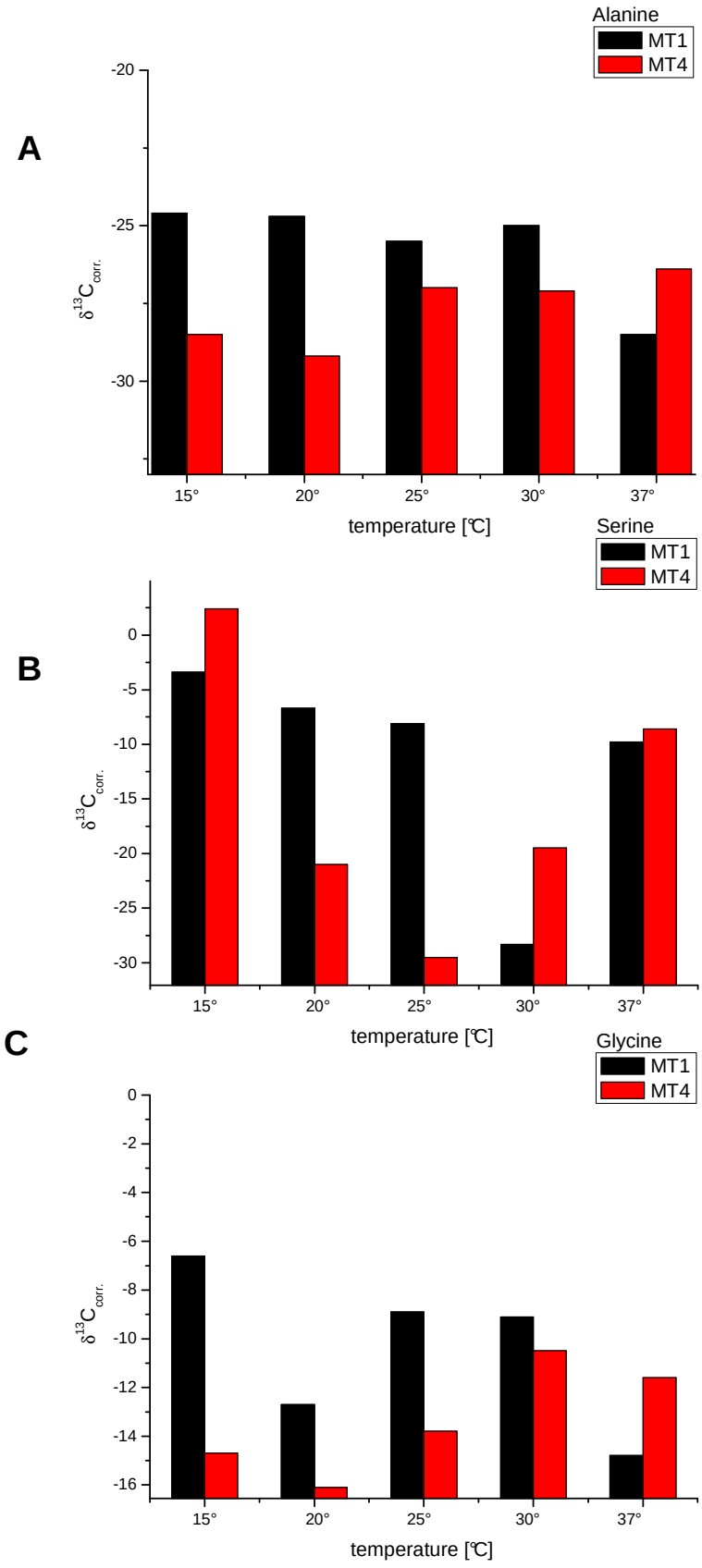

Fig. 3.4: Carbon fractionation of the bacterial amino acids. $\delta^{13}C$ values of the amino acid **A** alanine, **B** serine and **C** glycine extracted from cell of strains MT1 (black bars) and MT4 (red bars) grown at different temperatures.

Table 3.2: Carbon fractionation of the amino acids ($\delta^{13}C$ [‰])

MT1	15°C	20°C	25°C	30°C	37°C
Alanine	-24,6	-24,7	-25,5	-25,0	-28,5
Glycine	-6,6	-12,7	-8,9	-9,1	-14,8
Threonine	-23,1	-25,4	-27,2	-24,6	-12,2
Valine	-29,9	-26,4	-31,2	-34,6	-34,5
Serine	-3,4	-6,7	-8,1	-28,3	-9,8
Leucine	-35,7	-34,8	-36,1	-33,5	-36,5
Isoleucine	-27,3	-27,9	-32,3	-34,0	-31,6
Proline	-26,0	-22,7	-24,8	-22,3	-24,2
Aspartic Acid	-32,0	-29,8	-31,5	-29,8	-32,2
Glutamic Acid	-36,7	-25,8	-28,0	-37,5	-27,1
Phenylalanine	-34,9	-33,9	-41,1	-32,2	-41,4
Lysine	-34,0	-30,1	-33,6	-31,2	-28,5

MT4	15°C	20°C	25°C	30°C	37°C
Alanine	-28,5	-29,2	-27,0	-27,1	-26,4
Glycine	-14,7	-16,1	-13,8	-10,5	-11,6
Threonine	-28,6	-31,6	-32,5	-26,7	-29,3
Valine	-37,0	-31,1	-40,1	-40,0	-32,4
Serine	2,4	-21,0	-29,5	-19,5	-8,6
Leucine	-37,0	-39,3	-38,8	-37,0	-36,7
Isoleucine	-23,6	-27,5	-33,3	-36,3	-29,5
Proline	-23,5	-26,6	-25,4	-21,4	-23,4
Aspartic Acid	-29,6	-33,6	-31,6	-31,4	-31,6
Glutamic Acid	-25,7	-36,5	-37,9	-38,3	-33,0
Phenylalanine	-39,2	-35,3	-32,3	-32,0	-34,3
Lysine	-31,9	-28,1	-34,8	-24,5	-28,0

3.2.5 Dependency of the Growth Temperature on the Percentage of the Bacterial Amino Acids

The analysis of the percentage consistency of the extracted amino acid derivatives from strains *Pseudomonas reinekei* MT1 and *Pseudomonas veronii* MT4 harvested in proliferation phase revealed similar distribution patterns. Glutamic acid, aspartic acid, leucine and alanine turned out to be the most abundant amino acids in both strains. A dependency of the percentage distribution on the growth temperature could be found in many amino acids of both strains. The content of serine in the cells of MT1 and MT4 increased towards rising growth temperatures, likewise the percentage of leucine and alanine. In contrast, the ratio of aspartic acid decreased in MT1 when grown at higher temperature, equally to the content of glutamic acid in this strain, whereas the percentage of those amino acids in strain MT4 did not change at rising temperatures. Likewise in strain MT1 the percentage of lysine and threonine in MT4 increased slightly when cells were grown at higher temperatures. In both strains the content of glycine, valine, isoleucine, proline and phenylalanine remained on a constant level when cells were grown at different temperatures. A variation in the growth temperature dependency on the amino acid percentage could be found in the content of tyrosine. In strain MtT1 the percentage increased with rising temperature while in strain MT4 the content decreased (Fig 3.5).

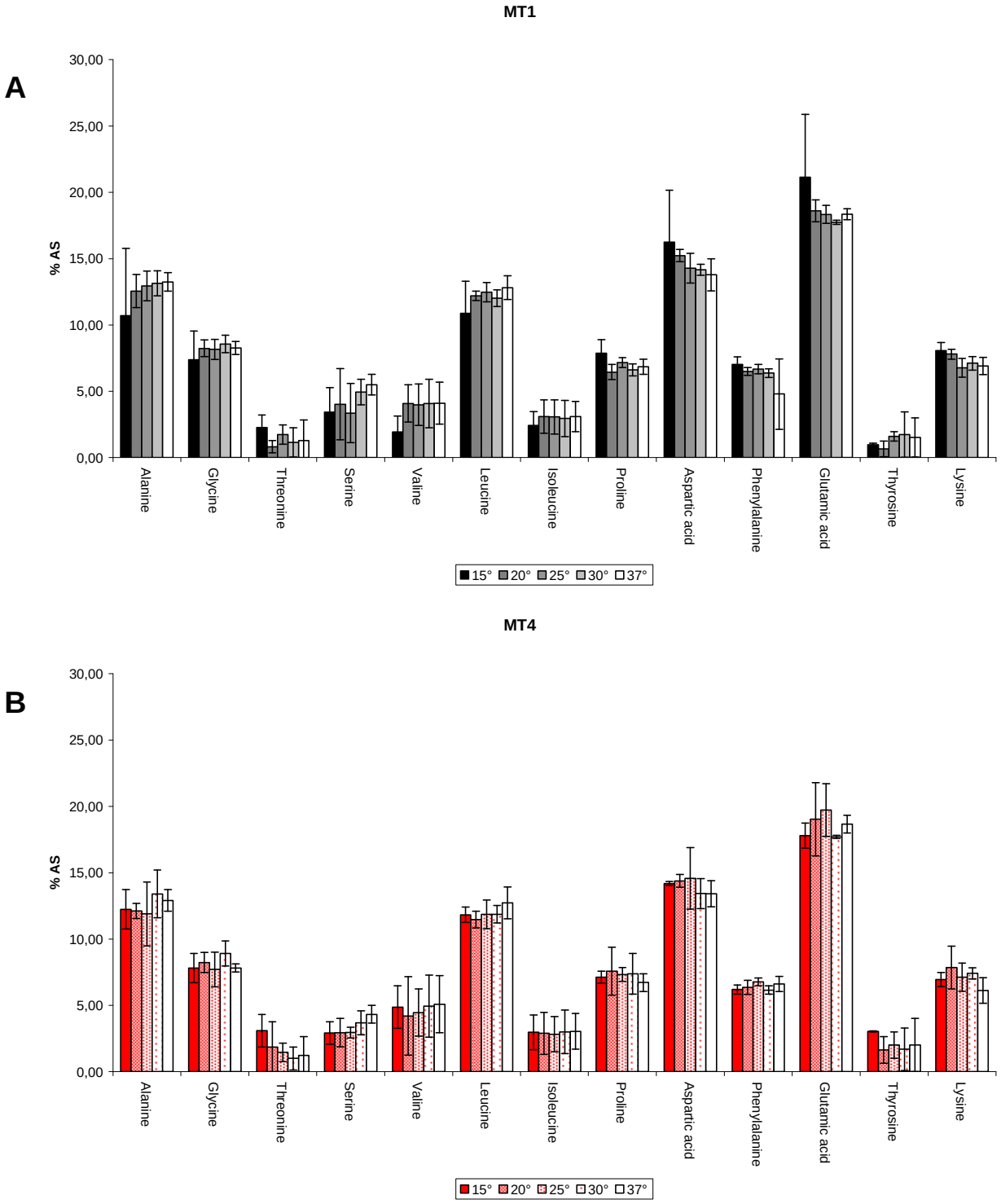

Fig. 3.5: Percentage of the bacterial amino acids. Percentage of the extracted amino acids from **A** strain MT1 and **B** strain MT4 grown at different temperatures.

3.2.6 Dependency of the Growth Temperature Percentage of Bacterial Fatty Acids

The influence of the growth temperature on the consistency of the fatty acids extracted from the bacterial strains *Pseudomonas reinekei* MT1 and *Pseudomonas veronii* MT4 in exponential growth phase was dissected in this part of the thesis. Those strains showed similar trends concerning the proportions of their fatty acids when grown on increasing temperatures.

In both strains the percentage of the fatty acid $C_{16:1}\omega7c$ decreased with increasing growth temperature from 15° up to 37°C. Meanwhile, the proportion of fatty acid $C_{16:0}$ increased in both strains regarding to rising growth temperature. The proportion of the cyclic fatty acid cyclo-$C_{17:0}$d7,8 increased in both strains when cells were grown on higher temperatures. In both strains, the percentage of the fatty acid $C_{18:1}\omega7c$ decreased with rising growth temperature.

In strain MT1 the consistency of the fatty acids is rather similar when cells were grown at different temperatures, only from cells that were grown at 37°C two additional fatty acids could be extracted, $C_{18:0}$ and 2-OH-$C_{12:0}$. Those fatty acids were abundant in the in all samples extracted from strain MT4. The proportion of the fatty acid cyclo-$C_{19:0}$d8,9, only present in strain MT4, was very low and decreased with rising growth temperature. The fatty acid $C_{18:1}\omega7t$ could only be found in MT4 cells grown at 15°C, fatty acid $C_{18:0}$ was very low abundant in cells grown at 20°, 30° and 37°C (Fig. 3.6).

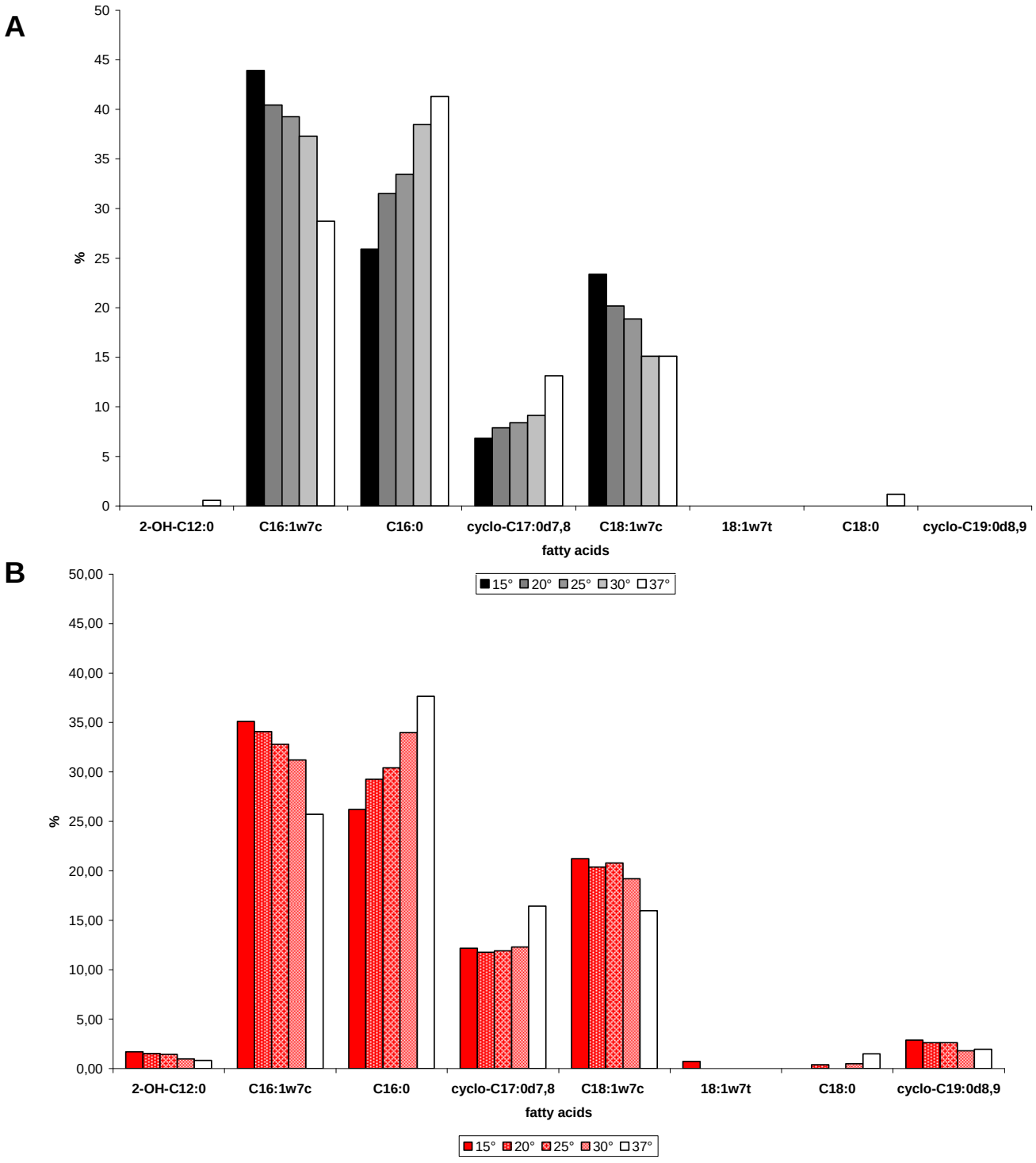

Fig. 3.6: Percentage of the bacterial fatty acids. Percentage of the extracted fatty acids from **A** strain MT1 and **B** strain MT4 grown at different temperatures.

3.2.7 Carbon Fractionation of the Bacterial Fatty Acids

The $\delta^{13}C$ values of the extracted fatty acids from cells of *Pseudomonas reinekei* MT1 and *Pseudomonas veronii* MT4 harvested in the logarithmic phase of growth were analysed for the dependency on the growth temperature on the carbon fractionation. With rising growth temperature an enrichment of the heavier isotope resulting in lower $\delta^{13}C$ values could be shown in literally all extracted straight chain fatty acids of strains MT1 and MT4 except the cyclic fatty acids cyclo-$C_{17:0}$d7,8 and cyclo-$C_{19:0}$d8,9. For both strains, no significant change of the isotopic ratio of fatty acid cyclo-$C_{17:0}$d7,8 could be monitored at different growth temperatures (Fig.3.7). The $\delta^{13}C$ values of the fatty acid $C_{16:0}$ showed a clear dependence on the growth temperature, in both strains, MT1 and MT4, resulting in a higher depletion of the lighter isotope with rising growth temperature. The same trend in both strains followed the fatty acid $C_{16:1}\omega7c$ which is synthesised from fatty acid $C_{16:0}$ by the introduction of a double bound. (Fig.3.7). The $\delta^{13}C$ values of fatty acid $C_{16:1}\omega5c$, which could - due to its low abundance - only be detected by GC-IRMS analysis, revealed in both strains MT1 and MT4 no dependency on the growth temperature, although it is likewise the fatty acid $C_{16:1}\omega7c$ synthesised from $C_{16:0}$ (Table 3.3). Due to the low abundance of the fatty acid $C_{18:0}$ in strain MT1 no significant isotopic ratio could be obtained. The $\delta^{13}C$ values of its resulting fatty acid $C_{18:1}\omega7c$ revealed an increasing tendency towards rising growth temperature. The same characteristics can be seen in the $\delta^{13}C$ values of strain MT4 for this fatty acid.

A

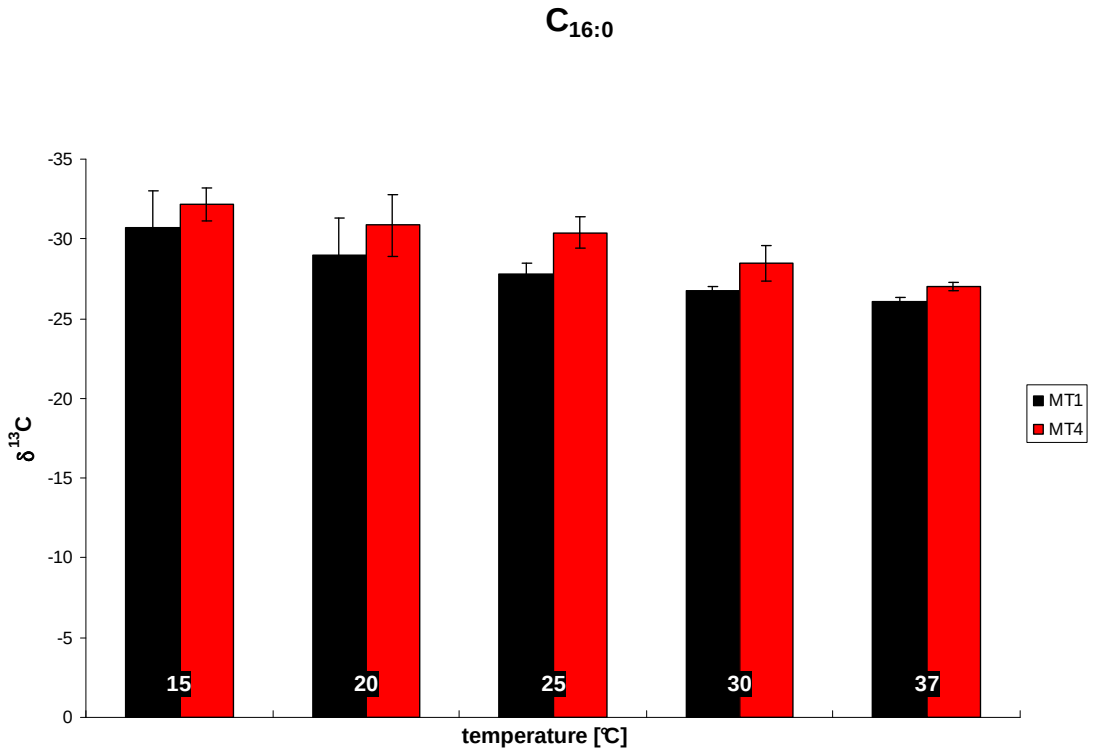
C16:0
-35
-30
-25
-20
-15
-10
-5
0
δ13C
15
20
25
30
37
temperature [℃]
MT1
MT4

B

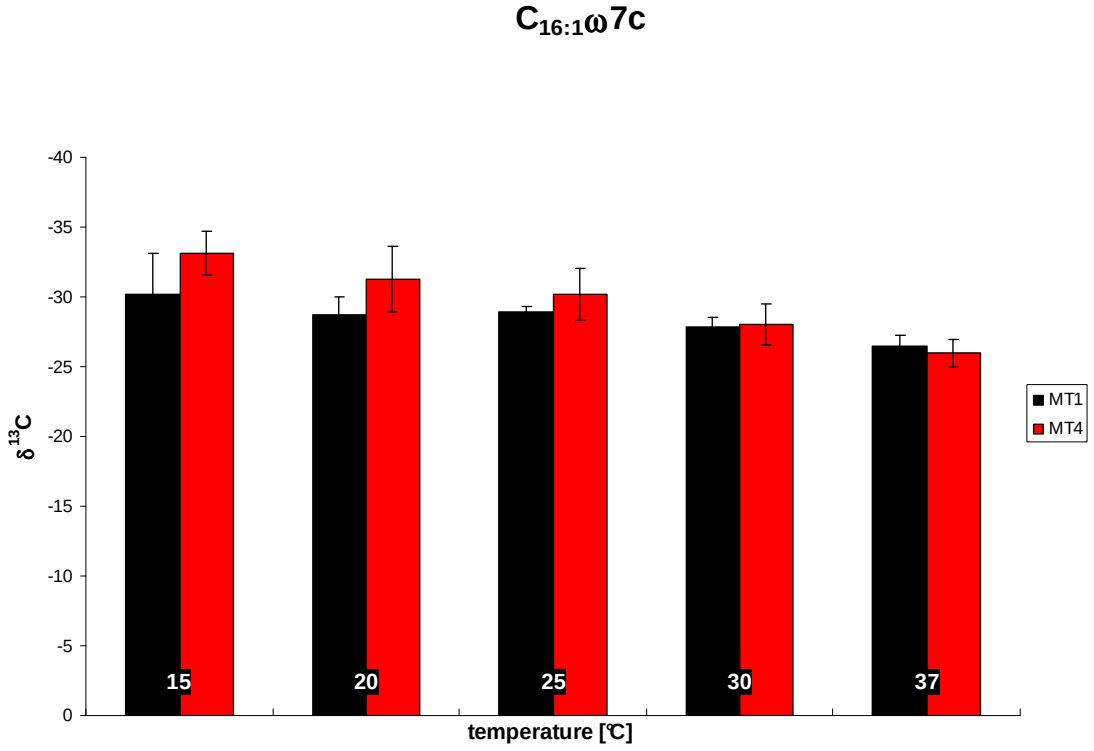
C16:1ω7c
-40
-35
-30
-25
-20
-15
-10
-5
0
δ13C
15
20
25
30
37
temperature [℃]
MT1
MT4

C

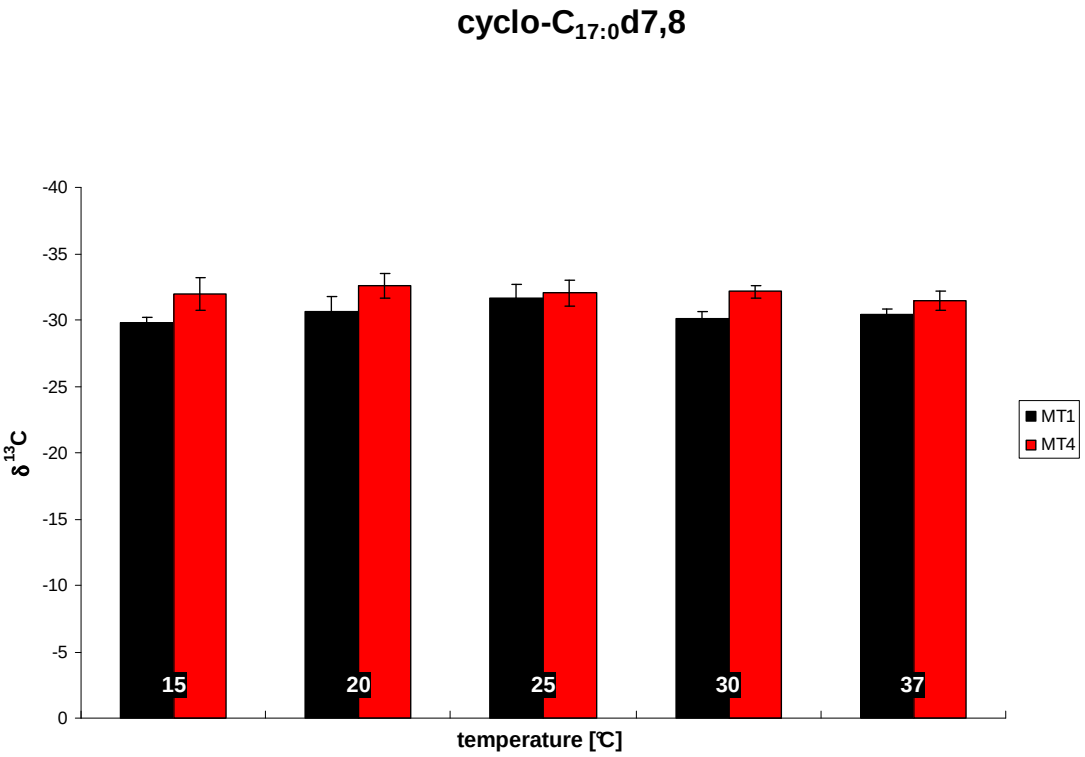

Fig. 3.7: Carbon Fractionation of the Bacterial Fatty Acids. $\delta^{13}C$ values of the fatty acid **A** $C_{16:0}$, **B** $\delta^{13}C$ values of the fatty acid $C_{16:1}\omega7$ and **C** $\delta^{13}C$ values of the fatty acid cyclo-$C_{17:0}$ extracted from cell of strains MT1 (black bars) and MT4 (red bars) grown at different temperatures.

Table 3.3: Carbon fractionation of the bacterial fatty acids ($\delta^{13}C$ [‰], STD = Standard Deviation)

			MT1		
	15°C	20°C	25°C	30°C	37°C
16:1w7	-30,24	-28,68	-28,88	-27,89	-26,52
STD (±)	2,8629	1,2926	0,4174	0,6877	0,7103
16:1w?	-33,70	-30,90	-28,87	-31,07	-35,49
STD (±)	0,5961	2,2760	0,6180	0,0000	0,0000
16:0	-30,68	-28,96	-27,79	-26,80	-26,06
STD (±)	2,3071	2,3382	0,6638	0,2340	0,3050
cy17:0d7,8	-29,84	-30,66	-31,64	-30,15	-30,44
STD (±)	0,3987	1,0732	1,0385	0,4297	0,4403
18:1w7	-31,56	-30,03	-29,47	-28,11	-27,19
STD (±)	2,1114	2,2712	0,9076	0,3526	0,3554
18:0	-27,68	n.d.	-23,75	-25,02	-24,72
STD (±)	n.d.	n.d.	n.d.	1,7898	1,0089
cy19:0d8,9	n.d.	n.d.	-29,19	-27,66	-30,57
STD (±)	n.d.	n.d.	n.d.	n.d.	0,2435

			MT4		
	15°C	20°C	25°C	30°C	37°C
16:1w7	-33,13	-31,26	-30,20	-28,03	-25,94
STD (±)	1,6039	2,3593	1,8600	1,4966	0,9751
16:1w?	-33,73	-30,44	-33,45	-30,14	-28,54
STD (±)	0,8052	1,9403	4,9493	2,2555	2,1460
16:0	-32,15	-30,86	-30,38	-28,50	-27,06
STD (±)	1,0129	1,9435	0,9962	1,1368	0,2577
cy17:0d7,8	-31,95	-32,53	-32,02	-32,15	-31,47
STD (±)	1,2802	0,9246	0,9974	0,4750	0,7065
18:1w7	-34,46	-32,44	-31,37	-29,83	-28,51
STD (±)	1,5985	2,2720	1,6666	0,9244	0,2516
18:0	-28,40	-27,69	-28,37	-26,74	-25,69
STD (±)	0,9383	0,6225	0,9730	0,7557	0,1407
cy19:0d8,9	-29,46	-30,57	-29,99	-28,87	-30,17
STD (±)	1,1866	2,0311	1,0668	2,2154	1,7876

3.3 Kinetics of Substrate Uptake in Pure Bacterial Cultures

To analyse the kinetics of substrate uptake in pure cultures of three members of the 4-chlorosalicylate degrading community, *Pseudomonas reinekei* MT1, *Achromobacter spanius* MT3 and *Pseudomonas veronii* MT4, cells were grown on minimal medium containing 5 mM sodium acetate as sole carbon source. After pulse dosing of [U-^{13}C]-labelled sodium acetate at discriminative growth stages samples were taken at different time points after labelling. The extracted fatty acids from those samples were dissected for their isotopic ratio to calculate the kinetics of substrate uptake by employing pseudo-first order kinetics.

For each series of experiments the isotope ratios of the fatty acids were determined three times and used to calculate the maximal incorporation **a** and the incorporation rate **b** (2.6.5.1, Equation 2) and the resulting constants were used for the calculation of the incorporation curves (Fig. 3.8). The resulting calculated incorporation curves fitted well the measurements confirming that the application of a pseudo first-order kinetic could reliably describe the incorporation of ^{13}C into individual fatty acids in bacteria. For some data sets no mathematical solution could be found and the corresponding sampling point had to be omitted in the progress of the analyses.

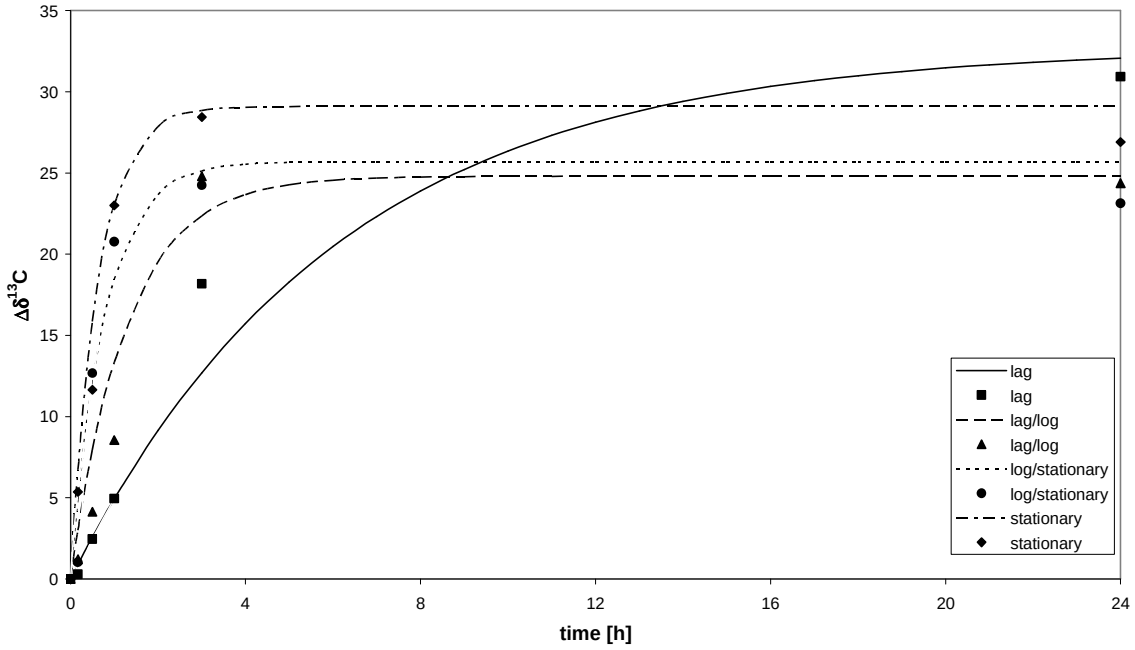

Fig. 3.8: Simulated incorporation curves for $C_{16:0}$ in *Pseudomonas reinekei* MT1. $\Delta\delta^{13}C$ is the increase in $\delta^{13}C$ and is the difference between $\delta^{13}C_{t=0}$ and $\delta^{13}C$ given in [‰].

The maximal incorporation **a** was rather similar between the individual fatty acids at all stages of the growth curve (Table 3.4). Some fatty acids showed a slightly smaller incorporation of the labelled carbon and a good example for that is the fatty acid $C_{18:0}$ which was always less enriched compared to $C_{16:0}$. This observation was valid for all strains and it fits well with results reported before by Tillmann (Tillmann, 2004). Comparing the individual strains for the maximal carbon incorporation ($\mathbf{a_{mean}}$) it was found that there were some differences between the strains (Table 3.4). While *P.reinekei* MT1 and *A. spanius* MT3 showed similar values (MT1: $\mathbf{a}_{mean}$ = 26.2 ± 4.5, MT3: $\mathbf{a}_{mean}$ = 27.7 ± 6.1), *P. veronii* MT4 revealed a significantly higher incorporation ($\mathbf{a}_{mean}$ = 47.9 ± 15.7) compared to the other strains. In the two *Pseudomonas* strains the two unsaturated C_{16}-fatty acids displayed smaller labellings than $C_{16:0}$, here $C_{16:1}$ω5c was less labelled than $C_{16:1}$ω7c. In *A. spanius* MT3 the opposite was found (Table 3.4). The C_{18}-fatty acids showed a different behaviour and $C_{18:1}$ω7c had higher incorporations of the label than $C_{18:0}$ in strains MT1 and MT3 but in strain MT4 this trend was reversed.

As for the maximal incorporation **a** no big differences were observed for the incorporation rates **b** for the individual fatty acids at a given growth phase. Earlier experiments showed a slightly slower incorporation in the fatty acid $C_{18:0}$ compared to $C_{16:0}$ (Tillmann, 2004) and this could be confirmed in the present study (Table 3.4). Cyclo-$C_{17:0}$d7,8 showed in all strains the lowest incorporation rates, while $C_{16:1}$ω5c showed in all strains the largest incorporation rate **b**. In the unsaturated fatty acids $C_{16:1}$ω5c and $C_{16:1}$ω7c the label was always faster incorporated compared to the corresponding saturated fatty acid $C_{16:0}$. The opposite was found for $C_{18:0}$ which was faster labelled in MT1 and MT3 than $C_{18:1}$ω7c. A complete different picture emerged when incorporation rates of a given fatty acid were compared along the growth stages. Here a clear tendency is seen for all strains and significant increases of the incorporation rates with growing age of the cultures were found (Table 3.4, Fig. 3.9). For all strains and all fatty acids at least a fivefold increase in the stationary phase compared to the early log-phase was determined, while for *P. veronii* MT4 this increase was up to 25-fold. All strains gave comparable **b**-values during exponential growth, but *P. veronii* MT4 deviated significantly in the stationary phase showing much higher **b**-values than the other two strains (Table 3.4). When individual fatty acids of a given strain were compared for their increase of the incorporation rates no statistically significant tendency could be derived. This lack of differences in the

increase of **b** between the individual fatty acids pointed to a common cause for the increase of **b** towards the stationary phase (Fig. 3.10).

To compare the maximal incorporations **a** with growth rates the specific growth rate µ was determined for all strains. While rather similar values for *Pseudomonas reinekei* MT1 (µ= 0.23 h^{-1}) and *Achromobacter spanius* MT3 (µ=0.20 h^{-1}) were determined an almost twofold value (µ=0.40 h^{-1}) was derived for *Pseudomonas veronii* MT4. No inhibition of *P. reinekei* MT1 was observed for the chosen acetate concentrations (Ferenci, 1996).

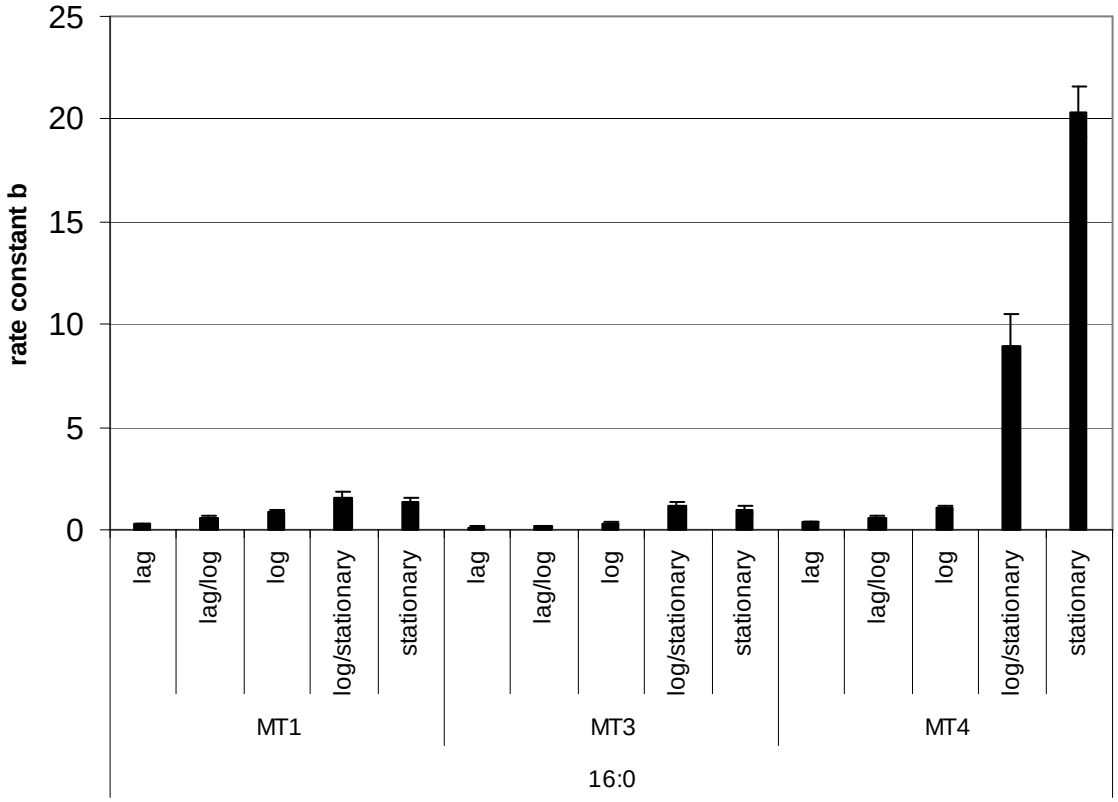

Fig. 3.9: Calculated incorporation rates **b** for fatty acid 16:0 of the three strains tested at different growth stages. The increase of **b** with growing age of the culture can clearly be seen. Errors are shown as halve-bars.

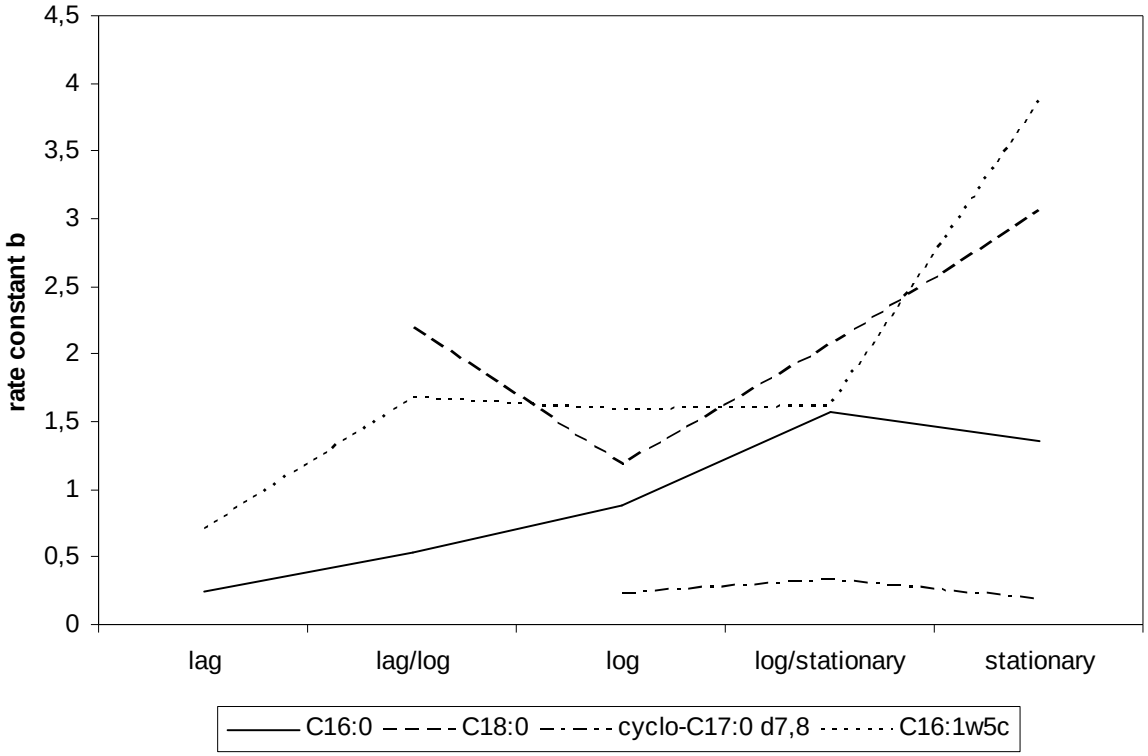

Fig. 3.10: Calculated incorporation rates b for four different fatty acids of *Pseudomonas reinekei* MT1 at different growth stages

Table 3.4: Maximal incorporation **a**, rate constant of substrate incorporation **b** and R^2 calculated for the individual fatty acids of the three strains in the lag, the transition lag to logarithmic, the logarithmic, the transition logarithmic to stationary and the stationary phase.

		$C_{16:0}$	$C_{16:1}\omega5$	$C_{16:1}\omega7$	$C_{18:0}$	$C_{18:1}\omega7$	cyclo-$C_{17:0}$
MT1							
Lag	**a**	31.2±1.5	18.7±4.1	21.0±2.1	n. d.	21.2±1.1	n. d.
phase	**b**	0.25±0.03	0.70±0.50	0.35±0.09	n. d.	0.38±0.05	n. d.
	R^2	0.9892	0.8240	0.9585	n. d.	0.9881	
Lag-log	**a**	26.0±2.5	13.2±6.9	26.0±3.8	19.5±2.4	18.8±2.0	n. d.
phase	**b**	0.54±0.15	1.67±2.6	0.62±0.26	2.19±0.97	0.79±0.25	n. d.
	R^2	0.9592	0.3159	0.9070	0.8316	0.9279	
Log	**a**	32.5±0.9	25.9±3.0	28.6±1.0	25.1±1.5	22.4±0.5	29.8±0.8
phase	**b**	0.88±0.07	1.59±0.6	1.37±0.15	1.18±0.22	1.54±0.11	0.23±0. 02
	R^2	0.9953	0.8868	0.9897	0.9735	0.9957	0.9966
Log-stationary	**a**	25.6±1.5	17.8±2.4	20.6±2.0	16.6±2.1	12.8±1.7	25.5±1.7
phase	**b**	1.57±0.30	1.62±0.7	1.93±0.64	2.06±0.95	1.56±0.68	0.33±0. 06
	R^2	0.9735	0.8833	0.9263	0.8679	0.8899	0.9762
Stationary	**a**	28.2±1.3	17.6±5.0	22.0±1.6	21.0±1.4	21.4±1.1	31.1±1.6
phase	**b**	1.35±0.19	3.87±5.2	1.53±0.36	3.06±0.82	1.75±0.31	0.19±0. 03
	R^2	0.9838	0.4973	0.9571	0.9493	0.9747	0.9879
MT3							
Lag	**a**	31.0±0.6	11.7±2.0	31.3±2.1	28.6±3.5	28.1±2.8	n. d.
phase	**b**	0.14±0.01	0.44±0.20	0.25±0.05	0.13±0.05	0.21±0.06	n. d.
	R^2	0.9989	0.8240	0.9752	0.9490	0.9506	
Lag-log	**a**	31.8±1.0	20.1±1.5	26.0±1.8	24.2±4.0	29.4±2.1	n. d.
phase	**b**	0.22±0.02	2.58±0.70	0.38±0.07	0.42±0.18	0.16±0.04	n. d.
	R^2	0.9949	0.9530	0.9724	0.8328	0.9782	
Log	**a**	33.3±1.6	42.5±2.1	35.5±1.8	20.1±2.7	31.5±2.1	n. d.
phase	**b**	0.34±0.04	0.47±0.06	0.41±0.05	0.40±0.14	0.36±0.06	n. d.
	R^2	0.9889	0.9866	0.9877	0.9234	0.9782	
Log-stationary	**a**	25.2±0.7	26.4±5.9	27.9±1.2	17.2±1.6	17.6±1.6	25.7±2.1
phase	**b**	1.21±0.11	0.78±0.52	1.04±0.13	1.32±0.39	0.88±0.23	0.26±0 .06
	R^2	0.9934	0.8032	0.9880	0.9201	0.9498	0.9698
Stationary	**a**	23.0±1.4	26.5±1.8	25.7±3.0	19.4±1.6	18.0±2.0	20.2±5.7
phase	**b**	0.95±0.18	1.62±0.40	1.39±0.52	0.54±0.12	0.42±0.13	0.48±0 .39
	R^2	0.9762	0.9582	0.9061	0.9689	0.9447	0.7563
MT4							
Lag	**a**	50.8±1.2	47.4±1.4	46.8±2.2	47.2±1.5	47.2±1.5	51.1±3.5
phase	**b**	0.38±0.03	0.75±0.08	1.76±0.32	0.35±0.03	0.83±0.14	0.11±0 .02
	R^2	0.9856	0.9690	0.8536	0.9790	0.8999	0.9546
Lag-log	**a**	48.9±1.6	41.1±1.77	50.6±1.7	41.4±0.9	47.4±1.6	40.6±1.8
phase	**b**	0.62±0.07	0.85±0.12	1.03±0.13	0.82±0.08	0.87±0.1	0.22±0. 03
	R^2	0.9676	0.9419	0.9447	0.9865	0.9484	0.9655
Log	**a**	56.6±1.2	47.6±1.4	54.0±1.9	43.5±0.5	52.0±1.4	45.2±3.4
phase	**b**	1.11±0.09	2.78±0.37	1.81±0.24	1.12±0.05	1.97±0.21	0.30±0 .06
	R^2	0.9777	0.9397	0.9266	0.9938	0.9543	0.9005
Log-stationary	**a**	41.7±1.1	35.0±1.3	38.1±1.5	23.2±0.5	27.2±1.4	38.3±0.6
phase	**b**	8.91±1.57	35.5±35	n. d.	10.8±1.63	n.d.	0.82±0.04
	R^2	0.9302	0.8994	0.8375	0.9591	0.7366	0.9914
Stationary	**a**	66.8±0.2	n.d.	59.9±3.8	113.9±1.1	54.2±2.1	31.8±1.3
phase	**b**	20.35±1.23	n.d.	n. d.	5.83±0.31	n.d.	1.31±0.20
	R^2	0.9991		0.7195	0.9917	0.8403	0.8983

3.4 Proliferation Assay of a Bacterial Consortium

3.4.1 Estimation of the Activity States via Proliferation Patterns

The bacterial DNA content offers data about the duration of cell cycle phases and thus for cell growth and proliferation activity. The shape of the distributions of a DNA histogram provides such information (Cooper, 1991). The proportion of cells in different stages is a crucial parameter for evaluating the duration of these phases and to estimate the proliferation activity of the population.

The four bacterial strains (MT1, MT2, MT3, MT4) were grown in pure cultures on different substrates and analysed regarding their growth and proliferation characteristics. The resulting DNA distribution patterns provided different types of valuable information (Fig. 3.11).

Since the correlation of proliferation activity with the appearance of a major part of cells within a distinct stage of the cell cycle is a strain-specific feature, a determination of the typical DNA-pattern for different growth states was performed for each strain involving the batch-cultivation procedure. These patterns were determined during growth on different substrates to enhance reliability of the DNA pattern allocation.

The typical eukaryotic like DNA proliferation patterns were determined by growing all strains on different substrates. Since strains MT3 and MT4 were not able to metabolise 4-chlorosalicylate the DNA patterns of those strains were only obtained from cells grown on peptone and acetate. MT2 cells did neither grow on 4-chlorosalicylate nor on acetate. DNA patterns for this strain were obtained from cells grown on peptone (Fig. 3.11).

In populations of MT1 a majority of the cells (up to 48.43 %) displayed a single chromosome equivalent during the exponential growth phase (C_1). This was observed for growth on peptone. Comparing the shapes of the DNA distributions during growth on this substrate, it seems likely that replication is immediately followed by cell division. During growth on acetate and 4-chlorosalicylate the quantities of cells presenting a C_1 content decreased to 42.01 % and 17.30 %, respectively. The quantities of cells containing a C_2-content aroused under stationary cultivation conditions for this species (between 67.62 % and 86.04 % for the three substrates).

The shapes of the DNA distributions of MT3 were found to be much more variable during growth on peptone and acetate than those of MT1. It became clear that the individual MT3 cells contained chromosome contents correlating to 1, 2, 3, 4 and more chromosome equivalents per cell, using the linear scale of DNA fluorescence intensity values. Subpopulations containing C_2, C_3, and C_4 chromosome equivalents dominated the exponential growth phase with 95.57 % (peptone) and 43.10 % (acetate) of these cells. The corresponding mode values of all subpopulations clearly point to asynchronous cell cycle behaviour. At the end of the cultivation, under substrate depletion, the cells always stayed mainly within the second subset of subpopulations.

MT4 and MT2 showed increasing amounts of cells containing two and four chromosome equivalents during exponential growth on peptone (78.40 % and 83.41 %, respectively, Figure 2). In comparison to MT4 (73.39 % for peptone, 84.06 % for acetate), there was a lower percentage of cells in the C_1-subpopulation (33.8 %) in MT2 during stationary cultivation, indicating that the latter requires more time for replication and cell division events.

Summarising, to describe the state of high proliferation the quantities of cells with the following chromosome equivalents were used: percent C_1 for MT1; percent C_2+C_3+C_4 for MT3; percent C_2+C_4 for MT4 and MT2, respectively.

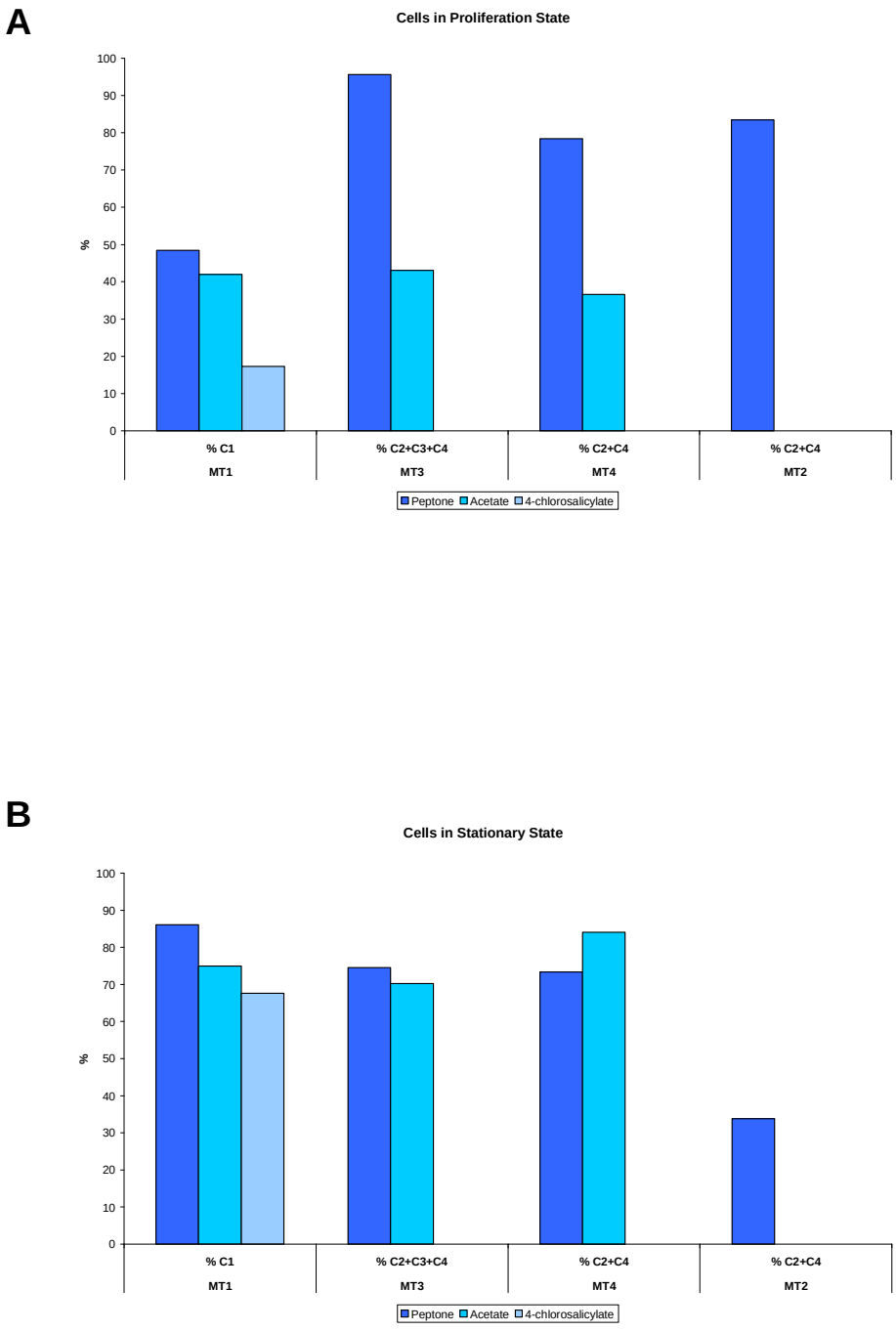

Fig. 3.11: Estimation of the Activity States via Proliferation Patterns. **A** Percentage of the sum of chromosome equivalents counting for proliferation state of cells of strains MT1, MT2, MT3 and MT4 obtained from cells of those strains grown on three different media. **B** Percentage of the sum of chromosome equivalents counting for stationary phase state of cells of strains MT1, MT2, MT3 and MT4 obtained from cells of those strains grown on three different media.

3.4.2 Differentiation of the Consortium during Growth on 4-Chlorosalicylate

To study the degradation of 4-chlorosalicylate that requires a mixed culture it is essential to monitor the proportions and to control the proliferation population dynamics of the component species. For these purposes a combination of immuno-staining, quantitative DNA labelling and multi-parametric flow cytometry were used. While the four strains can grow together in constant proportions in mixed cultures on 4-chlorosalicylate, it was shown that the compound could not be mineralized as a sole substrate by each species alone.

To get information about their multiplication activity within the consortium each species was followed by measuring the chromosome content every few hours and, at the same time, estimates of changes in species quantities were obtained by counting the cells.

The proliferation activities of the consortiums member are shown in Fig. 3.12. Samples were taken at different times during the chemostat cultivation and species related antibody vs. DNA fluorescence intensities determined. The species related shapes of the population patterns are evident; also the chromosome equivalents are clearly distinguished. The gates for the DNA distribution patterns (red circles) were set according to the mean values of the DNA subpopulations [relative fluorescence]: MT1: 38.82 for C_1, 79.06 for C_2, 123.11 for C_4; MT2: 43.92 for C_1, 84.92 for C_2, 243.43 for C_4; MT3: 35.24 for C_1, 72.35 for C_2, 109.82 for C_3, 148.64 for C_4; MT4: 51.50 for C_1, 97.73 for C_2, 220.18 for C_4. Since all the data were comparable which each other as beads alignment of the MoFlo allows, the similar range of the relative intensities of DNA labelling is obvious. Therefore, the sizes of the four genomes lied within the same order of magnitude and could not be used for differentiations of the species from each other without involving immuno-staining.

Detailed information about the contribution of each species can be obtained by analysing their proliferation patterns (Fig. 3.13). Due to stability reasons, the chemostat culture was built up strain by strain.

An increase in proliferation activity was shown for MT1 at the start of cultivation up to day 14 and decreased until cultivation was aborted on day 82. The percentage of MT1 cells in stationary phase of growth increased over this time period. MT3 was added to the chemostat culture after 14 days and the fraction of those cells in proliferation phase declined until day 51 of incubation and rose then again. After 82

days the proportion of cells in stationary and proliferation phase were equal. The part of MT3 cells in stationary phase was increasing up to day 51 and decreasing until day 76. After 24 days of incubation strain MT4 was adjoined to the continuous culture. The fraction of MT4 cells in stationary phase raised up to the end of cultivation, the part of cells of this strain in proliferation phase decreased continuously. The DNA pattern for strain MT2 showed a high proportion for cells in proliferation phase beginning at day 39 – appending of MT2 – up to the abortion of cultivation after 82 days. The contingent of cells showing the DNA pattern of cells of this strain in stationary phase was relatively low and decreased to day 82. This finding could be contributed to the fact that *Wautersiella falsenii* MT2 was not able to degrade 4-chlorosalicylate or any of its metabolites; it was the “necrotiser” within the community. Due to the fact that high numbers of cells of the other strains were in stationary phase in the last third of the cultivation a high amount of dead or injured cells probably served as substrates for MT2.

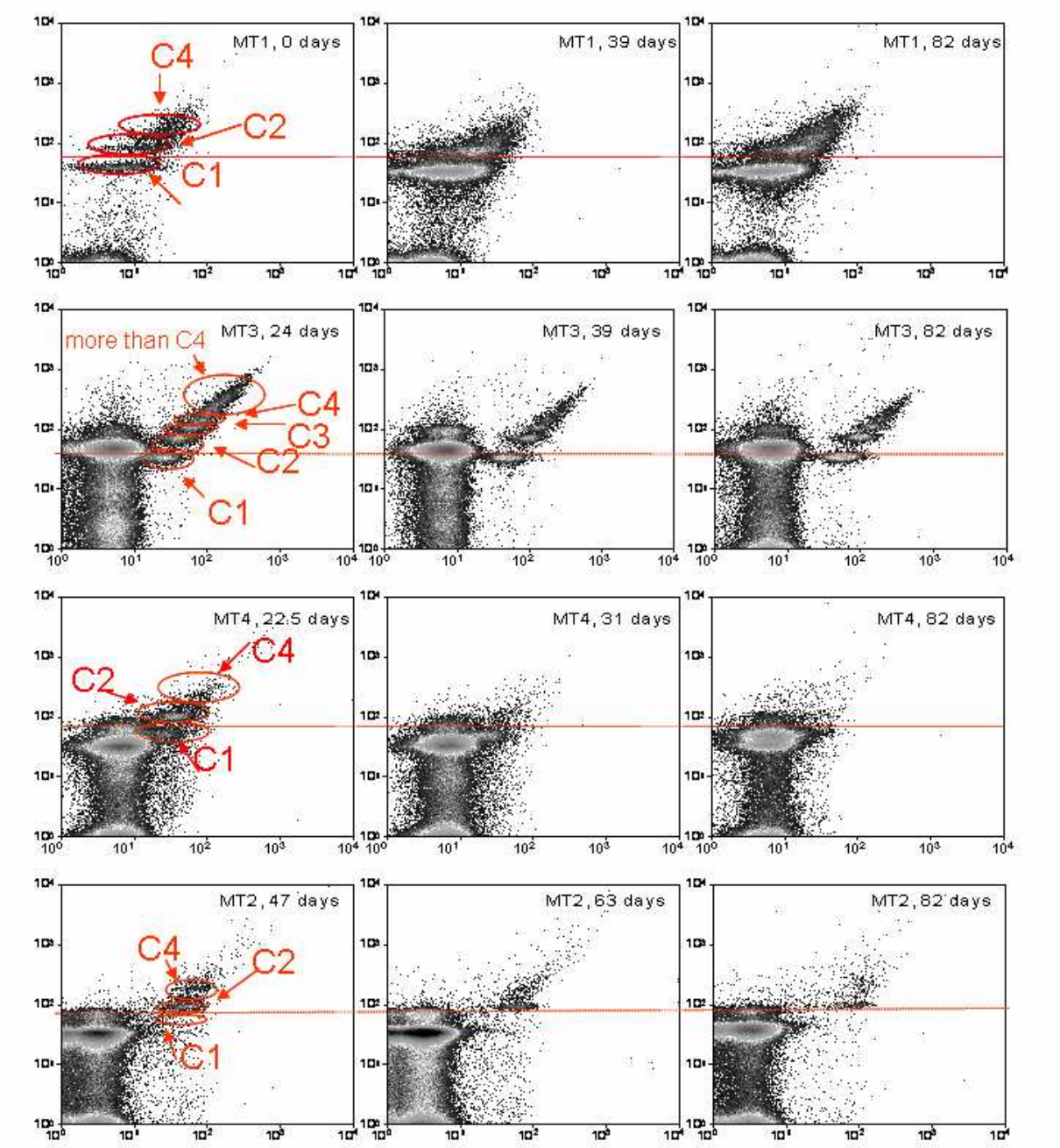

Fig. 3.12: Differentiation of the Consortium during Growth on 4-Chlorosalicylate. Dot Blot analysis of the flow cytometric dissection of samples from the consortium for obtaining DNA patterns for the analysis of the proliferation and stationary phase state of the individual members.

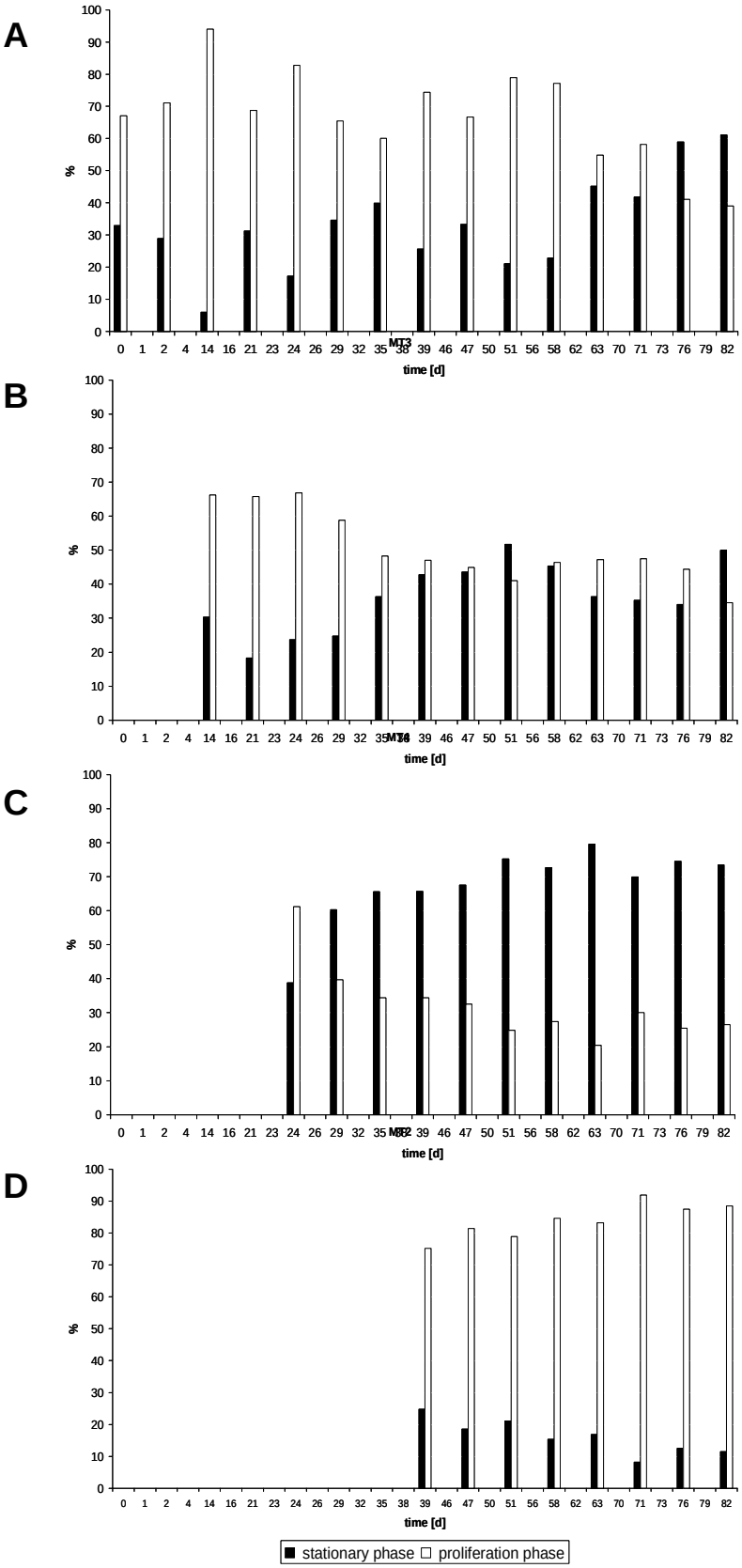

Fig. 3.13: Differentiation of the consortium during growth on 4-chlorosalicylate I. Percentage of **A** MT1 cells, **B** MT3 cells, **C** MT4 cells and **D** MT2 cells within the consortium in proliferation and stationary phase state.

3.4.3 Analysis of the 4-Chlorosalicylate Degradation by the Bacterial Consortium

Due to reasons of stability the bacterial community in the chemostate culture was build up strain by strain. The HPLC analysis revealed that in the first period of incubation when the chemostate culture consisted only of strains MT1 and MT3 the initial concentration of the carbon source 4-chlorosalicylate decreased from 5 mM to 0.04 mM. After introducing strains MT4 and MT2 to the chemostate culture the concentration of the substrate remained on a constant low level. The first intermediate of the degradation pathway of 4-chlorosalicylate formed by strain MT1, 4-chlorocatechol, was detected by HPLC analysis at very low concentrations of on average 0 – 3 µM. Irrespectively of some high peak concentration and a short period of increased 4-chlorocatechol concentration the proportion of this metabolite remained at a constant low level.

By HPLC analysis the formation of protoanemonin and cis-dienlactone, dead-end metabolites of the 4-chlorosalicylate degradation pathway by strain MT1, could also be detected (Fig. 3.14). In case of cis-dienlactone, the concentration of this metabolite could be shown to decrease rapidly in the presence of strain MT3 and remained also on a constant level. The formation of protoanemonin was clearly detectable in the chemostate culture of MT1 and MT3. Its concentration decreased from 0.37 to 0.01 mM in the first 30 days of incubation. After adding MT4 and MT2 the concentration of protoanemonin decreased over the cultivation time of the chemostate although peaks of high concentrations of this metabolite could be detected.

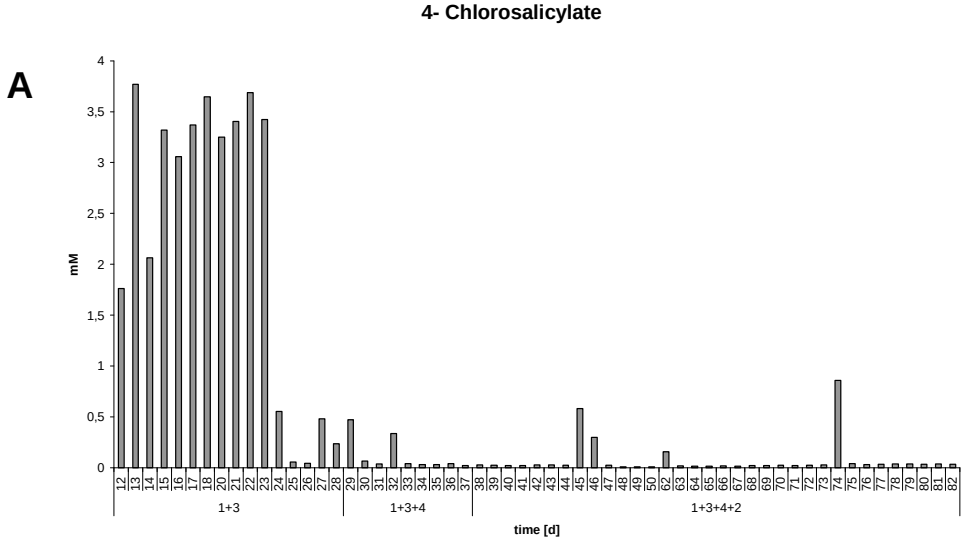

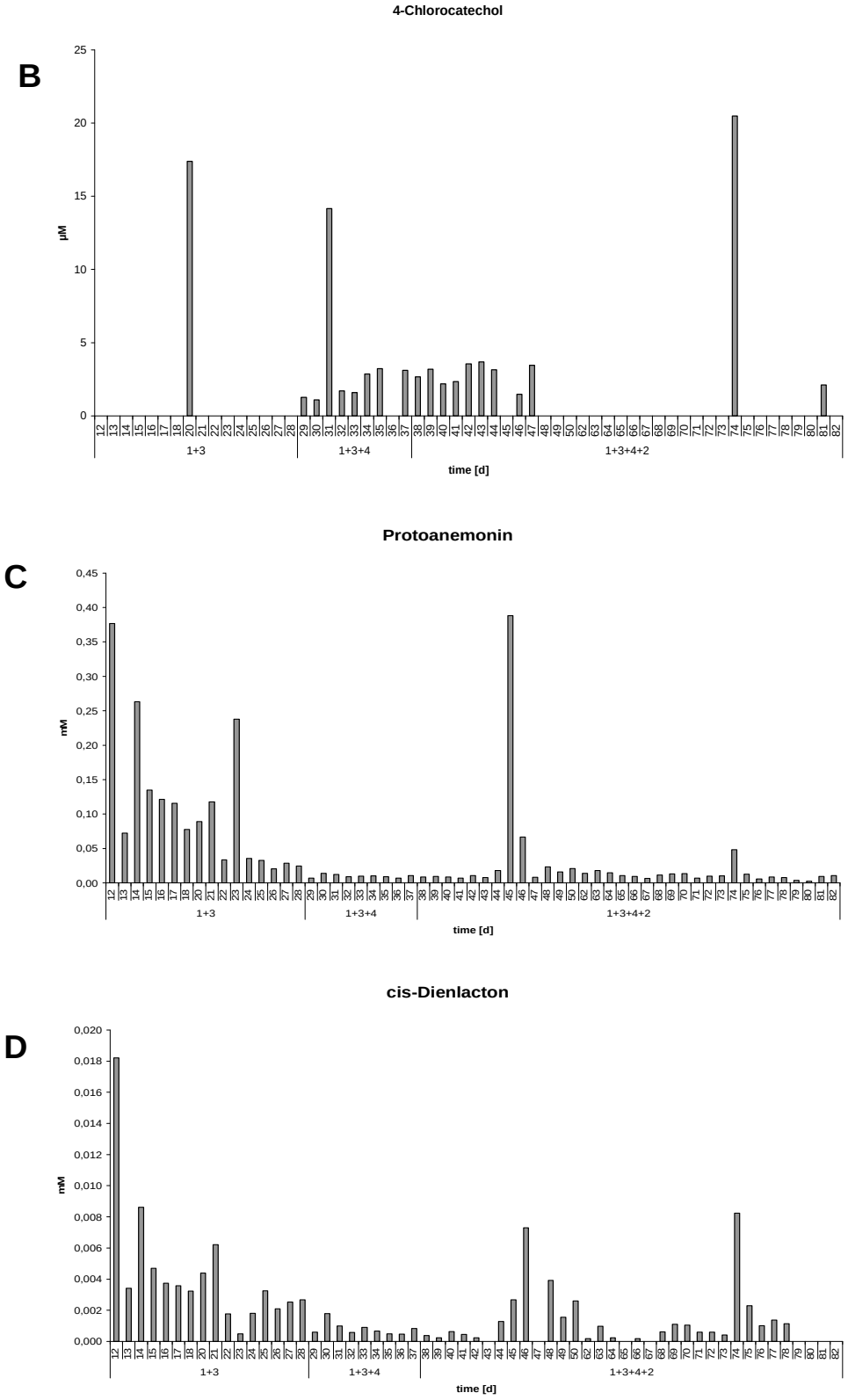

Fig. 3.14: HPLC-Analysis of the 4-chlorosalicylate degradation by the bacterial consortium. Concentration of **A** 4-chlorosalicylate, **B** 4-chlorocatechol, **C** protoanemonin and **D** cis-dienlactone in the microbial consortium analysed by HPLC. Note the different scaling of the Y-axis.

3.5 Kinetics of Carbon Sharing in a Bacterial Consortium Revealed by a Novel Combination of Immuno-Staining, Stable Isotope Probing and FACS

The kinetics of carbon sharing within a 4-chlorosalicylate degrading consortium consisting of strains *Pseudomonas reinekei* MT1, *Wautersiella falsenii* MT2, *Achromobacter spanius* MT3 and *Pseudomonas veronii* MT4 were dissected by a novel combination of three well established analytical methods: stable isotope probing, immuno-staining and FACS. To achieve this goal, the chemostate culture was pulse-dosed with [U-^{13}C]-labelled 4-chlorocatechol and samples were taken at different time points after labelling and stained with strain specific antibodies against the two most abundant strains of the community, MT1 and MT3. The stained strains were separated by FACS sorting. The fatty acids, the biomarkers of choice in this study, were extracted from the separated bacterial fractions and analysed for their isotopic ratios by IRMS.

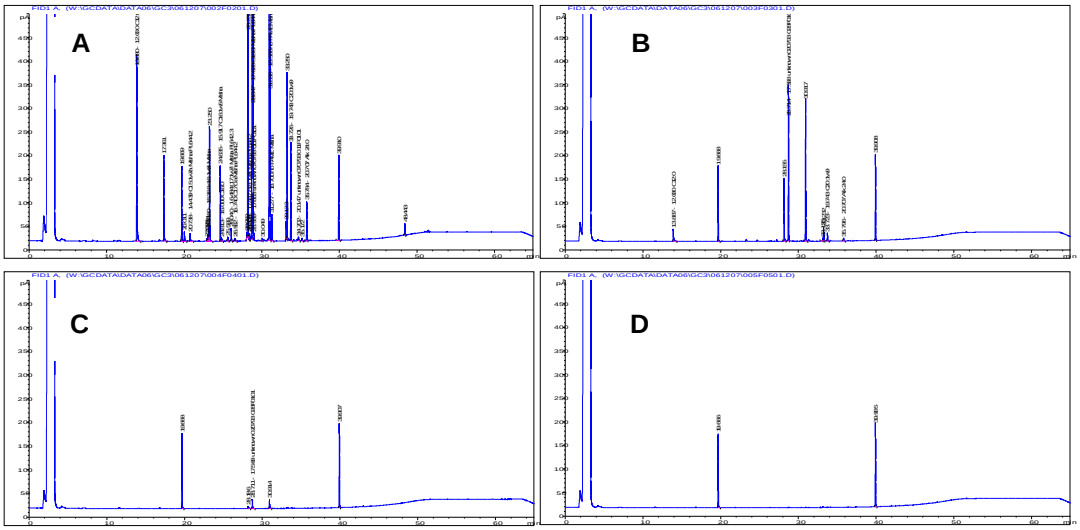

Fig. 3.15 : GC-Analysis of the extracted fatty acids from chemostate samples differing in their amounts of cells/ ml. Fatty acid profile of a sample containing **A** 2.15 x 10^8 cells, **B** containing 2.15 x 10^7cells, **C** containing 2.15 x 10^6 cells. **D** containing 2.15 x 10^5 cells.

Due to the restricted amount of MT3 cells within the bacterial community, its percentage of 8 % within the community was analysed by epifluorescence cell counting (Pelz, 1999), the sensitivity of the GC-IRMS analysis had to be tested. Therefore, fatty acids were extracted from samples with different concentrations of

cells of a chemostate sample and analysed by GC to determine the analytical threshold of the method. Those analyses revealed 2 x 10^7 cells as the lowest number of cells which should be employed for the GC-IRMS analysis of the bacterial fractions after separating them by FACS (Fig 3.15).

3.5.1 Immuno-Staining of Two Members of the Community

For the separation of individual members from the chemostat community cells had to be stained with fluorescence-labelled antibodies. Therefore, cells were first incubated with a primary strain specific antibody followed by incubation with a fluorescence-labelled secondary antibody which binds to the immunoglobulin of the primary antibody. The fluorescence microscopy analysis of the antibody stained cells of either strain MT1 or strain MT3 within the bacterial community revealed a high strain specificity of the used antibodies. Therefore, the separation of those stained bacterial fractions of MT1 and MT3 cells within the community seemed to be possible by flow cytometry.

As shown in Fig 3.16 the immunofluorescence staining of strain MT1 within the bacterial consortium with a strain specific antibody corroborated the percentage data determined by Pelz (Pelz, 1999) who dissected strain MT1 as the most abundant member of the community. The fluorescence microscopy analysis of the separated fraction of immuno-stained MT1 cells from the consortium sample after FACS reflected the high specificity of the sorting. Respectively, the fluorescence microscopy image of the fraction of the unstained part of the community showed no fluorescence (Fig. 3.16). The fluorescence microscopy analysis of the immunofluorescence stained fraction of MT3 cells in the consortium also reflected the strain specifity of the employed antibody (Fig. 3.17). The percentage of MT3 cells within the community seemed to be lower as the percentage of strain MT1, also corroborating the findings of Pelz (Pelz, 1999).

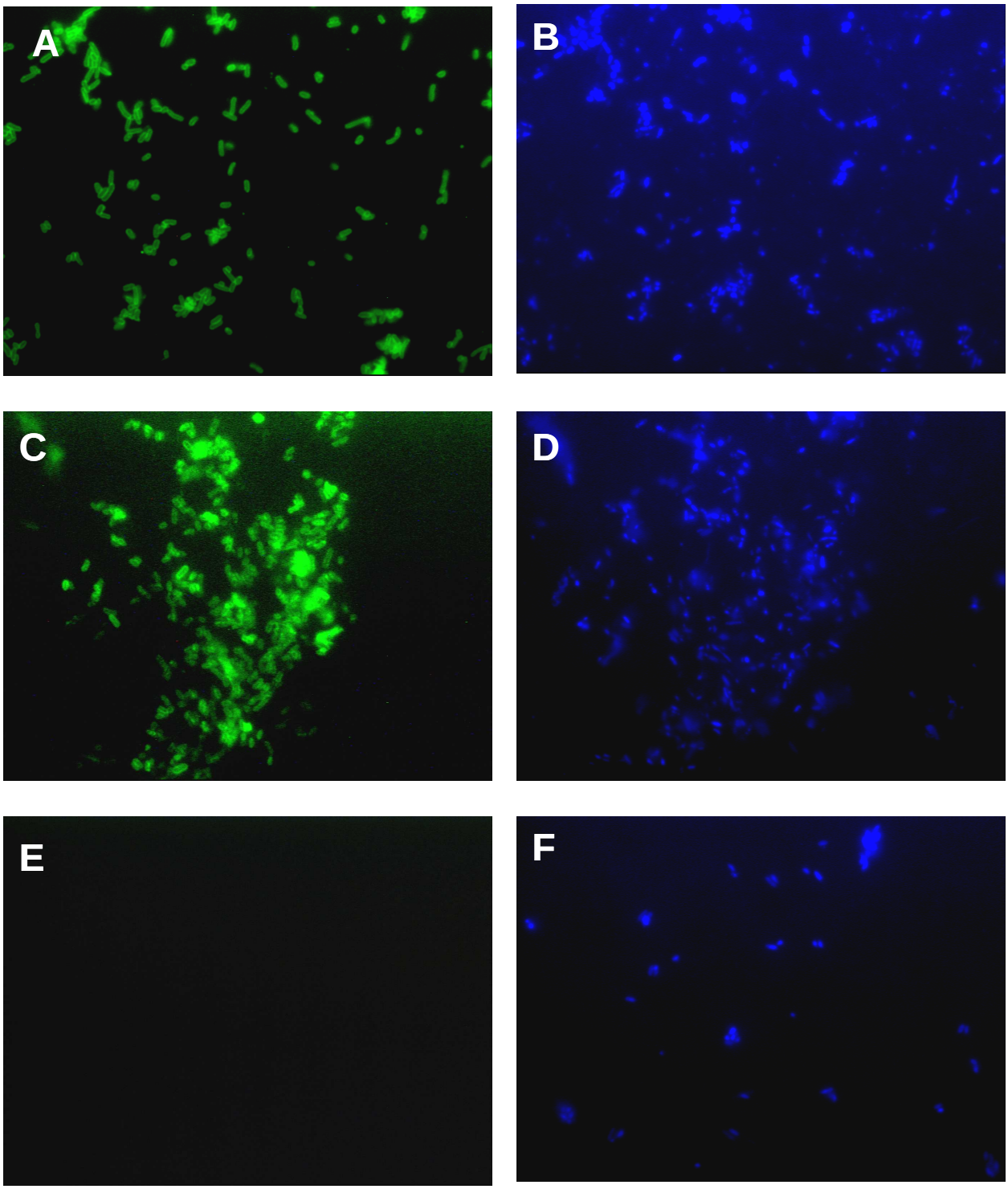

Fig. 3.16: Fluorescence microscopy images of stained strain MT1 cells (green fluorescence channel) within the community counterstained with DAPI (blue fluorescence channel). **A** MT1 cells immunofluorescence (green) stained within a sample of the the consortium before sorting. **B** Counterstaining of the sample of the consortium before sorting with DAPI (blue). **C** Fraction of immunostained MT1 cells sorted from the community (green). **D** Fraction of immunostained MT1 cells sorted from the community (blue). **E** Fraction of the remaining cells of the non-immunostained community (MT2, MT3 and MT4; green channel). **F** Fraction of the remaining cells of the non-immunostained community (MT2, MT3 and MT4; blue channel).

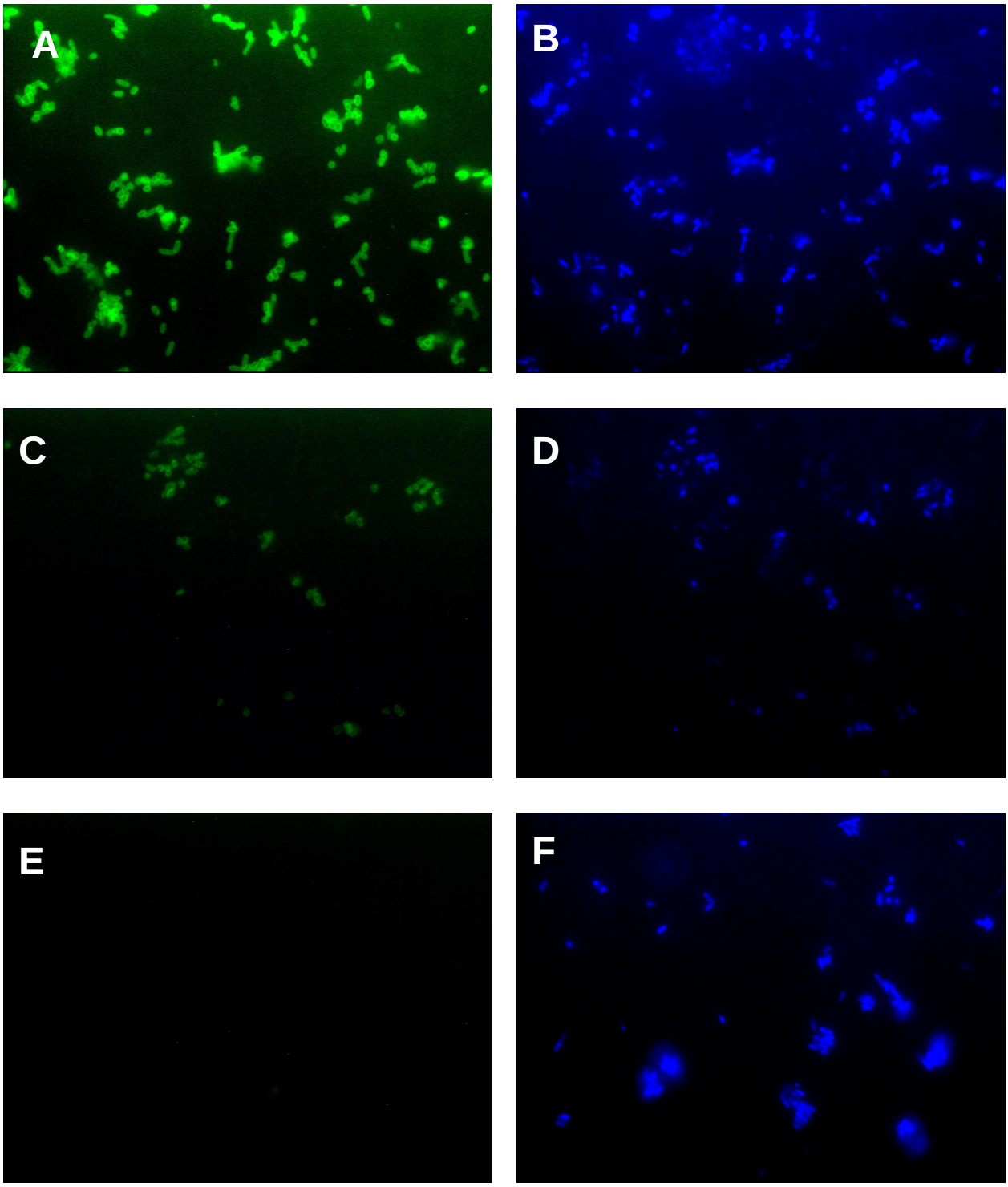

Fig. 3.17: Fluorescence microscopy images of stained strain MT3 cells (green fluorescence channel) within the community counterstained with DAPI (blue fluorescence channel). **A** MT3 cells immunofluorescence (green) stained within a sample of the the consortium before sorting. **B** Counterstaining of the sample of the consortium before sorting with DAPI (blue). **C** Fraction of immunostained MT3 cells sorted from the community (green). **D** Fraction of immunostained MT3 cells sorted from the community (blue). **E** Fraction of the remaining cells of the non-immunostained community (MT1, MT2 and MT4; green channel). **F** Fraction of the remaining cells of the non-immunostained community (MT1, MT2 and MT4; blue channel).

3.5.2 Fluorescence Activated Cell Sorting of the Bacterial Community

For the analysis of the carbon sharing in a 4-chlorosalicylate degrading community grown as a continuous culture cells were pulse-dosed with [U-^{13}C]-labeled 4-chlorocatechol. In order to reveal the kinetics of substrate incorporation into the fatty acids of the bacteria samples were taken from the chemostat culture after 0 min, 1 h, 3 h, 6 h, 12 h, 24 h and 48 h.

For the separation of individual strains from the rest of the bacterial community immunostaining of those fractions in combination with Fluorescence Activated Cell Sorting (FACS) was employed. The fluorescence signal of the antibody stained cells therefore enabled their separation by the flow cytometric approach. For the calibration of the FACS DAPI- and DAPI/antibody-stained pure cells of strains MT1 and MT3 were utilized (Fig. 3.18). The dotblot-analysis of the pure cells showed the fluorescence signal of the DNA-intercalating dye DAPI plotted versus the fluorescence signal of the immuno-staining. Appropriate gates were set for the separation of the immuno-stained cell fraction showing high fluorescence intensity for both signals (P4, Fig 3.18). Gate P5 (Fig. 3.18) included cell showing only the DAPI fluorescence signal. To exclude the influence of autofluorescence signals of the bacteria, pure DAPI-stained cells of strains MT1, MT2 MT3 and MT4 were analysed by FACS. Those dotblot-analyses showed no fluorescence signal in the gated region (Fig. 3.19).

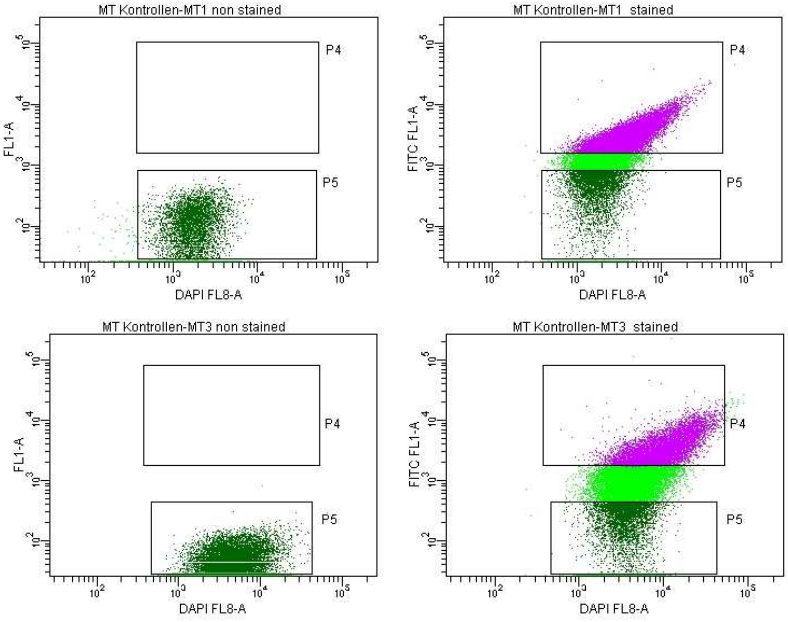

Fig. 3.18: Dotblot analysis of pure cultures of non stained and stained MT1 and MT3 cells

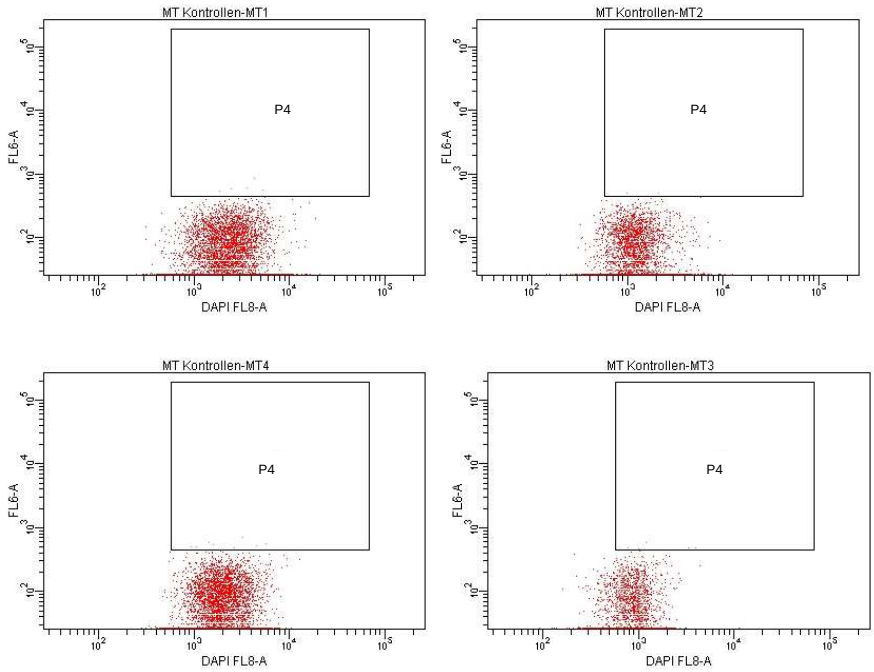

Fig. 3.19: Dotblot analysis of pure unstained MT1, MT2, MT3 and MT4 cells

The dotblot-analysis of the immuno-stained fraction of MT1 cells within the bacterial consortium showed a clear assignment of those cells from the rest of the community by their gated fluorescence signals. Due to the fluorescence signal emitted by the cells they could be separated by the FACS sorter by setting the appropriate gates P4 and P5 (Fig. 3.20) obtained from the calibration analysis (Fig. 3.18). The dotblot-analysis of the immuno-stained MT3 cell fraction showed similar results (Fig. 3.21). Here, the dotblot-analysis also revealed the separation of those fractions by using the appropriate gates from the calibration analysis with pure cultures of strain MT3 (Fig. 3.18). The separated fractions of pure MT1 and accordingly MT3 cells and the respective rest of the bacterial consortium were re-analysed by FACS to confirm the purity of the sorted fractions. The resort of the FACS-separated immuno-stained bacterial fraction of strains MT1 and MT3 from the samples revealed a conspicuous enrichment of the immunofluorescence-labelled bacteria (Fig. 3.22). Due to the sorting conditions the resorts of the separated fractions of MT1 and MT3 cells showed a negligible amount of unstained cells in those fractions (Fig. 3.22).

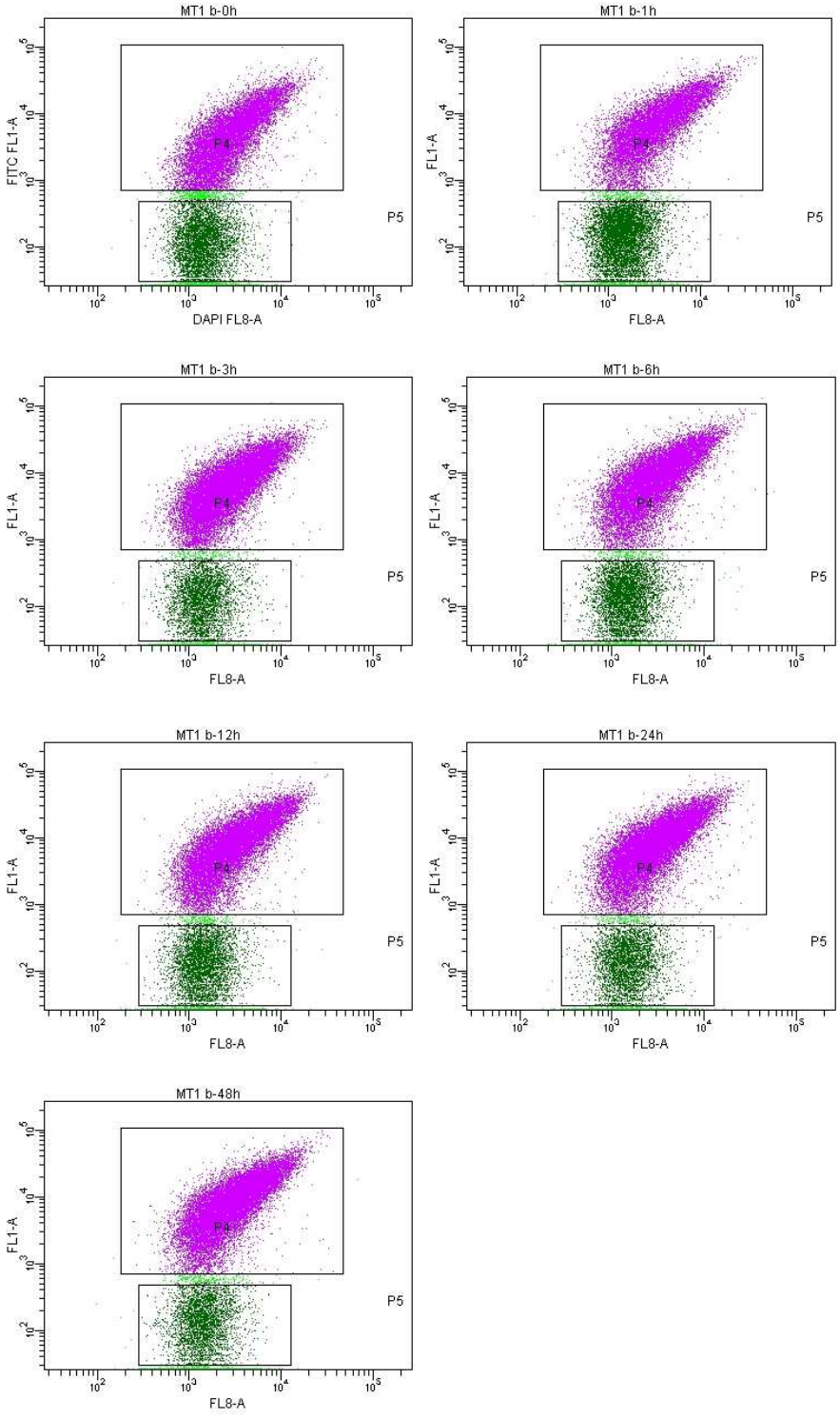

Fig. 3.20: Dotblot analysis of the FACS-separation of MT1 (violet) from the consortium (green). Samples from the chemostate culture of the bacterial consortium were taken at indiccated time points after pulse-dosing with [U-^{13}C]-labelled 4-chlorocatechol. The fraction of MT1 cells within the consortium was stained in every sample with strain-specific antibodies. The fluorescence signal of the immunostained cells enabled their separation by FACS.

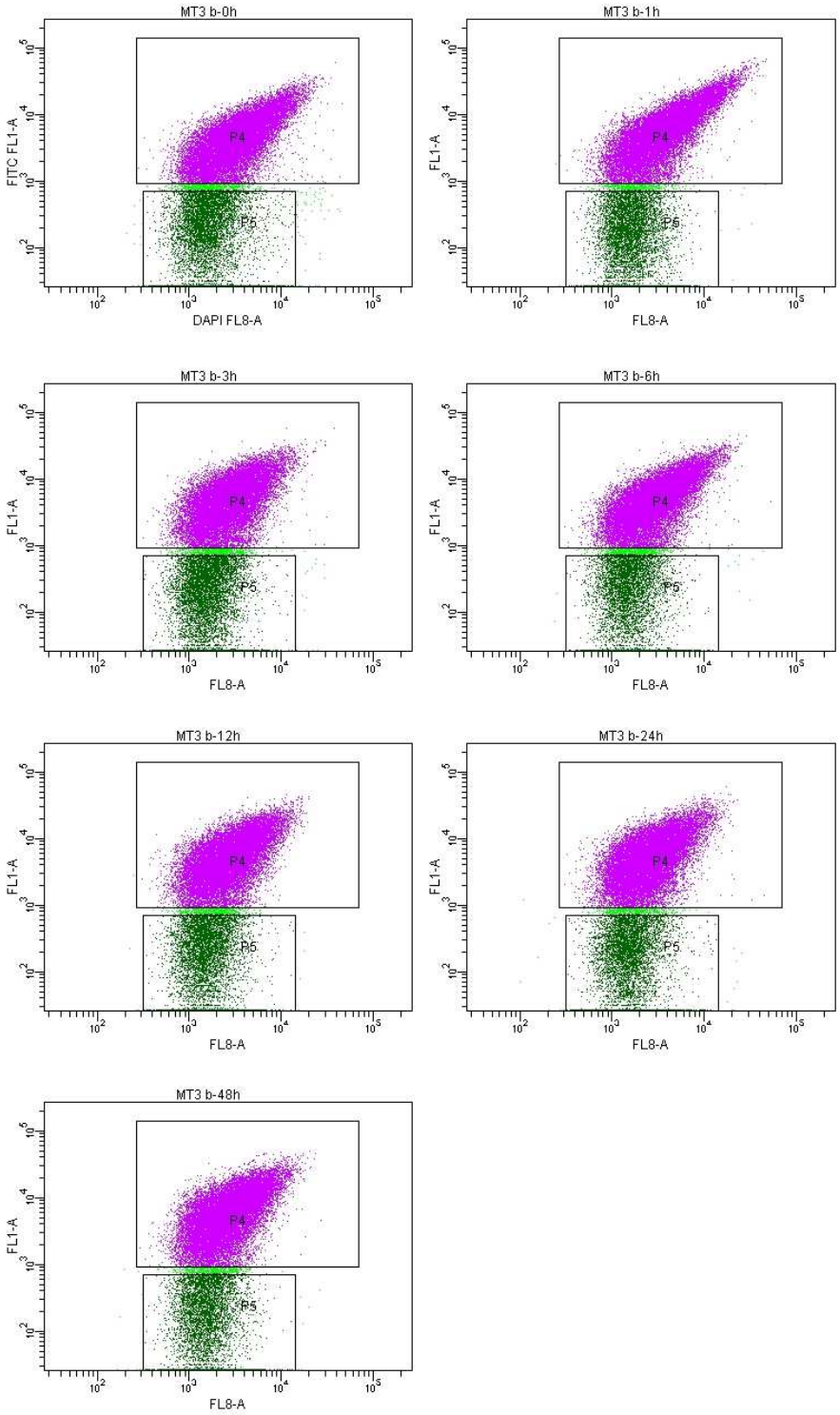

Fig. 3.21: Dotblot analysis of the FACS-separation of MT3 (violet) from the consortium (green). Samples from the chemostate culture of the bacterial consortium were taken at indicated time points after pulse-dosing with [U-^{13}C]-labelled 4-chlorocatechol. The fraction of MT3 cells within the consortium was stained in every sample with strain-specific antibodies. The fluorescence signal of the immunostained cells enabled their separation by FACS.

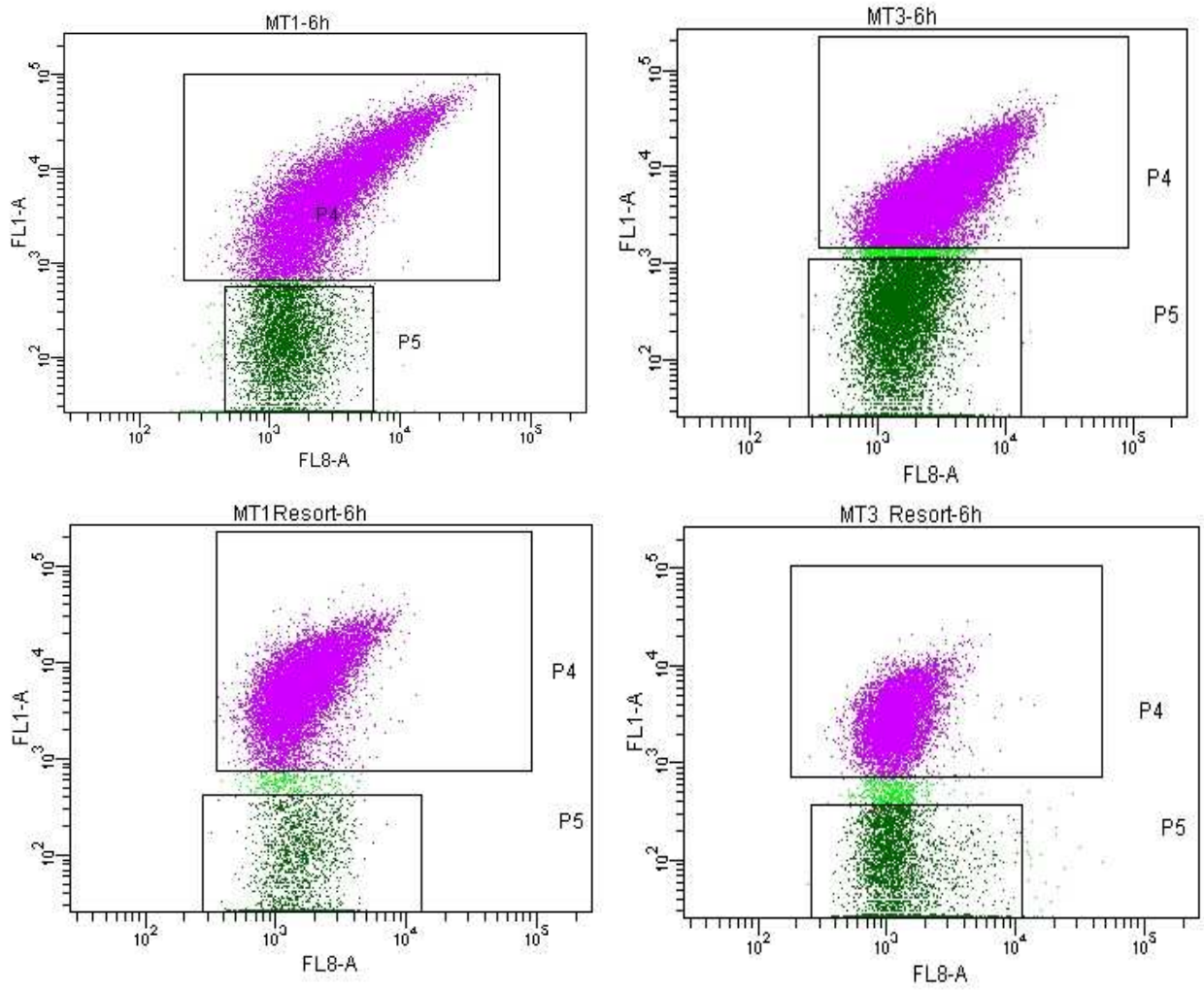

Fig. 3.22: Dotblot analysis of the FACS- separation and resort results. The separated fractions of pure MT1 and accordingly MT3 cells and the respective rest of the bacterial consortium were re-analysed by FACS to confirm the purity of the sorted fractions.

3.5.3 Analysis of the Kinetics of the [U-^{13}C]-labelled Substrate Incorporation into the Fatty Acids of the Separated Fractions of the Bacterial Consortium

The separated fractions of the 4-chlorosalicylate degrading bacterial consortium were analysed for the kinetics of the incorporation of the [U-^{13}C]-labelled substrate 4-chlorocatechol into the fatty acids of the bacteria at different time points after pulse dosing. Therefore, the fatty acids of the FACS-separated fractions of pure MT1 and accordingly MT3 cells and the respective rest of the bacterial consortium were extracted and analysed for their isotopic ratios. The obtained δ^{13}C values of the separated cell fractions of MT1 and MT3 at different time points after pulse-dosing with the [U-^{13}C]-labelled substrate were plotted versus time. From the resulting curves the incorporation rate **b** and the maximal incorporation value **a** were calculated by employing pseudo-first order kinetics. From the **a** and **b** values obtained standard curves were calculated and plotted together with the measured δ^{13}C values in a diagram (Fig. 3.23).

All six fatty acids -extracted from strains MT1 and MT3 after separation by FACS- examined in this study revealed similar trends towards the rate constant and the maximal level of substrate incorporation. Strain MT3 showed a higher level of incorporation of the ^{13}C-labelled substrate 4-chlorocatechol indicated by the high **a** values. The incorporation rate constant **b**, calculated from the δ^{13}C values of the extracted fatty acids after pulse-dosing with the labelled substrate, was found to be higher for strain MT1 compared to strain MT3 (Table 3.5). The maximal incorporation of the labelled substrates was reached after 12 h in nearly all analysed fatty acids in both strains. The only exception of this trend could be found for the cyclic fatty acid cyclo-$C_{17:0}$d7,8. In both strains MT1 and MT3 this fatty acids reached its maximal incorporation **a** after 24 h.

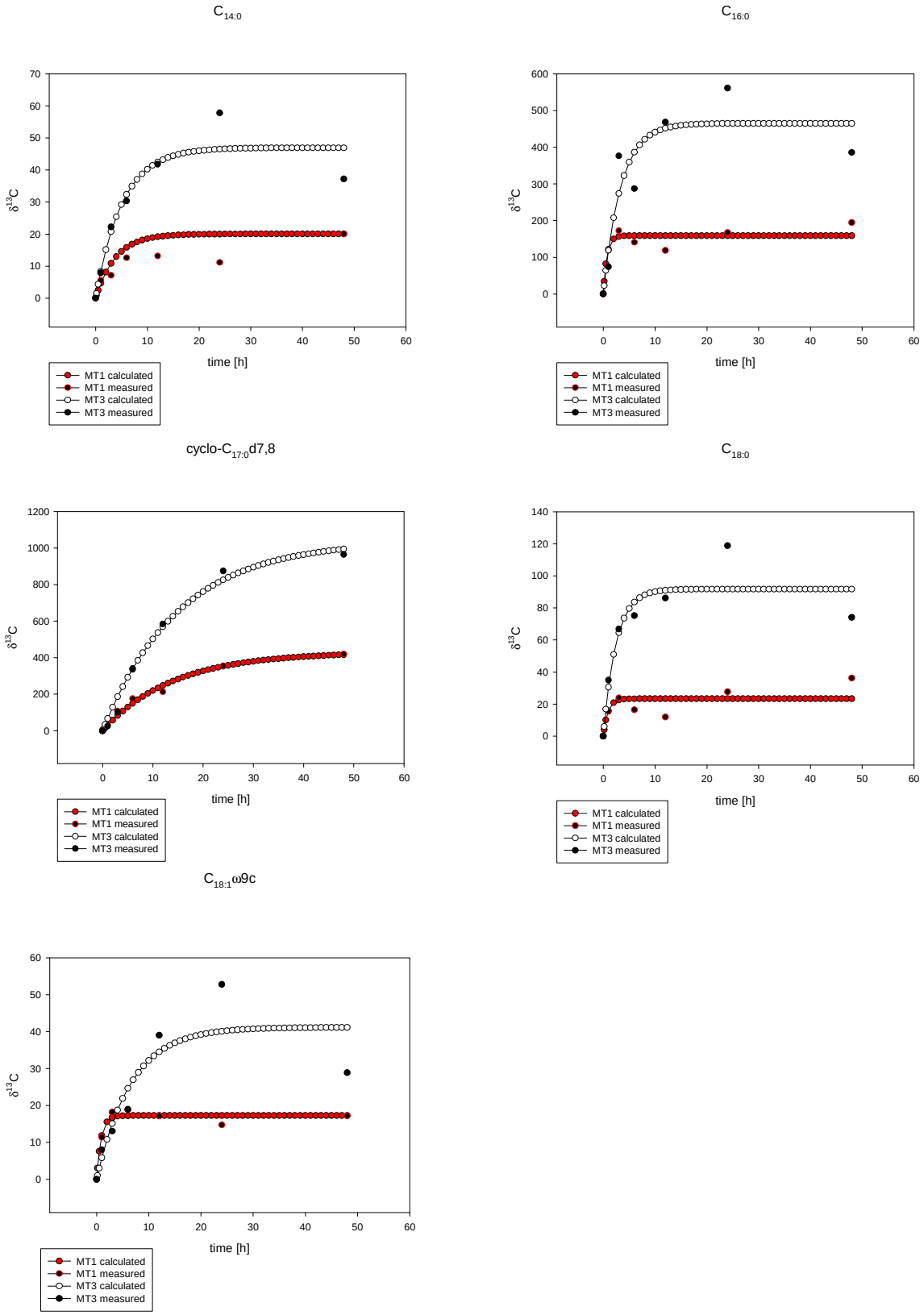

Fig. 3.23 : $\delta^{13}C$ values of the extracted fatty acids from FACS separated cell fractions of strain MT1 and MT3 taken after different time points after pulse-dosing with ^{13}C-chlorocatechol. From the resulting curves the incorporation rate **b** and the maximal incorporation value **a** were calculated by employing pseudo-first order kinetics. From those obtained **a** and **b** values standard curves were calculated and plotted together with the measured $\delta^{13}C$ values in a diagrams: **A** $C_{14:0}$, **B** $C_{16:0}$, **C** cyclo-$C_{17:0}$d7,8, **D** $C_{18:0}$, **E** $C_{18:1}\omega9c$.

Table 3.5: Maximal incorporation **a**, rate constant of substrate incorporation **b** and R^2 calculated for the individual fatty acids of strains MT1 and MT3

		$C_{14:0}$	$C_{16:0}$	$cycloC_{17:0}$	$C_{18:1\omega9}$	$C_{18:0}$
MT1	R^2	0,8097	0,8565	0,9833	0,9564	0,5587
	a	15.15 ± 1.94	158.71 ± 12.23	429.69± 26.77	17.24 ± 0.71	23.37 ± 4.05
	b	0.26 ± 0.12	1.45 ± 0.78	0.07 ± 0.01	1.16 ± 0.30	1.12 ± 1.16
MT3	R^2	0,9039	0,8472	0,9871	0,8178	0,8654
	a	46.94 ± 4.70	464.99 ± 53.72	1037.64 ± 64.78	41.13 ± 6.51	91.78 ± 8.7 1
	b	0.19 ± 0.06	1.45 ± 0.13	0.07 ± 0.01	0.15 ± 0.80	0.41 ± 0.16

4. Discussion

4.1 Phylogenetic Analysis of the 4-Chlorosalicylate Degrading Community

By sequencing their 16S rRNA genes the four community members showed the highest homology towards following bacterial strains: *Pseudomonas putida* MT1, *Empedobacter brevis* MT2, *Achromobacter spanius* MT3 and *Pseudomonas veronii* MT4. Hereby, the classification of strains MT3 and MT4 is not as definite as in the case of strains MT1 and MT2. A distinct classification of those strains would be possible by DNA-DNA hybridization. The report of the ad hoc committee on reconciliation of approaches to bacterial systematics proposed therefore a bacterial species a group of strains (including the type strain) sharing 70% or greater DNA-DNA relatedness with 5℃ or less difference of melting temperature (Wayne, 1987). Major disadvantages of this method are the laborious nature of pair wise cross-hybridizations, the requirement for isotope use and the impossibility of establishing a central database. Due to the fact that the identification of the strains was not in the main focus of this thesis the time-consuming method of DNA-DNA hybridization was not employed for the distinct classification of strains MT3 and MT4.

4.2 Temperature Dependency of Carbon Fractionation in *Pseudomonas*

Under diverse cultural or environmental conditions, for example depletion of nutrients, changes in pH, temperature etc., bacteria launch “stress responses” which significantly improve their chances of survival under, or successful adaptation to, the challenges posed by such unfavourable environments. In this study the influence of the stress factor growth temperature towards the changes in the isotopic ratio of the biomass, amino acids and fatty acids of two *Pseudomonas* strains, *P. reinekei* MT1 and *P. veronii* MT4 was analysed. Although the monitoring of carbon fractionation has been shown to deliver a helpful tool in the analysis of the degradation of hazardous substances in environment (Morasch, 2001; Kaschl, 2005), no study dealt with the influence of the growth temperature on the carbon fractionation in bacteria, yet.

The optimal growth temperature, obtained from the calculation of the growth rate µ of *Pseudomonas reinekei* MT1 and *Pseudomonas veronii* MT4, was dissected in order

to relate any dependency of carbon fractionation to this. The fractionation of carbon and nitrogen in cells of both species was analysed by combusting cells of both strains harvested in exponential phase of growth in a gas chromatograph-coupled elementar analyser. The isotopic ratio of the hereby released gases CO_2 and N_2 was dissected by Isotopic Ratio Mass Spectrometry (IRMS). The influence of the growth temperature on the carbon fractionation on the bacterial amino acids and fatty acids was also dissected by analysing the $\delta^{13}C$ values of the extracted acids by GC-IRMS. Additionally, the temperature dependency of the percentage consistency of the extracted amino acids and fatty acids of strains *P. reinekei* MT1 and *P. veronii* MT4 were investigated.

Nearly all bacteria are able to synthesize the 20 amino acids de novo, which are necessary for protein synthesis. The carbon skeletons of the amino acids are derived from intermediates of metabolic pathways. The amino groups are introduced by direct amination or transamination. The conveyance of inorganic nitrogen in organic compounds always refers to ammonia. First, nitrate, nitrite and molecular nitrogen are assimilatory reduced to ammonia and then transferred to organic compounds.

The pathways for the biosynthesis of amino acids are diverse. However, they have an important common feature: their carbon skeletons come from intermediates of glycolysis, the pentose phosphate pathway, or the citric acid cycle. On the basis of these starting materials, amino acids can be grouped into six biosynthetic families (Fig. 4.1; modified after Berg, 2002).

The analysis of the carbon and nitrogen fractionation in the biomass of strains MT1 and MT4 showed no clear dependency on the growth temperature and therefore, no significant dependence on the optimal growth temperature.

In contrast, the isotopic ratios of some extracted amino acids of both strains MT1 and MT4 showed a relation towards the growth temperature. As visualized in Fig. 3.4 for the $\delta^{13}C$ values of the amino acids alanine, serine and glycine an influence on the growth temperature could be detected. Interestingly, the precursor-grouped amino acids show no trend of fractionation concerning the dependency on the growth temperature. This leads to the assumption that specific enzymatic steps -involved in the biosynthesis of the different bacterial amino acids- are temperature dependent.

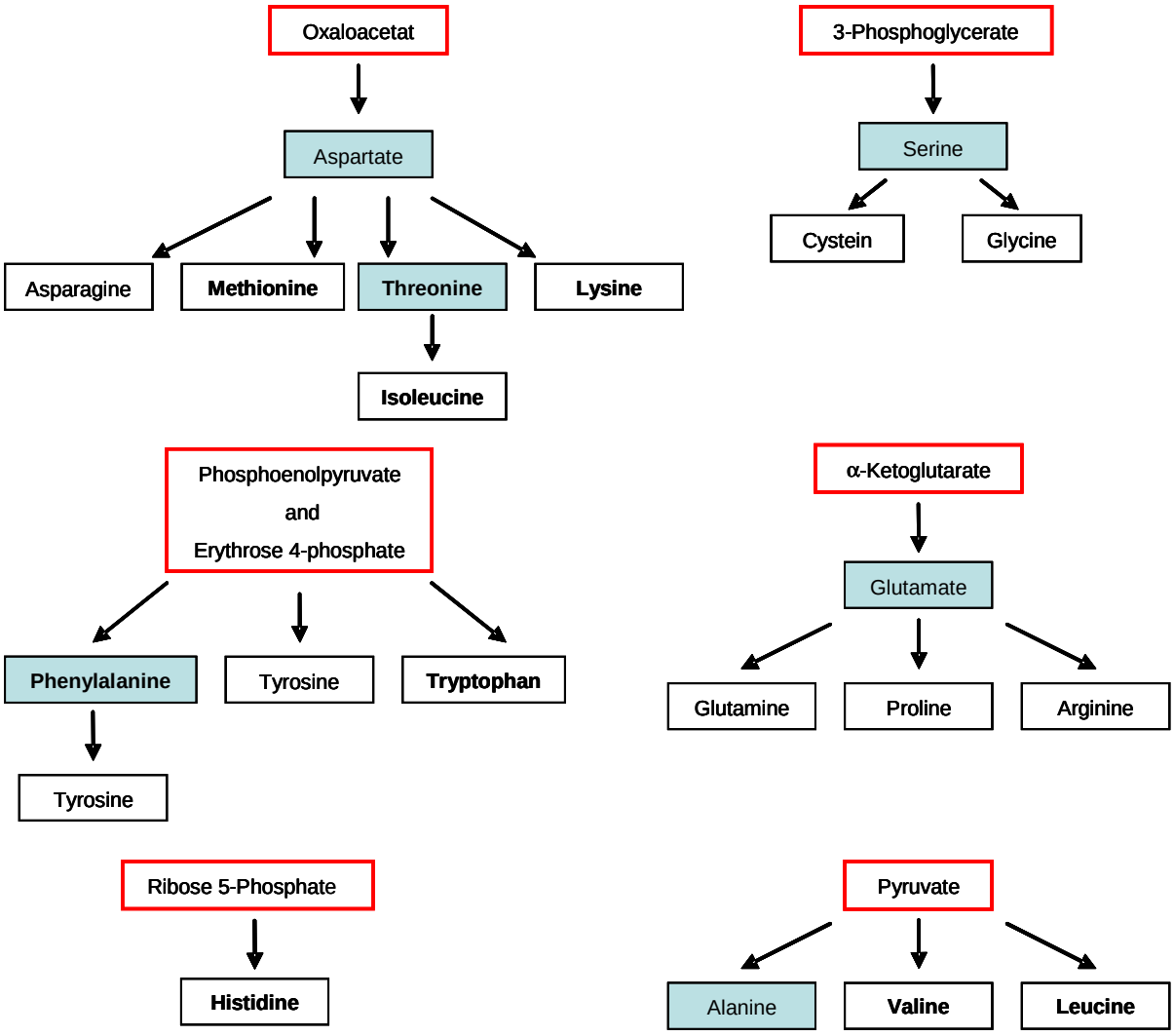

Fig. 4.1: Biosynthetic Families of Amino Acids in Bacteria and Plants. Major metabolic precursors are framed red. Amino acids that give rise to other amino acids are shaded blue. Essential amino acids are in boldface type (modified after Berg, 2002)

Three different mechanisms are known to be responsible for isotopic fractionation: equibrillium, kinetic and nuclear spin. Equilibrium fractionation reactions are those in which the distribution of isotopes differs between chemical substances (reactant vs. product) or phases (e.g., vapor vs. liquid) when a reaction is in equilibrium. In these reactions the reactants and products remain in close contact in a closed, well-mixed system such that back reactions can occur and chemical equilibrium can be attained. Nuclear spin isotope effects are not mass dependent; rather, they arise because of differences in the nuclear structure among isotopes and lead to differences in nuclear

spin. It is not clear how important nuclear spin fractionation is in most circumstances, but it does allow one to couple tracers (e.g., a 13C-labeled substrate) with nuclear magnetic resonance (NMR) techniques. Kinetic isotope effects arise in irreversible or unidirectional reactions because for some reason the reverse reaction is inhibited or not occurring, such as evaporation in an open system when water vapor moves away from the liquid water pool. In kinetic reactions, both bond strength and isotope velocity are important. Kinetic fractionation reactions are normally associated with processes like evaporation, diffusion, dissociation reactions, and enzymatic effects. Kinetic fractionations are often quite large, usually much larger than equilibrium fractionations, and result in the lighter isotope accumulating in the product (lighter is faster). In contrast to equibrillium and kinetic effects, the isotopic fractionation resulting from nuclear spin effects is not mass dependent (Sulzman, 2007).

The isotopic fractionation of the biomass, the fatty acids and amino acids in bacteria analysed on the dependence on the growth temperature are resulting from kinetic effects, due to the fact that at least the formation of fatty and amino acids in cells are irreversible reactions. It could be hypothesed that the occurring isotopic fractionation in those biomolecules results from enzymatic preferences towards lighter isotopes at different temperatures.

The preference of enzymes towards the lighter isotope ^{12}C in the biosynthesis of bacterial fatty acids was reported for the pyruvate dehydrogenase by Melzer and co-workers (Melzer, 1987). They could show that the isotope fractionation at C-2 of pyruvate gives strong evidence that the well known relative ^{13}C depletion in lipids from biological material is mainly caused by the isotope effect on the pyruvate dehydrogenase reaction. Monson and colleagues (Monson, 1982) revealed in their analysis that fatty acids biosynthesized by *Escherichia coli* grown aerobically with glucose as the sole carbon source and harvested at late log phase are depleted by approximately 3‰ in ^{13}C relative to the glucose. This fractionation arises in the formation of acetyl-coenzyme A by pyruvate dehydrogenase and is localized at the carboxyl position in the acetyl-coenzyme A product. For the isotopic fractionation amino acids it was reported by Yoneyama and co-workers that the reaction of glutamine synthetase led to the production of glutamine (amide) with lower $\delta^{15}N$ values than that of the ammonia supplied, while the $\delta^{15}N$ values of ammonia were significantly increased during the incubation (Yoneyama, 1993).

The consistency of the amino acid profiles in both strains showed a clear common dependency on the growth temperature in both strains but no general trend. The percentage of some amino acids was rising with increasing growth temperature, while others were decreasing at higher temperatures. No correlation towards the groupings (Fig. 4.1) of the precursor compounds and the rising or decreasing percentage of the therefrom resulting amino acids could be detected. The different growth temperatures demand different tertiary structures of many proteins which is reflected in the changing amino acid composition.

The dependency on the growth temperature of the percentage consistency of the bacterial fatty acids could be clearly shown in Fig. 3.6. Both strains MT1 and MT4 showed an increasing ratio of the fatty acid $C_{16:0}$ while the ratio of the fatty acid $C_{16:1}\omega7c$ decreased with rising growth temperature. This could be due to the fact that the activity of the desaturase, the enzyme which is involved in the biotransformation of fatty acid $C_{16:1}\omega7c$ from its precursor fatty acid $C_{16:0}$, is temperature-sensitive. Those findings corroborate with analysis of Sakamoto and colleagues (Salamoto, 1997) who could show for the cyanobacterium *Synechococcus sp.* PCC 7002 that the ambient growth temperature, and not some other growth rate-related process, regulates the expression of acyl lipid desaturation in this cyanobacterium. Also the formation of the cyclic fatty acid cyclo-$C_{17:0}$d7,8 from its precursor $C_{16:0}$ underlies an enzymatic biotransformation by the cyclopropane-fatty acid synthase. It could be assumed that the increasing ratio of the cyclo-$C_{17:0}$d7,8 fatty acid with rising growth temperature is also resulting from a temperature-sensitivity of this enzyme.

This study dealt for the first time with the influence of the stress factor temperature on the isotopic fractionation of ^{13}C and ^{15}N in bacterial fatty acids and amino acids. A general dependency of the growth temperature and the resulting isotopic fractionation could not be detected. However, slight changes were seen in some fatty acids. Mutation studies are necessary helping to identify enzymes which are involved in the temperature dependent isotopic fractionation of those compounds.

4.3 Kinetics of Substrate Uptake in Pure Bacterial Cultures

The observation that strain *P. veronii* MT 4 incorporates carbon from the substrate acetate more efficiently than strains *P. reinekei* MT1 or *Achromobacter spanius* MT3 showing a larger **a**-value than the other two strains points to differences between the three strains in the efficiency of the incorporation of acetate into fatty acids. This finding probably simply mirrors the higher growth rate observed for *P. veronii* MT4 compared to *P. reinekei* MT1 or *A. spanius* MT3. The growth rate of MT4 is about twice as high as the ones of MT1 and MT3 and it fits well to $\mathbf{a}_{mean}$ of MT4 which is twice as high as well. Since there was no statistically significant increase in the maximal incorporation with increasing age of the culture it can be assumed that these differences are based on different physico-chemical constants of enzymes involved in the transportation of acetate into the cell and the synthesis of the fatty acids (Koch, 1997). Key enzymes are here acetate kinase, phosphotransacetylase and acetyl CoA synthetase, the latter being the main scavenger for exogenous acetate because of its higher affinity for this substrate (Treves, 1998). Some strains are known which synthesize acetyl-CoA using the acetyl-CoA synthetase (ACS) reaction while others achieve this reaction only via the acetate kinase (ACK)/ phosphotransacetylase (PTA) sequence. A third group of microorganisms is known which possesses both pathways and activate them depending on the concentration of acetate in the medium. In strains of the genus *Pseudomonas* either the ACS or the ACK/PTA route has been reported (Kretschmar, 2001) but it is not known which route is used by strains MT1 and MT4. Because **a**-values of different fatty acids in a given strain were rather similar it can be deduced that the differences in the maximal incorporation **a** between different strains arise from reaction steps within the fatty acid synthesis.

The picture found for the incorporation rate **b** is completely different to that seen for the maximal incorporation **a**. All strains showed a pronounced dependence of the incorporation rate **b** with the age of the cultures while the maximal incorporation **a** did not show such a trend. It is tempting to assume that the transportation process for acetate changed towards the stationary phase of the growth curve (Figure 3.9). Such changes of transportation processes have been described for several species, e. g. *Escherichia coli* (Clark, 1996; Ferenci, 1996) and *Corynebacterium glutamicum* (Gerstmeier, 2003) where they ensure the constant supply of the substrate in the cell under decreasing substrate concentrations in the medium.

The comparison of the individual fatty acids of a given strain revealed no statistically significant tendency for the increase of the incorporation rates **b**, but since all fatty acids displayed an increase of b in the stationary phase of growth a common cause can be indicated. Because all three species showed this phenomenon it can be deduced that the increase of **b** is caused by changes in some enzymatic steps very early in the fatty acid synthesis or, more probably, in the transport of acetate into the bacterial cell. This study gave for the first time quantitative data on the increase of the incorporation rates in the biosynthesis of fatty acids demonstrating that the substrate is indeed faster but not better converted to cell compounds in the stationary than in the exponential growth phase.

Another reason for the high incorporation rates can be assumed due to the fact that the cell density in the suspension cultures rises with the age of the culture. Therefore, the high incorporation rates in the change from log to stationary phase and in stationary phase could be explained by the higher cell densities in those samples. This theory can be confuted if one considers the optical densities of the cell suspensions before adding the labelled substrate. Those optical densities do not differ much in the pure cell suspensions of the three strains up to the logarithmic phase of growth (Table 4.1). In the change between logarithmic and stationary phase and in stationary phase of growth the difference in the optical density become more obvious. While strain MT1 reached the stationary phase of growth with an OD_{600} value of 0.44 strains MT3 and MT4 showed slightly higher optical densities in this growth phase. Due to the fact that of those both strains showed nearly identical OD_{600} values in stationary phase of growth when the labelled substrate was added to the suspension cultures, the tremendous differences in the maximal incorporation and the rate constant of incorporation between the strains (Table 3.4) makes the cell density a negligible parameter in this study.

Table 4.1: Optical density at 600 nm measured in different growth phases in strains MT1, MT3 and MT4

	OD600				
	lag	lag/log	log	log/stationary	stationary
MT1	0,20	0,20	0,32	0,44	0,45
MT3	0,14	0,15	0,30	0,53	0,52
MT4	0,18	0,26	0,32	0,62	0,57

Furthermore, the results show that the carbon of the substrate is more rapidly incorporated in some fatty acids while others react more slowly. The faster labelling of the unsaturated fatty acids $C_{16:1}\omega5$ which is formed by dehydrogenation from the saturated precursor fatty acid $C_{16:0}$ is reasonable if the biosynthesis leads directly to $C_{16:1}\omega5$ and has no or only little exchange with the $C_{16:0}$ pool. If the saturated fatty acid precursor is in equilibrium with the pool of this fatty acid in the cell the final unsaturated fatty acid should show slower labelling as has been found for $C_{18:0}$ and $C_{18:1}\omega7$. An interesting case is the cyclic fatty acid cyclo-$C_{17:0}$ which is formed in *P. reinekei* in the late logarithmic growth phase by $C_{17:cyclopropane}$ synthases from $C_{16:1}$ (Muñoz-Rojas, 2006). This seems to be a rather slow process as can be seen from the fact that this fatty acid showed always the slowest incorporation of the label and fits to the finding that this fatty acid contributes to the change of the cell membrane to a more rigid one in the stationary phase (Muñoz-Rojas, 2006).

In both *Pseudomonas* strains the unsaturated C_{16}-fatty acids showed lower labellings than $C_{16:0}$, here $C_{16:1}\omega5c$ showed less labelling than $C_{16:1}\omega7c$. In contrast, in *A. spanius* MT3 the opposite was found. The C_{18}-fatty acids showed a different behaviour. $C_{18:1}\omega7c$ presented higher incorporations of the label than $C_{18:0}$ in strains MT1 and MT3 but in strain MT4 this trend was converse. This tendency was observed for all growth stages and one of the reasons maybe a more efficient synthesis of fatty acids starting from the labelled acetate. However, which of the many enzymatic steps is responsible or whether other reasons may have led to these differences in incorporation is still an open question and further experiments are required to identify the contributing factors in each strain.

It is interesting that the two *Pseudomonas* species reacted very differently to the supply of substrate in the stationary phase. *P. veronii* showed in general a larger incorporation of the carbon of the substrate into fatty acids than *P. reinekei*. However, the main difference was observed in the stationary phase where the incorporation rates increased in *P. veronii* tremendously while *P. reinekei* showed only a moderate increase. In the microbial consortium this should give *P. veronii* an advantage over *P. reinekei* in the competition for scarce nutrients because the former species can react much faster to a sudden addition of substrates, at least to acetate, than *P. reinekei*. One can speculate that this may be one reason why a number of *P. veronii* strains have been observed in the environment (Adhikari, 2001; Hong, 2004; Ajithkumar,

2003) where they degrade various compounds including xenobiotics along gradients of pollution (Hong, 2004; Kaschl, 2005).

4.4 Proliferation Assay of a Bacterial Consortium

Under natural conditions consortia consisting of very different species of bacteria are involved in the process of degrading organic compounds. Typically, these habitats provide neither optimal nor balanced growth conditions, since even the substrate flow tends to be discontinuous and highly variable. The basic intend of this study was to investigate the interspecies relationship in a bacterial consortium and the nature of the interdependence that enables the component species to mineralise 4-chlorosalicylate.

Multiparameter flow cytometry was used to get quantitative information on the community dynamics and for the identification of active populations. The method is well established for depicting bacterial consortia in natural environments and was recently combined with cell sorting as a prerequisite for phylogenetic analyses of subcommunities (Kleinsteuber, 2006).

In this thesis the technique was used for quantifying the degree of replicative activity as a sensitive measurement of the bacterial ability to grow under the micro-environmental conditions applied. The DNA patterns indicating cells in proliferation and stationary state of growth were obtained from pure cultures of the individual members of the 4-chlorosalicylate degrading community. Those patterns could be applied on samples of a chemostate culture of the consortium to unravel the physiological status of each individual member. This method enabled therefore an insight in the percentage of cells the proliferation and stationary of each community member.

High growth rates are associated with uncoupled DNA synthesis, typically found only under optimal growth conditions on lab-scale but not in natural water or soil environments. This behaviour was observed for the very short time ranges of 1 to 3 hours during the exponential growth phases for MT1 and MT3 during growth on peptone and acetate and for M4 and MT2 during growth on peptone (not shown). General initiation of uncoupled DNA replication might be genetically determined in the first place, but is promoted by the presence of substrates that can be metabolised

at high rates, thereby allowing substantial amounts of carbon, other nutrients and energy to be used exclusively for DNA synthesis. Due to low growth rates uncoupled DNA synthesis was not expected during the concertedly degradation of 4-chlorosalicalyte the pattern of theses states were not further involved in the evaluation of the data.

Due to reasons of stability the chemostate culture of the community was built up strain by strain, starting with MT1. The adapted proliferation and stationary phase patterns revealed a high amount of cells of *P.reinekei* MT1 in proliferation phase of growth in the first period of incubation but it decreased until day 82, the end of cultivation. The proportion of those cells in stationary phase of growth is slightly increasing during the whole incubation period. This could be due to the fact that the degradation of 4-chlorosalicylate by strain MT1 involves the formation of the highly toxic dead-end metabolite protoanemonin. This intermediate can be mineralised by strain *P. veronii* MT4. Since the main proportion of cells of this strain seemed to be in stationary phase of growth after appending to the chemostate culture after 24 days of incubation – resulting in a reduced metabolic activity of those cells - protoanemonin could be utilized only by a small proportion of MT4 cells in proliferation phase. The HPLC analysis of the supernatant of the chemostate samples showed a high concentration of protoanemonin in the beginning of the incubation, resulting from the active degradation of the substrate 4-chlorosalicylate by strain MT1. After adding MT4 to the chemostate culture the concentration decreased to a relatively constant amount of approximately 0.02 mM. The high peak at day 45 of incubation revealed a sudden increase up to 0.38 mM. This tremendous increase of proteanemonin could be referred to the unpleasant physiological status of strain MT4. Strain *Wautersiella falsenii* MT2 showed a completely different physiological status. The predominant proportion of cells of this strain are in proliferation state of growth while only a small and even decreasing part of this population was shown to be in stationary state of growth. This corroborates the findings of Pelz (Pelz, 1999) who described strain MT2 as the “necrotiser” of the consortium, due to the fact that this strain is living on the remains of dead or injured cells of the community.

Similar proliferation patterns obtained by flow cytometry were already successfully employed to study the dynamics of binary bacterial communities under various cultivation conditions (Müller, 2002). Such an analysis based on DNA contents can be regarded as highly reliable and quantitative since there is no risk of active

excretion of the dye by fixed cells. Nevertheless, those studies always require the necessity to separate the different fractions of bacteria in community. Müller and colleagues described first the combination of fluorochromising techniques and flow cytometry to dissect the physiological status of a xenobiotic degrading binary bacterial culture (Müller, 2002). Here, for the first time strain specific immuno-staining in combination with flow cytometry was employed to unravel the physiological status of individual members in a bacterial 4-chlorosalicylate degrading consortium. This combination of well established techniques allowed a direct insight in the percentages of cells in proliferation and stationary phase of growth of the different strains of the community. Furthermore, it could also be applied in combination with the method of FISH which would allow the analysis of proliferation patterns of not yet cultivated bacteria in complex bacterial communities.

4.5 Kinetics of Carbon Sharing in a Bacterial Consortium Revealed by a Novel Combination of Immunostaining, Stable Isotope Probing and FACS

The analysis of metabolic networks was the basic goal of many studies in the last decades (Webster, 2006). Those studies often employed stable isotopes to reveal the metabolic active member of such communities by the incorporation of the ^{13}C-labelled substrates in biomarkers of the cells (Webster, 2006; Zhang, 2002; Whiteley, 2007). The most challenging aspect of those studies lies in the complexity of bacterial communities. A method described by Nogales and co-workers involves the extraction of bacterial RNA from contaminated sites in order to reveal the metabolic active members in such consortia (Nogales, 1999). Another useful tool in the elucidation of those bacteria actively metabolising specific compound in polluted soils or sediments is delivered by stable isotope probing (SIP). Hereby, a ^{13}C-labelled substance is introduced into the system, for example ^{13}C-labelled benzene (Kasai, 2006). This technique involves incubation of soils or sediments with ^{13}C-labeled substrates, extraction of labelled nucleic acids (DNA or rRNA) by bead beating, and separation of light and heavy fractions using density gradient centrifugation, which occurs because of differences in the density of ^{13}C- versus ^{12}C-DNA. The amplification of the 16S-rRNA genes from the extracted isotopic heavier DNA and cDNA (obtained from the extracted RNA) by PCR techniques enables the sequencing of those genes. The comparison of the obtained sequences with the database of the National Centre for Biotechnology Information delivers an insight into the consistency of such a bacterial consortium and its actively degrading members. This application of SIP delivers therefore an essential tool in the elucidation of those problems of “who is eating what” in bacterial consortia but it gives no information about the kinetics of substrate fluxes in those networks. A disadvantage of SIP is the requirement of high incorporation labels of the substrate. This important limitation of DNA-SIP is the prerequisite for DNA synthesis and cell division to obtain incorporation of sufficient label into DNA for gradient separation. In the presence of 100% 13C-labeled compound, with each cell division, the heavy carbon fraction of DNA increases by 50%, as one parent chromosome strand is retained by each progeny. As a result, increasing the number of cell divisions increases the successful

isolation of labelled nucleic acid, but may increase the enrichment bias of the SIP experiment (Neufeld, 2006).

In this thesis a system was developed which allows the analysis of the kinetics of carbon sharing in a bacterial community by applying a novel combination of three well established techniques: stable isotope probing, immuno-staining and FACS. Therefore, a bacterial consortium, grown as a chemostate culture on 4-chlorosalicylate as sole carbon source, was pulse-dosed with [U-^{13}C]-4-chlorocatechol, an intermediate of the degradation pathway of 4-chlorosalicylate. Samples of the biomass were taken at different time points after labelling. Individual bacterial fractions were stained with strain specific antibodies and separated from the community by FACS. The fatty acids from the separated fractions were extracted. The incorporation of the labelled substrate into those biomarkers was analysed by a GC-IRMS approach.

A similar approach was employed by Pelz (Pelz, 1999) who combined stable isotope probing and immunocapture to elucidate the carbon flux of a ^{13}C-labelled substrate in a bacterial consortium. This method proofed to be useful in order to unravel the substrate sharing in a microbial network but also hereby, no information was obtained about the kinetics of the carbon flux in the system. For the unravelling of the velocity of the substrate uptake in the 4-chlorosalicylate degrading model consortium extensively studied in the last years (Faude, 1995; Pelz, 1999; Tillmannn, 2004) the method of Pelz was modified in regard of a sufficient cell number which is indispensable for the analysis of the fatty acids, the biomarkers chosen in this study. Pelz employed immunocapture for the separation of individual bacterial fractions of the community after pulse-dosing with ^{13}C-labelled substrate. This approach delivers only small cell numbers, which were described as not sufficient enough for the extraction of an adequate amount of fatty acids for further GC- IRMS analysis (Pelz, 1999). Therefore, analyses within this study were performed to obtain sufficient cell numbers which are suitable for the extraction of a fair amount of bacterial fatty acids. Those analyses revealed 2 x 10^7 as the lowest but still adequate number of cells. The application of preferably small cell numbers played an important role in this analysis, due to the low percentage of strain MT3 (8 %) in the bacterial community. Because of the very low percentage of only 1-2 % (Pelz, 1999) the two other members of this community, *Wautersiella falsenii* MT2 and *Pseudomonas veronii* MT4, were not considered in this study. The total volume of 500 ml of cell suspension of the

chemostate culture of the consortium would not allow sufficient cell numbers of these strains in samples taken after pulse-dosing with the labelled substrate.

To elucidate the carbon sharing in the 4-chlorosalicylate degrading community two individual bacterial strains of this consortium had to be separated in order to extract the fatty acids from each fraction for the analysis of the incorporation of the ^{13}C-labelled substrate into these biomarkers. Therefore, the fractions of strains *Pseudomonas reinekei* MT1 *and Achromobacter spanius* MT3 were immuno-stained with strain specific antibodies and separated by FACS. Although time-consuming, this approach allows the separation of a suitable number of cells from each of the immunostained bacterial fractions within the community samples for the further extraction of the microbial fatty acids. The isotopic ratio of these biomarkers revealed differences in the kinetics of substrate incorporation of strains MT1 and MT3. In general, *P. reinekei* MT1 showed a faster incorporation of the ^{13}C-labelled substrate into the fatty acids of this strain displayed by higher **b** values, while the maximal incorporation **a** was higher in strain *A. spanius* MT3. For the calculation of those parameters -the incorporation rate **b** and the maximal incorporation **a**- from the obtained isotopic ratios of the fatty acids the law of first order kinetics was employed. This was valid because of the low amounts of the added ^{13}C-labelled substrate used for the pulse-dosing of the chemostate culture. This was therefore not the limiting factor for at least 4 of the 6 sampling points. In both strains the maximal incorporation of the ^{13}C-labelled substrate into their analysed fatty acids was reached after 12 h, exceptionally into the fatty acid cyclo-$C_{17:0}$d7,8. Here, the maximal incorporation was obtained after 24 h. Those data indicated that within the 4-chlorosalicylate degrading bacterial community strain *Pseudomonas reinekei* MT1 was able to incorporate the labelled substrate faster than strain *Achromobacter spanius* MT3. In contrast, strain MT showed a higher maximal incorporation of the ^{13}C-labelled 4-chlorocatechol in its synthesised fatty acids.

This combination of the well described methods immunohistochemistry, stable isotope probing and flow cytometric cell sorting delivers therefore a suitable tool in the analysis of metabolic networks and the kinetics in such systems. The approach is not only applicable in the analysis of bacterial consortia in the fields of environmental microbiology; it also could be employed in the elucidation of carbon fluxes in host-pathogen interactions. Therefore, this new combination of methods delivers a versatile tool in the dissection of substrate fluxes for all fields of science. It could also

be employed in combination with FISH to elucidate carbon fluxes in complex communities harbouring not yet cultivable groups of bacteria.

5. Conclusion

Within this thesis a 4-chlorosalicylate degrading bacterial consortium was the basis for the application of different techniques to elucidate different problems in microbial consortia. This consortium was analysed in many studies in the last few years towards its consistency (Faude, 1995), its metabolic networks (Pelz, 1999), the degradation pathway of 4-chlorosalicylate by one of its members (Nicodem, 2004) and the dissection of the metabolic active members by IRMS (Tillmann, 2004). On the basis of these studies this consortium delivers a perfect model community to dissect different aspects in such a well analysed system. In this thesis the consortium was employed to unravel the following questions:

1. **The phylogenetic classification of the consortium members**

   The four bacterial members of the 4-chlorosalicylate degrading consortium isolated from the sediment of the creek Spittelwasser (Faude, 1995) were identified by sequencing their 16S rRNA genes. Database research in BLAST and the phylogenetic analysis of the sequences revealed the homology to following type strains by sequence alignment: *Pseudomonas reinekei* MT1, *Wautersiella falsenii* MT2, *Achromobacter spanius* MT3 and *Pseudomonas veronii* MT4.

2. **The Temperature Dependency of Carbon and Nitrogen Fractionation in Pseudomonas**

   Two members of the consortium, *Pseudomonas reinekei* MT1 and *Pseudomonas veronii* MT4 were dissected towards the dependency of the stress factor growth temperature on the isotopic fractionation in the bacterial biomass, amino acids and fatty acids. This part of the thesis revealed that the growth temperature showed no general dependency on the carbon and nitrogen fractionation within the biomass of the two *Pseudomonas* stains although differences in the carbon fractionation in some amino acids extracted from strains MT1 and MT4 could be detected. Those findings were hypothesised to be dependent on enzymatic preferences on lighter isotopes at different temperatures.

   An influence of the stress factor growth temperature could only be found in the consistency of the amino acid and fatty acid profiles in both strains.

3. The Kinetics of Substrate Uptake in Pure Bacterial Cultures

To analyse the kinetics of substrate uptake in pure cultures of three members of the 4-chlorosalicylate degrading community, *Pseudomonas reinekei* MT1, *Achromobacter spanius* MT3 and *Pseudomonas veronii* MT4, cells were grown on minimal medium containing 5 mM sodium acetate as sole carbon source. After pulse dosing of [$U^{13}C$]-labelled sodium acetate at discriminative growth stages samples were taken at different time points after labelling. The extracted fatty acids from those samples were dissected for their isotopic ratio to calculate the kinetics of substrate uptake by employing pseudo-first order kinetics**.**

This analysis revealed that the maximal incorporation and the incorporation rate of the [$U^{13}C$]-labelled substrate in the stationary phase in strain MT4 is significantly higher compared to those in strains MT1 and MT3. In the microbial consortium this should give *P. veronii* MT4 an advantage over *P. reinekei* MT1 in the competition for scarce nutrients because the former species can react much faster to a sudden addition of substrates, at least to acetate, than *P. reinekei*.

It can be assumed that these differences are based on different physico-chemical constants of enzymes involved in the transportation of acetate into the cell and the synthesis of the fatty acids. This study gave for the first time quantitative data on the increase of the incorporation rates in the biosynthesis of fatty acids demonstrating that the substrate is indeed faster but not better converted to cell compounds in the stationary than in the exponential growth phase.

4. The Proliferation Assay of a Bacterial Consortium

The physiological status of the individual members of the 4-chlorosalicylate degrading consortium was dissected by strain specific antibody staining in combination with flow cytometry. Therefore, the four bacterial members of the consortium were grown in pure cultures on different substrates and analysed by flow cytometry regarding their growth and proliferation characteristics. The resulting DNA distribution patterns were applied to samples of a chemostate culture of the consortium in order to analyse the physiological status of each individual member of the community. This system revealed for strains *Pseudomonas reinekei* MT1, *Achromobacter spanius* MT3 and *Pseudomonas veronii* MT4 decreasing proportions of cells in proliferation phase of growth during the incubation period, while the proportion of *Wautersiella falsenii* MT2 cells in

proliferation phase was increasing during incubation. Since strain MT2 was assumed to live on cell debris and other metabolites (Pelz, 1999) its active proliferation status could allocated the decreasing physiological status of the other three members. The high proportion of cells of the remaining strains in stationary phase of growth towards the end of incubation was allocated to the formation of toxic intermediates of the degradation of 4-chlorosalicylate.

5. The Kinetics of Carbon Sharing in a Bacterial Consortium Revealed by a Novel Combination of Stable Isotope Probing, Immunostaining and FACS

A system was developed which allows the analysis of the kinetics of carbon sharing in a bacterial community by applying a novel combination of three well established techniques: stable isotope probing, immunostaining and FACS. Therefore, a bacterial consortium, grown as a chemostate culture on 4-chlorosalicylate as sole carbon source, was pulse-dosed with [U-^{13}C]-4-chlorocatechol, an intermediate of the degradation pathway of 4-chlorosalicylate. Samples of the biomass were taken at different time points after labelling. Individual bacterial fractions were stained with strain specific antibodies and separated from the community by FACS. The fatty acids from the separated fractions of the two most prominent members, strains MT1 and MT3, were extracted. The incorporation of the labelled substrate into those biomarkers was analysed by a GC-IRMS approach. The maximal incorporation and the incorporation rate of the labelled substrate into the bacterial fatty acids were calculated by employing pseudo-first order kinetics. This approach revealed that the incorporation rate of the isotopic-labelled substrate into those biomarkers was much faster in strain MT1, while the maximal incorporation of the label into the fatty acids of strain MT3 was much higher. In this part of the thesis a system was developed which allows the analysis of the kinetics of substrate sharing in bacterial consortia by the combination of three well established analytical techniques. The sensitivity of fatty acid-stable isotope probing in combination with fluorochromizing staining of individual members of bacterial consortia - such as immunohistochemistry methods or FISH – and FACS delivers a new tool in the analysis of functional diversity of microbial communities.

6. Literature

Abraham, W.-R., Meyer, H., Lindholst, S., Vancanneyt, M. and Smit, J. (1997) Phospho- and sulfolipids as biomarkers of *Caulobacter*, *Brevundimonas* and *Hyphomonas. Syst. Appl. Microbiol.* **20**:522-539

Abraham, W.-R., Hesse, C. and Pelz, O. (1998) Ratios of carbon isotopes in microbial lipids as an indicator of substrate usage. *Appl. Environ. Microbiol.* **64**(11):4202-4209

Abraham, W.-R. and Hesse, C. (2003) Isotope fractionations in the biosynthesis of cell components by different fungi: a basis for environmental carbon flux studies. *FEMS Microbiol. Ecol.* **46**:121-128

Adhikari, T. B., Joseph, C. M., Yang, G., Phillips, D. A. and Nelson, L. M. (2001) Evaluation of bacteria isolated from rice for plant growth promotion and biological control of seedling disease of rice. *Can. J. Microbiol*. **47:**916-924

Ajithkumar, B., Ajithkumar, V. P. and Iriye, R. (2003) Degradation of 4-amylphenol and 4-hexylphenol by a new activated sludge isolate of *Pseudomonas veronii* and proposal for a new subspecies status. *Res. Microbiol*. **154:**17-23

Allman, R., Schjerven, T. and Boye, E. (1991) Cell cycle parameters of *Escherichia coli* K-12. *J. Bacteriol.* **173**(24):7970-4

Antic, M.P., Jovancicevic, B.S., Ilic, M., Vrvic, M.M. and Schwarzbauer, J. (2006) Petroleum pollutant degradation by surface water microorganisms*. Environ. Sci. Pollut. Res. Int.* **13**(5):320-7

Amann, R.I., Ludwig, W., and Schleifer, K.H. (1995) Phylogenetic identification and in situ detection of individual microbial cells without cultivation. *Microbiol. Rev*. **59**: 143–169

Balkwill, D. L., Leach, F. R., J. T. Wilson, McNabb, J. F. and White, D. C. (1988) Equivalence of microbial biomass measures based on membrane lipid and cell wall components, adenosine triphosphate and direct counts in subsurface aquifer sediments. *Microb. Ecol.* **16:**73-84

Batisson, I., Pesce, S., Besse-Hoggan, P., Sancelme, M. and Bohatier, (2007) Isolation and characterization of diuron-degrading bacteria from lotic surface water. *Microb. Ecol.* (E-Pub)

BD Bioscience (2000) Introduction to flow cytometry: a learning guide. Manual Part Number: 11-11032-01

Bernander, R., Stokke, T. and Boye, E. (1998) Flow cytometry of bacterial cells: comparison between different flow cytometers and different DNA stains. *Cytometry* **31**(1):29-36

Berg, J., Tymoczko, J. and Stryer, L. (2002) Biochemistry, 5th Edition, *W. H. Freeman and Company*. ISBN 0716746840

Bigeleisen, J. and Wolfsberg, M. (1959) Theoretical and experimental aspects of isotope effects in chemical kinetics. *Adv. Chem. Phys*. **1**:15– 76

Boschker, J.T., Nold, S.C., Wellsbury, P., Bos, D., de Graaf, W., Pel, R., Parkes, R.J., Cappenberg, T.E. (1998) Direct linking of microbial populations to specific biogeochemical processes by ^{13}C-labelling of biomarkers. *Nature* **392**: 801– 805

Brack, W., Kind, T., Schrader, S., Möder, M. and Schüürmann, G. (2003) Polychlorinated naphthalenes in sediments from the industrial region of Bitterfeld. *Environ. Pollut.* **121**:81-5

Brack, W., Altenburger, R., Ensenbach, U., Möder, M. and Schüürmann, G. (1999) Bioassay-directed identification of organic toxicants in river sediment in the industrial region of Bitterfeld (Germany) - a contribution to hazard assessment. *Arch. Environ. Contam. Toxicol.* **37**:164–174

Caldwell, D. E., E. Atuku, K. P. Wivcharuk, S. Karthikeyan, D. R. Korber, D. R. Schmid and G. M. Wolfaardt. (1997). Germ theory versus community theory in understanding and controlling the proliferation of biofilms. *Adv. Dental Res.* **11**:4-13

Camara, B., Strömpl, C., Verbarg, S., Spröer, C., Pieper, D.H. and Tindall BJ. (2007) *Pseudomonas reinekei* sp. nov., *Pseudomonas moorei* sp. nov. and *Pseudomonas mohnii* sp. nov., novel species capable of degrading chlorosalicylates or isopimaric acid. *Int. J. Syst. Evol. Microbiol.* **57**:923-31

Campbell, J. W., and Cronan, J. E. Jr. (2001) Bacterial fatty acid biosynthesis: targets for antibacterial drug discovery. *Annu. Rev. Microbiol.* **55:**305-332

Chemie AG Bitterfeld- Wolfen (1993) Bitterfelder Chronik, Bitterfeld.

Cho, J.-C. and Tiedje, J.M. (2001) Bacterial species determination from DNA-DNA hybridization by using genome fragments and DNA microarrays. *Appl. Environ. Microbiol.* **67**(8): 3677–3682

Christensen, B. B., Haagensen, J. A. ,Heydorn, A. and Molin, S. (2002) Metabolic commensalism and competition in a two-species microbial consortium. *Appl. Environ*. *Microbiol* **68**: 2495-502

Clark, D. P. and Cronan Jr., J. E. (1996) Two-carbon compounds and fatty acids as carbon sources. *Escherichia coli* and *Salmonella*: cell and molecular biology, *ASM Press*, Washington, D.C. ISBN 1555811647

Cooper, S. (1991) Bacterial growth and division. *Academic Press*, San Diego, CA. ISBN 0121879054

Coenye, T., Vancanneyt, M., Falsen, E., Swings, J. and Vandamme, P. (2003) *Achromobacter insolitus* sp. nov. and *Achromobacter spanius* sp. nov. from human clinical samples. *Int. J. Syst. Evol. Microbiol.* **53**:1819-24

Craig, H. (1953) The geochemistry of the stable carbon isotopes. *Geochim. Cosmochim. Acta* **3**:53-92

Cullington, J.E. and Walker, A. (1999) Rapid biodegradation of diuron and other phenylurea herbicides by a soil bacterium. *Soil Biol. Biochem* **31**: 677–686

DeLong, E.F., Wickham, G.S. and Pace, N.R. (1989) Phylogenetic stains: ribosomal RNA based probes for the identification of single cells. *Science* **243**: 1360–1363

Descheemaker, P. and Swings, J. (1995) The application of fatty acid methyl ester analysis (FAME) for the identification of heterotrophic bacteria present in decaying lede-stone of the St. Bavo Cathedral in Ghent. *Sci. Total Environ.* **167:**241-247

Dethlefsen , L., Eckburg, P.B, Bik, E.M. and David A. Relman, D. A. (2006) Assembly of the human intestinal microbiota. *TRENDS Ecol. Evol.* **21** (9): 517:523

Dumont, M.G., Murrell, J.C. (2005) Stable isotope probing - linking microbial identity to function. *Nat. Rev. Microbiol.* **(6)**:499-504

El-Fantroussi, S. (2000) Enrichment and molecular characterization of a bacterial culture that degrades methoxy-methyl urea herbicides and their aniline derivatives. *Appl. Environ. Microbiol* . **66**: 5110–5115

Elomari, M., Coroler, L., Hoste, B., Gillis, M., Izard, D. and Leclerc H. (1996) DNA relatedness among Pseudomonas strains isolated from natural mineral waters and proposal of *Pseudomonas veronii* sp. nov. *Int. J. Syst. Bacteriol.* **46**(4):1138-1144

Falk, P. G., Hooper L. V., Midtvedt T. and Gordon J.I. (1998) Creating and maintaining the gastrointestinal ecosystem: what we know and need to know from gnotobiology. *Microbiol. Mol. Biol. Rev.* **62** (4):1157-1170

Fang, J., Barcelona, M. J. and Semrau, J. D. (2000) Characterization of methanotrophic bacteria on the basis of intact phospholipid profiles. *FEMS Microbiol. Lett.* **189:**67-72.

Faude, U. C. (1996). Immunochemische Analyse mikrobieller Lebensgemeinschaften. PhD Thesis. University of Leipzig

Ferenci, T. (1996) Adaptation to life at micromolar nutrient levels: the regulation of *Escherichia coli* glucose transport by endoinduction and CAMP. *FEMS Microbiol. Rev*. **18**: 301-317

Findlay, R H. (1996) The use of phospholipid fatty acids to determine microbial community structure. *Molecular microbial ecology manual. Kluwer Academic Publishers.* ISBN 0792339436

Frech, G. (1996). Struktur und Dynamik eines 4-Chlorsalicylat abbauenden Chemostat-Konsortiums. PhD Thesis. Technical University Braunschweig

Fuhrmann, J.A. and Campbell, L.. (1998) Microbial microdiversity. *Nature* **393**:410-411

Gans, J., Wolinsky, M. and Dunbar, J. (2005). Computational improvements reveal great bacterial diversity and high metal toxicity in soil. *Science* **309:**1387-1390

Gerstmeir, R., Wendisch, V. F., Schnicke, S., Ruan, H., Farwick, M., Reinscheid, D. and Eikmanns. B. J. (2003) Acetate metabolism and its regulation in *Corynebacterium glutamicum*. *J. Biotechnol.* **104:**99-122

Goodman, K. J. and Brenna, J. T. (1992) High sensitivity tracer detection using high-precision gas chromatography-combustion isotope ratio mass spectrometry and highly enriched [U-^{13}C]-labeled precursors. *Anal. Chem.* **64:**1088-1095

Green, T. and Scow, K.M. (2000) Analysis of phospholipid fatty acids (PLFA) to characterize microbial communities in aquifers. *Hydrogeol. J.* **8**(1):126-141

Guarner, F. and Malagelada J.R. (2003). Gut flora in health and disease. *Lancet* **361**(9356), 512-519

Haug, W., A. Schmidt, B. Nörtemann, D. C. Hempel, A. Stolz, and Knackmuss, H. J. (1991) Mineralization of the sulfonated azo dye Mordant Yellow 3 by a 6-aminonaphthalene- 2-sulfonate-degrading bacterial consortium. *Appl. Environ. Microbiol.* **57:**3144-3149

Hay, M. E., Parker, J. D., Burkepile, D. E., Caudill, C. C., Wilson, A. E. , Hallinan, Z. P. and Chequer A. D. (2004). Mutualisms and aquatic community structure: the enemy of my enemy is my friend. *Annu. Rev. Ecol. Evol. Syst.* **35**: 175–197

Hong, H. B., Nam, I. H., Murugesan, K., Kim, Y. M. and Chang, Y. S. (2004) Biodegradation of dibenzo-p-dioxin, dibenzofuran, and chlorodibenzo-p-dioxins by *Pseudomonas veronii* PH-03*. Biodegradation* **15:**303-313

Kämpfer, P., Avesani, V., Janssens, M., Charlier, J., De Baere, T. and Vaneechoutte, M. (2006) Description of *Wautersiella falsenii* gen. nov., sp. nov. to accommodate clinical isolates phenotypically resembling members of the genera *Chryseobacterium* and *Empedobacter*. *Int. J. Syst. Evol. Microbiol*. **56**:2323-2329

Kacmar, J., Gilbert, A., Cockrellm J. and Srienc, F. (2006) The cytostat: a new way to study cell physiology in a precisely defined environment. *J. Biotechnol*. **126**(2):163-172

Kalbitz, K. and Popp, P. (1999) Seasonal impacts on b-hexachlorocyclohexane concentration in soil solution*. Environ. Pollut.***106**:139–141

Karle, I. and Karle, J. (1966) The crystal and molecular structure of anemonin, $C_{10}H_8O_4$. *Acta Cryst.* **20**:555-559

Kaschl, A., Vogt, C., Uhlig, S., Nijenhuis, I., Weiß, H., Kästner, M., Richnow, H.-H. (2005) Isotopic fractionation indicates anaerobic monochlorobenzene biodegradation *Environ.Toxicol.Chem.* **24**(6):1315-1324

Kasai, Y., Takahata, Y., Manefield, M. and Watanabe, K. (2006) RNA-based stable isotope probing and isolation of anaerobic benzene-degrading bacteria from gasoline-contaminated groundwater. *Appl. Environ. Microbiol*. **72**(5): 3586–3592

Kaneda, T. (1991) Iso- and anteiso-fatty acids in bacteria: biosynthesis, function and taxonomic significance. *Microbiol. Mol. Biol. Rev.* **55**(2): 288-302

Kell, D.B., Ryder, H.M., Kaprelyants, A.S. and Westerhoff, H.V. (1991). Quantifying heterogeneity: flow cytometry of bacterial cultures. *Antonie Van Leeuwenhoek.* **60**(3-4):145-58

Kleinsteuber, S., Riis, V., Fetzer, I., Harms, H. and S. Müller (2006) Population dynamics of a microbial consortium during growth on diesel fuel in saline environments. *Appl. Environ. Microbiol*., **72**(5):3531-3542

Koch, A. L. (1997) Microbial physiology and ecology of slow growth. *Microbiol. Mol. Biol. Rev.* **61**:305-318

Kohring, L.L., Ringelberg, D.B., Devereux, R., Stahl, D.A., Mittelman, M.W. and White, D.C. (1994) Comparison of phylogenetic relationships based on phospholipid fatty acid profiles and ribosomal RNA sequence similarities among dissimilatory sulfatereducing bacteria. *FEMS Microbiol. Lett.* **119** :303–308

König, C., Eulberg, D., Gröning, J., Lakner, S., Seibert, V., Kaschabek, S.R. and Schlömann, M. (2004) A linear megaplasmid, p1CP, carrying the genes for chlorocatechol catabolism of *Rhodococcus opacus* 1CP. *Microbiol.* **150**:3075-87

Kuballa, J., Wilken, R.-D., Jantzen, E., Kwan, K.K., Chau, Y.K. (1995) Speciation and genotoxicity of butyltin compounds. *Analyst.* **120**:667–673

Kumar, S., Tamura, K. and M Nei, M. (2004) MEGA3: Integrated software for Molecular Evolutionary Genetics Analysis and sequence alignment. *Brief. Bioinformatics* **5**:150-163

Kretzschmar, U., Schobert, M. and Görisch, H. (2001) The *Pseudomonas aeruginosa acsA* gene, encoding an acetyl-CoA synthetase, is essential for growth on ethanol. *Microbiol.* **147:**2671-2677

Lebaron, P. and Joux, F. (1994) Flow cytometric analysis of the cellular DNA content of *Salmonella typhimurium* and *Alteromonas haloplanktis* during starvation and recovery in seawater. *Appl. Environ. Microbiol.* **60**(12):4345-4350

Leclerc, L. and Labeyrie, L. (1987) Temperature dependence of the oxygen isotopic fractionation between diatom silica and water. *Earth Planet. Sci. Lett.* **84**:69-74

Lechevalier, M. P. (1977) Lipids in bacterial taxonomy: a taxonomist's view. *Crit. Rev. Microbiol.* **7**:109–210

Lee, M. D., Odom, J. M. and Buchanan, J. R. (1998). New perspectives on microbial dehalogination of chlorinated solvents: insights from the field. *Annu. Rev. Microbiol.* **52**:423–52

Lerman, L. and Fisher, S. (1979). Length-independent separation of DNA restriction fragments in two-dimensional gel electrophoresis. *Cell* **16**:191-200

Liu, W.T., Marsh, T. L., Cheng, H. and Forney, L. J. (1997). Characterization of microbial diversity by determining terminal restriction fragment length polymorphisms of genes encoding 16S rRNA. *Appl. Environ. Microbiol.* **63**:4516-4522

Lu, Y., Abraham, W.R. and Conrad, R. (2007). Spatial variation of active microbiota in the rice rhizosphere revealed by in situ stable isotope probing of phospholipid fatty acids. *Environ. Microbiol.* **9**(2):474-481

Madsen, E.L. (2006) The use of stable isotope probing techniques in bioreactor and field studies on bioremediation. *Curr. Opin. Biotechnol.* **17**(1):92-97

Mauclaire, L., Thullner, M., Pelz,O., Abraham, W.-R. and Zeyer, J. (2003) Assimilation of toluene carbon along a bacteria–protist food chain determined by ^{13}C-enrichment of biomarker fatty acids. *J. Microbiol. Methods* **55**:635-649

Meckenstock, R.U., Morasch, B.,Griebler, G. and Richnow, H.H. (2004) Stable isotope fractionation analysis as a tool to monitor biodegradation in contaminated acquifers. *J. Contam. Hydrol.* **75**:215– 255

Melzer, E. and Schmidt, H.L.. (1987) Carbon isotope effects on the pyruvate dehydrogenase reaction and their importance for relative carbon-13 depletion in lipids. *J. Biol. Chem.* **262**(17): 8159-8164

Monson, K.D. and Hayes, J.M. (1982) Carbon isotopic fractionation in the biosynthesis of bacterial fatty acids. Ozonolysis of unsaturated fatty acids as a means of determining the intramolecular distribution of carbon isotopes. *Geochim. Cosmochim. Acta* ***46***:139-149

Miller, L. and Berger, T. (1985) Bacteria identification by gas chromatography of whole cell fatty acids. Application Note (Hewlett Packard), 228–241

Morasch, B., H. Richnow, H.-H., Schink, B. and Meckenstock, R.U. (2001) stable hydrogen and carbon isotope fractionation during microbial toluene degradation: mechanistic and environmental aspects. *Appl. Environ. Microbiol.* **67**(10):4842-4849

Moss, C. W., Lambert, M. A. and Merwin, W. H. (1974) Comparison of rapid methods for analysis of bacterial fatty acids. *Appl. Microbiol.* **28**:80-85

Müller, S., Lösche, A., Bley, T. and Scheper, T. (1995) A flow cytometric approach for characterization and differentiation of bacteria during microbial processes. *Appl. Microbiol. Biotechnol.* **43**:93-101

Müller, S., Strauber, H., Lösche, A. and Babel, W. (2002). Population analysis of a binary bacterial culture by multi-parametric flow cytometry. *J. Biotechnol.* **97**:163–176

Müller, S. and Babel, W. (2003) Analysis of bacterial DNA patterns—an approach for controlling biotechnological processes. *J. Microbiol. Methods* **55**:851– 858

Mullis, Kary (1990) The unusual origin of the polymerase chain reaction. *Scientific American* **262**(4):56-61, 64-65

Muñoz-Rojas, J., Bernal, P., Duque, E., Godoy, P., Segura, A. and Ramos, **J.-L. (2006)** Involvement of cyclopropane fatty acids in the response of *Pseudomonas putida* KT2440 to freeze-drying*. Appl. Environ. Microbiol.* **72**:472-477

Narbad, A., Hewlins, M. J. and Callely. A. G. (1989) ^{13}C-NMR studies of acetate and methanol metabolism by methylotrophic *Pseudomonas* strains. *J. Gen. Microbiol*. **135:**1469-1477

Neufeld, J.D., Dumont, M.G., Vohra, J. and Murrell, J.C. (2006) Methodological considerations for the use of stable isotope probing in microbial ecology. *Microb. Ecol.* **53**(3):435-42

Neufeld, J.D., Vohra, J., Dumont, M.G., Lueders, T., Manefield, M., Friedrich, M.W. and Murrel,l J.C. (2007) DNA stable isotope probing. *Nat. Protoc*. **2**(4):860-866

Nogales, B., Moore, E.R.B., Abraham, W.R. and Timmes, K. (1999) Identification of the metabolically active members of a bacterial community in a polychlorinated biphenylpolluted moorland soil. *Environ. Microbiol.* **1**(3):199–212

Nicodem, P. (2004) New bacterial pathway of 4- and 5-chlorosalicylate degradation via 4-chlorocatechol and maleylacetate in a *Pseudomonas* strain. PhD Thesis, Technical University Braunschweig

Nwachukwu, S.C., James, P. and Gurney, T.R. **(2001)** Inorganic nutrient utilisation by "adapted" *Pseudomonas putida* strain used in the bioremediation of agricultural soil polluted with crude petroleum. *J. Environ. Biol*. **22**(3):153-162

Orita, M., Suzuki, Y., Sekiya,T. and Hayashi, K. (1989) Rapid and sensitive detection of point mutations and DNA polymorphisms using the polymerase chain reaction. *Genomics* **5**: 874-879

Pel, R., Floris, V. and Hoogveld, H. (2004) Analysis of planktonic community structure and trophic interactions using refined isotopic signatures determined by combining fluorescence-activated cell sorting and isotope ratio mass spectrometry. *Freshw. Biol.* **49**:546-562

Pelz, O., Tesar, M., Wittich, R.-M., Moore, E.R.B., Timmis, K.T. and Abraham, W.-R. (1999) Towards elucidation of microbial community metabolic pathways: unravelling the network of carbon sharing in a pollutant-degrading bacterial consortium by immunocapture and isotopic ratio mass spectrometry. *Environ. Microbiol.* **1**(2):167-174

Pelz, O. (1999a) Functional characterisation of a 4-chlorosalicylate-degrading bacterial community by $\delta^{13}C$ labeling of biomarkers. PhD Thesis, Technical University Braunschweig

Pieper, D.H. (2005) Aerobic degradation of polychlorinated biphenyls. *Appl. Microbiol. Biotechnol.* **67**(2):170-191

Popp, P., Kalbitz, K., Oppermann, G. (1994) Application of solidphase microextraction and gas chromatography with electron-capture and mass spectrometric detection for the determination of hexachlorocyclohexanes in soil solutions. *J. Chromatogr.* **687**:133–140

Prosser, J.I., Rangel-Castro, J.I.and Killham, K.. (2006) Studying plant-microbe interactions using stable isotope technologies. *Curr. Opin. Biotechnol*. **17**(1):98-102

Rainey, P. B., Bailey, M. J. and Thompson. I. P. (1994). Phenotypic and genotypic diversity of fluorescent pseudomonads isolated from field-grown sugar beet. *Microbiol.* **140:**2315-2331

Rock, C. O. and Cronan, J. E. (1996) *Escherichia coli* as a model for the regulation of dissociable (type II) fatty acid biosynthesis. *Biochim. Biophys. Acta* **1302:**1-16.

Radajewski, S., Ineson, P., Parekh, N. and Murrell, J. (2000).Stable-isotope probing as a tool in microbial ecology. *Nature* **403**:646–649

Sackett, W. M., Eckelmann, W. R., Bender, M. L. and Bé, A..W.H. (1965) Temperatur dependence of carbon isotope composition in marine plankton and sediments. *Science* **148**:235-237

Sakamoto, T., Higashi, S., Wada, H., Murata, N. and Bryant, D.A. (1997) Low-temperature-induced desaturation of fatty acids and expression of desaturase genes in the *Cyanobacterium synechococcus* sp. PCC 7002. *FEMS Microbiol. Lett.* **152**(2):313-20

Sakamoto, M., Umeda, M. and Benno, Y. (2005) Molecular analysis of human oral microbiota. *J. Periodont. Res.* **40**(3):277-85

Schopf, J. W. (1993) Microfossils of the Early Archean Apex chert: new evidence of the antiquity of life. *Science* **260**:640-646

Seckbach, J. (2000) Journey to diverse microbial worlds: adaptation to exotic environments. *Kluwer Academic Publishers.* ISBN 0792360206

Shapiro, H.M. (2003) Practical Flow Cytometry. 4th ed*. Wiley & Sons*, New York. ISBN 0471411256

Shapiro, J. A. (1998) Thinking about bacterial populations as multicellular organisms. *Annu. Rev. Microbiol*. **52:**81-104

Skarstad, K., Boye, E. and Steen, H.B. (1986) Timing of initiation of chromosome replication in individual Escherichia coli cells. *EMBO J*. **5**:1711– 1717

Smith, B., Herath, H.M.W. and Chase, J.B. (1973) Effect of growth on carbon isotopic ratios in barley, pea and rape. *Plant Cell Physiol.* **14**:177-182

Spiers, A. J., Buckling, A. and Rainey, P. B. (2000) The causes of *Pseudomonas* diversity. *Microbiol.* **146**:2345-2350

Stolyar, S., Van Dien, S., Hillesland, K. L., Pinel, N., Lie, T. J., Leigh, J. A. and Stahl, D. A. (2007). Metabolic modeling of a mutualistic microbial community. *Mol.Syst. Biol*. **1**:3-92

Stanier, R. Y., Palleroni, N. J. and Doudoroff. M. (1966) The aerobic pseudomonads: a taxonomic study. *J. Gen. Microbiol.* **43:**159-271

Tesar, M., Hoch, C., Moore, E. R. B. and Timmis, K. N. (1996). Westprinting: Development of a rapid immunochemical identification for species within the genus *Pseudomonas* sensu stricto. *Syst. Appl. Microbiol.* **19**, 577-588

Tillmann, S. (2004). Assessment of the degradation potential of microbial biocenoses and identification of bacterial taxa involved in the organic degradation using isotope ratio mass spectrometry (IRMS). Ph. D. thesis, Technical University Braunschweig

Tillmann, S., Strömpl, C., Timmis, K.N. and Abraham, W.-R. (2005) Stable isotope probing reveals the dominant role of Burkholderia species in aerobic degradation of PCBs. *FEMS Microbiol. Ecol*. **52**:207-217

Treves, D. S., Manning, S. and Adams, J. (1998) Repeated evolution of an acetate-crossfeeding polymorphism in long-term populations of *Escherichia coli*. *Mol. Biol. Evol*. **15:**789-797

van Elsas, J.D., Jansson, J.K. and Trevors, J.T. (1997) Modern Soil Microbiology. CRC Press ISBN: 0-8247-2749-5

Vestal, J. R. and D. C. White (1989) Lipid analysis in microbial ecology. *Bioscience* **39**:535-541

Wayne, L. G., Brenner, D. J., Colwell, R. R., Grimont, P. A. D., Kandler, O., Krichevsky, M. I. and Truper, H.G. (1987) Report of the ad hoc committee on reconciliation of approaches to bacterial systematics. *Int. J. Syst. Bacteriol.* **37:**463-464

Webster, G., Watt, L.C., Rinna, J., Fry, J.C., Evershed, R.P., Parkes, R.J. and Weightman, A.J. (2006) A comparison of stable-isotope probing of DNA and phospholipid fatty acids to study prokaryotic functional diversity in sulfate-reducing marine sediment enrichment slurries *Environ. Microbiol.* **8**(9):1575–1589

Welch, D. F. (1991) Applications of cellular fatty acid analysis. *Clin. Microbiol. Rev.* **4:**422-438

White, D.C. and Ringelberg D.B. (1997) Utility of the signature lipid biomarker analysis in determining the *in situ* viable biomass, community structure, and nutritional/physiologic status of deep subsurface microbiota. The Microbiology of the Terrestrial Deep Subsurface. *CRC Press inc*, New York. ISBN 0849383625

Whiteley, A.S., Thomson B., Lueders T. and Manefield M._(2007) RNA stable isotope probing. *Nat. Protoc*. **2**(4):838-844

Wittich, R. M., Strömpel, C., Moore, E. R. B., Blasco, R. and Timmis, K. N. (1999) Interaction of *Sphingomonas* and *Pseudomonas* strains in the degradation of chlorinated dibenzofurans. *J. Ind. Microbiol. Biotechnol.* **23:**353-8

Yoneyama, T., Kamachi, K., Yamaya,T. and Mae, T. (1993) Fractionation of nitrogen isotopes by glutamine synthetase isolated from spinach leaves. *Plant Cell Physiol.* **34**(3): 489-491

Zelles, L., Bai, Q.Y., Beck, T. and Beese, F. (1992) Signature of fatty acids in phospholipids and lipopolysaccharides as indicators of microbial biomass and community structure in agricultural soils. *Soil Biol. Biochem.* **24:**317-323.

Zhang, C.L. (2002) Stable carbon isotopes of lipid biomarkers: analysis of metabolite sand metabolic fates of environmental microorganisms. *Curr. Opin. Biotechnol*. **13**:25–30

Name	Sonja Pawelczyk
Adresse	Neustadtring 5 38114 Braunschweig
Geburtsdatum	10.09.1977 (Berlin)
Email-Adresse	s.pawelczyk@gmx.de

AUSBILDUNG

Nov. 2004-Nov. 2007	Anfertigung einer Doktorarbeit im Rahmen des “Europäischen Graduiertenkollegs *Pseudomonas*: Biotechnology and Pathogenicity“, betreut durch Dr. W.-R. Abraham
Sept. 2004	Diplom im Studiengang Biotechnologie, TU Braunschweig
Aug. 2003-Mär. 2004	Diplomarbeit an der GBF Braunschweig, Arbeitsgruppe Infektionsgenetik (Charakterisierung und Lokalisierung des Phosphatidylserinrezeptors in transfizierten und nicht-transfizierten Zelllinien)
Dez. 2000	Vordiplom im Studiengang Biotechnologie, TU Braunschweig

1998-2004	Studium der Biotechnologie, TU Braunschweig
1997-1998	Studium der Biotechnologie, TU Berlin
1997	Abitur (Marie-Curie Gymnasium, Berlin)

AUSLANDSAUFENTHALT

Jan. 2001-Jul.2001	Studium der Biotechnologie, University of Dundee, Schottland
Mai/Jun. 2005	Lehrgang "Analytical Microbial Chemistry", Danmarks Tekniske Universitet, Dänemark

PRÄSENTATIONEN

Pawelczyk S, Macedo AJ, Kuhlicke U, Neu T and Abraham W-R. Biofilm formation and PCB-degradation of a 4-chlorosalicylate degrading consortium. Biofilms II-Attachment and Detachment in Pure and Mixed Cultures, Leipzig. 2006 (Poster Präsentation)

Pawelczyk S, Kuhlicke U, Neu T and Abraham W-R. Biofilm formation and PCB-degradation potential of a 4-chlorosalizylate degrading consortium. ISME, Wien. 2006 (Poster Präsentation)

Pawelczyk S, Kuhlicke U, Neu T and Abraham W-R. Immunohistochemical Analysis of a 4-Chlorosalicylate Degrading Biofilm Consortium. 4th ASM Conference on Biofilms, Quebec. 2007 (Poster Präsentation)

Hiermit möchte ich mich ganz herzlich bei Prof. Timmis und Prof. Lang für die Übernahme des Referats bzw. Koreferats der vorliegenden Arbeit bedanken.

Dem Europäischen Graduiertenkolleg „Pseudomonas: Biotechnology and Pathogenicity“ möchte ich für die Finanzierung dieser Doktorarbeit und den Teilnahmen an nationalen und internationalen Fachtagungen danken. Hier gilt mein Dank besonders Prof. Tümmler für viele interessante Diskussionen und Helga Riehn-Kopp für ihre organisatorische Unterstützung.

Ein besonderer Dank gilt Dr. W.-R. Abraham für die Betreuung dieser Arbeit. Ohne seine zahlreichen wissenschaftlichen Ratschläge und Anmerkungen wäre diese Arbeit nicht möglich gewesen. Esther Surges und Dr. Susann Müller sei für die Messungen aller Proben am IRMS und EA, bzw. am MoFlo gedankt.

Jennifer Skerra, Agnes Waliczek und Alexandre Jose Macedo möchte ich ganz besonders für ihre tägliche tatkräftige Unterstützung in wissenschaftlichen als auch allen anderen Lebenslagen danken. Auch den momentanen und besonders den ehemaligen Mitgliedern des Graduiertenkollegs gilt dieser Dank.

Auch bei allen anderen Mitarbeitern der Abteilung Mikrobiologie am Helmholtz Zentrum für Infektionsforschung möchte ich mich für die Unterstützung bedanken.

Ein ganz besonderer Dank gilt natürlich meiner Familie und Roman Fischer ohne deren Unterstützung abseits der Wissenschaft alles hier nicht möglich gewesen wäre. DANKE!